MANIPULATION OF MESENCHYMAL STEM CELLS FOR ALTERED THERAPEUTIC EFFECTS

by

SETH HENRY ANDREWS

(Under the Direction of Steven Stice and William Kisaalita)

ABSTRACT

Mesenchymal Stem Cells (MSCs) have been investigated for several decades for use in tissue engineering and regenerative medicine. Initially, they were only thought of as a source of multipotent cells for tissue transplantation. However, difficulties in maintaining the potency of transplanted MSCs and safety and regulatory concerns have prompted a shift in focus to their secretome, which can have regenerative and immunosuppressive effects on endogenous cells. This dissertation explores various ways to manipulate MSCs for different therapeutic benefits. First, we evaluated the ability of lentiviral transduced MSCs to express bone morphogenetic protein-2 (BMP-2) and heal critical sized bone defects compared to delivery of rhBMP-2 in scaffolds. We found that BMP-2 MSCs released the protein over a longer period of time than BMP-2 loaded scaffolds, and they induced comparable healing of critical sized defects to the loaded scaffolds. We next investigated the use of a parainfluenza-5 derived amplifying virus like particle (AVLP) to induce transgene expression in MSCs. This involved examining the transduction efficiency and stability of expression over time of both an EGFP and BMP-2 vector. We found that while MSCs could be reliably transduced to

express EGFP stably over time, transduction with the BMP-2 vector proved to induce much more variable expression. Finally, we compared the effect of acidic, hypoxic, and inflammatory culture on MSCs and their extracellular vesicles (EVs). We characterized the EVs produced in the various conditions and compared their ability to suppress T-cells to that of their parent cells. We found that EV secretion, size, and surface markers vary with the extracellular conditions of their secreting MSCs, and while MSCs are generally better at suppressing T-cell activation, EVs from acidic conditioned MSCs induce the formation of regulatory T-cells. We have identified various avenues for modifying the MSC secretome which could be of value for future therapeutics.
INDEX WORDS: Mesenchymal Stem Cells, bone morphogenetic protein 2, chondroitin sulfate glycosaminoglycan, lentivirus, bone, parainfluenza virus 5, amplifying virus like particle, extracellular vesicles, exosomes, immunomodulation, T-cells

MANIPULATION OF MESENCHYMAL STEM CELLS FOR ALTERED THERAPEUTIC EFFECTS

by

SETH HENRY ANDREWS

B.S., Cornell University, 2012

M.Eng., Cornell University, 2013

A Dissertation Submitted to the Graduate Faculty of The University of Georgia in Partial Fulfillment of the Requirements for the Degree

DOCTOR OF PHILOSOPHY

ATHENS, GEORGIA

2019

MANIPULATION OF MESENCHYMAL STEM CELLS FOR ALTERED THERAPEUTIC EFFECTS

by

SETH HENRY ANDREWS

Major Professor:	Steven Stice William Kisaalita
Committee:	Lohitash Karumbaiah Luke Mortensen Cheryl Gomillion

Electronic Version Approved:

Suzanne Barbour
Dean of the Graduate School
The University of Georgia
May 2019

ACKNOWLEDGEMENTS

I would like to thank my advisors, Dr. Steve Stice and Dr. William Kisaalita, and my committee members, Dr. Lohitash Karumbaiah, Dr. Luke Mortenson, and Dr. Cheryl Gomillion. I would also like to thank my friends and co-workers in the Stice Lab, the Regenerative Bioscience Center, and Aruna Biomedical, including Erin Jordan, Robin Webb, Raymond Swetenburg, Forrest Goodfellow, Christina Elling, Sam Spellicy, Austin Passaro, Meghan Logun, Ty Maughon, Taylor Ellison, Viviana Martinez, and Shelly Scoville.

I would also like to thank my parents, Brian and Susan Andrews. I would not be where I am today without them. Finally, I would like to thank my wife, Valerie Marcano, for always believing in me and pushing me to be my best.

Table of Contents

Page

INTRODUCTION 1
REFERENCES 4
CHONDROITIN SULFATE GLYCOSAMINOGLYCAN SCAFFOLDS FOR CELL AND RECOMBINANT PROTEIN-BASED BONE REGENERATION 7
2.1 ABSTRACT 8
2.2 INTRODUCTION 8
2.3 METHODS 11
2.4 RESULTS 19
2.5 DISCUSSION 22
REFERENCES 28
OVEREXPRESSION OF BMP-2 IN MESENCHYMAL STEM CELLS WITH AMPLIFYING VIRUS-LIKE PARTICLES 43
3.1 ABSTRACT 44
3.2 INTRODUCTION 44
3.3 METHODS 47
3.4 RESULTS 50
3.5 DISCUSSION 52
REFERENCES 54
LITERATURE REVIEW 70
4.1 INTRODUCTION 70
4.2 OSTEOGENIC MSC EVS 71
4.3 ORTHOIMMUNOLOGY 76
4.4 EV IMMUNOMODULATION 78
4.5 CONCLUSIONS 81
REFERENCES 82
ACIDIC PRECONDITIONED MSCS PRODUCE EXTRACELLULAR VESICLES THAT INCREASE REGULATORY T-CELL FREQUENCY IN VITRO 88

5.1 ABSTRACT 89
5.2 INTRODUCTION 89
5.3 METHODS 91
5.4 RESULTS 95
5.5 DISCUSSION 97
REFERENCES 103
CONCLUSION 120
REFERENCES 126

LIST OF FIGURES

Figure 2.1 Efficient transduction of MSCs with a lentiviral vector at 10 MOI……37

Figure 2.2: CS-GAG hydrogel is porous with stable rheology……38

Figure 2.3: Preparation of CS-GAG hydrogel and interactions with transduced MSCs..39

Figure 2.4: Defects bridge when treated with rhBMP-2 or BMP-2 MSCs……40

Figure 2.5: Newly formed bone similar between rhBMP-2 and BMP-2 MSC groups.....41

Figure 2.6: Histology reveals qualitative differences in bone maturity……...42

Figure 3.1: AVLP construct and transduction of MSCs……65

Figure 3.2: Flow cytometry of huMSC (AVLP-eGFP)……...66

Figure 3.3: AVLP-eGFP selection in huMSCs……...67

Figure 3.4: AVLP-BMP selection in huMSCs……68

Figure 5.1: EV characterization……....110

Figure 5.2: Relative expression of EV surface markers across MSC culture conditions as determined by MACSPLEX analysis……111

Figure 5.3: Comparative CFSE-EV uptake by T-cell subsets after 24 hours……112

Figure 5.4: Comparative proliferation of T-cell subsets 5 days after treatment with EVs or MSCs as measured by CFSE dilution……....113

Figure 5.5: Comparative activation of T-cell subsets 5 days after treatment with EVs or MSCs……114

Supplementary Figure 5.1: Experimental workflow……115

Supplementary Figure 5.2: Flow analysis diagram……116

Supplementary Figure 5.3: Dynamic Light Scattering of EVs……...117

Supplementary Figure 5.4: Comparative activation of T-cell subsets 24 hours after treatment with CFSE-EVs……...118

LIST OF EQUATIONS

Equation 3.1.....69

Equation 5.1.....119

Equation 5.2.....119

CHAPTER 1

INTRODUCTION

Regenerative medicine, which amplifies the body's own capacity to build and repair damage tissue, has been one of the most important medical advances in the last few decades (Mason & Dunnill, 2008). The discovery and application of stem cells, self-renewing cells that possess the potential to differentiate into multiple mature cell types, is critical to its continued success (Mahla, 2016). One of the most-studied stem cell types is mesenchymal stem cells, also called mesenchymal stromal cells (MSCs). Unlike other stem cell types, they can be easily harvested from adults, making them the most accessible stem cells. They are commonly described as adherent, fibroblast-like cells that can differentiate into bone, cartilage, and adipose tissue and lack hematopoietic markers (Campana et al., 2014).

MSCs have been used in a variety of applications since their discovery. Initially their value was seen in differentiating them into certain tissue types and transplanting them to injury sites. They have recently attracted interest for the pro-regenerative and anti-inflammatory properties of their secretome (Yeo et al., 2013). MSC conditioned media has improved healing of myriad conditions, including bone defects, myocardial infarction, osteoarthritis, and colitis (Vizoso, Eiro, Cid, Schneider, & Perez-Fernandez, 2017). These properties can be further improved through manipulation of the cells. This

work discusses several ways to modify the secretome of MSCs for therapeutic benefit, including genetic engineering and culture preconditioning.

Chapter 1, published as a research article in Stem Cells: Translational Medicine, is focused on the use of genetically modified mesenchymal stem cells to repair critically sized bone defects. The study compared the modified cells to naïve cells, and to cell-free options for synthetic bone grafting. These different methods were assessed both in vitro for release kinetics, and in vivo in a rodent model of critical sized femoral defects. This investigation tested the hypothesis that the modified MSCs would induce greater quality bone formation than any of the other options.

Chapter 2, published as a research article in the International Journal of Regenerative Medicine, summarizes a study assessing the ability of a new viral vector to transduce mesenchymal stem cells with transgenes. It investigated both initial transduction efficiency and stability of the transgene expression over time. It was hypothesized that the new vector would be a reliable, cost-effective method of inducing transgene expression in MSCs.

Despite the potential of MSCs, there have been numerous challenges in translating this to clinical success, including storage and safety issues. Recently thawed MSCs have found to have diminished efficacy and increased need for a recovery when compared to non-thawed MSCs (Galipeau, 2013). Additionally, transplantation of any live dividing cells raises concerns about tumorgenicity (Volarevic et al., 2018). Extracellular vesicles (EVs), derived from the MSC secretome, have emerged as a potential answer to some of these challenges.

Extracellular vesicles are nanoscale vesicles secreted by cells for intercellular signaling via the transfer of bioactive molecules including RNA, proteins, and lipids (Camussi, Deregibus, Bruno, Cantaluppi, & Biancone, 2010). They include exosomes, which are released through fusion of intracellular multivesicular bodies with the plasma membrane, and microparticles, which bud directly from the plasma membrane (Colombo, Raposo, & Thery, 2014). EVs are produced by all cells, but those derived from MSCs have shown regenerative effects in a wide range of applications. MSC-derived EVs have improved recovery from myocardial ischemia and reperfusion injury (Lai et al., 2010), stroke (Xin et al., 2013), gentamicin induced acute kidney injury (Reis et al., 2012), and allogeneic skin grafts (Zhang et al., 2014) in vivo. Being acellular, EVs are not subject to many of the safety concerns MSCS are, and they are easier to characterize and standardize for therapeutic use (Vishnubhatla, Corteling, Stevanato, Hicks, & Sinden, 2014). There is also substantial evidence that the cargo and function of EVs can be influenced by the extracellular environment of their parent cells, potentially increasing their therapeutic potency (de Jong et al., 2012; Kucharzewska & Belting, 2013).

Chapter 3 is a literature review yet to be published that summarizes the current understanding of the impact of the immune system on bone healing, and postulates that MSC EV induced osteogenesis in vivo is partly due to their immunomodulatory properties. Chapter 4 describes work yet to be published investigating the effects of different preconditioning environments on the immunosuppressive properties of MSCs and their EVs. MSCs were preconditioned in acidic, hypoxic, or inflammatory environments, and the cells or corresponding EVs were applied to activated immune

cells in vitro. It was hypothesized that preconditioning would improve the immunomodulatory properties of both the cells and EVs over normal culture conditions. Taken together, this work serves as an exploration of the diverse options available to alter MSCs for therapeutic benefit.

REFERENCES

Campana, V., Milano, G., Pagano, E., Barba, M., Cicione, C., Salonna, G., . . . Logroscino, G. (2014). Bone substitutes in orthopaedic surgery: from basic science to clinical practice. *J Mater Sci Mater Med, 25*(10), 2445-2461. doi:10.1007/s10856-014-5240-2

Camussi, G., Deregibus, M. C., Bruno, S., Cantaluppi, V., & Biancone, L. (2010). Exosomes/microvesicles as a mechanism of cell-to-cell communication. *Kidney Int, 78*(9), 838-848. doi:10.1038/ki.2010.278

Colombo, M., Raposo, G., & Thery, C. (2014). Biogenesis, secretion, and intercellular interactions of exosomes and other extracellular vesicles. *Annu Rev Cell Dev Biol, 30*, 255-289. doi:10.1146/annurev-cellbio-101512-122326

de Jong, O. G., Verhaar, M. C., Chen, Y., Vader, P., Gremmels, H., Posthuma, G., . . . van Balkom, B. W. (2012). Cellular stress conditions are reflected in the protein and RNA content of endothelial cell-derived exosomes. *J Extracell Vesicles, 1*. doi:10.3402/jev.v1i0.18396

Galipeau, J. (2013). The mesenchymal stromal cells dilemma--does a negative phase III trial of random donor mesenchymal stromal cells in steroid-resistant graft-versus-host disease represent a death knell or a bump in the road? *Cytotherapy, 15*(1), 2-8. doi:10.1016/j.jcyt.2012.10.002

Kucharzewska, P., & Belting, M. (2013). Emerging roles of extracellular vesicles in the adaptive response of tumour cells to microenvironmental stress. *J Extracell Vesicles, 2*. doi:10.3402/jev.v2i0.20304

Lai, R. C., Arslan, F., Lee, M. M., Sze, N. S., Choo, A., Chen, T. S., . . . Lim, S. K. (2010). Exosome secreted by MSC reduces myocardial ischemia/reperfusion injury. *Stem Cell Res, 4*(3), 214-222. doi:10.1016/j.scr.2009.12.003

Mahla, R. S. (2016). Stem Cells Applications in Regenerative Medicine and Disease Therapeutics. *International Journal of Cell Biology, 2016*, 24. doi:10.1155/2016/6940283

Mason, C., & Dunnill, P. (2008). A brief definition of regenerative medicine. *Regen Med, 3*(1), 1-5. doi:10.2217/17460751.3.1.1

Reis, L. A., Borges, F. T., Simoes, M. J., Borges, A. A., Sinigaglia-Coimbra, R., & Schor, N. (2012). Bone marrow-derived mesenchymal stem cells repaired but did not prevent gentamicin-induced acute kidney injury through paracrine effects in rats. *PLoS One, 7*(9), e44092. doi:10.1371/journal.pone.0044092

Vishnubhatla, I., Corteling, R., Stevanato, L., Hicks, C., & Sinden, J. (2014). The Development of Stem Cell-derived Exosomes as a Cell-free Regenerative Medicine. *Journal of Circulating Biomarkers*, 1. doi:10.5772/58597

Vizoso, F. J., Eiro, N., Cid, S., Schneider, J., & Perez-Fernandez, R. (2017). Mesenchymal Stem Cell Secretome: Toward Cell-Free Therapeutic Strategies in Regenerative Medicine. *International journal of molecular sciences, 18*(9), 1852. doi:10.3390/ijms18091852

Volarevic, V., Markovic, B. S., Gazdic, M., Volarevic, A., Jovicic, N., Arsenijevic, N., . . . Stojkovic, M. (2018). Ethical and Safety Issues of Stem Cell-Based Therapy. *International journal of medical sciences, 15*(1), 36-45. doi:10.7150/ijms.21666

Xin, H., Li, Y., Cui, Y., Yang, J. J., Zhang, Z. G., & Chopp, M. (2013). Systemic administration of exosomes released from mesenchymal stromal cells promote functional recovery and neurovascular plasticity after stroke in rats. *J Cereb Blood Flow Metab, 33*(11), 1711-1715. doi:10.1038/jcbfm.2013.152

Yeo, R. W., Lai, R. C., Zhang, B., Tan, S. S., Yin, Y., Teh, B. J., & Lim, S. K. (2013). Mesenchymal stem cell: an efficient mass producer of exosomes for drug delivery. *Adv Drug Deliv Rev, 65*(3), 336-341. doi:10.1016/j.addr.2012.07.001

Zhang, B., Yin, Y., Lai, R. C., Tan, S. S., Choo, A. B., & Lim, S. K. (2014). Mesenchymal stem cells secrete immunologically active exosomes. *Stem Cells Dev, 23*(11), 1233-1244. doi:10.1089/scd.2013.0479

CHAPTER 2

CHONDROITIN SULFATE GLYCOSAMINOGLYCAN SCAFFOLDS FOR CELL AND RECOMBINANT PROTEIN-BASED BONE REGENERATION[1]

[1] Seth Andrews, Albert Cheng, Hazel Stevens, Meghan T. Logun, Robin Webb, Erin Jordan, Boao Xia, Lohitash Karumbaiah, Robert E. Guldberg, Steven Stice. Accepted by Stem Cells Translational Medicine. Reprinted here with permission of publisher.

2.1 ABSTRACT

Bone morphogenetic protein 2 (BMP-2) loaded collagen sponges remain the clinical standard for treatment of large bone defects when there is insufficient autograft, despite associated complications. Recent efforts to negate co-morbidities have included biomaterials and gene therapy approaches to extend the duration of BMP-2 release and activity. In this study, we compared the collagen sponge clinical standard to chondroitin sulfate glycosaminoglycan (CS-GAG) scaffolds as a delivery vehicle for recombinant human BMP-2 (rhBMP-2) and rhBMP-2 expression via human BMP-2 gene inserted into mesenchymal stem cells (BMP-2 MSC). We demonstrated extended release of rhBMP-2 from CS-GAG scaffolds compared to their collagen sponge counterparts, and further extended release from CS-GAG gels seeded with BMP-2 MSC. When used to treat a challenging critically-sized femoral defect model in rats, both rhBMP-2 and BMP-2 MSC in CS-GAG induced comparable bone formation to the rhBMP-2 in collagen sponge, as measured by bone volume, strength, and stiffness. We conclude that CS-GAG scaffolds are a promising delivery vehicle for controlling the release of rhBMP-2 and to mediate the repair of critically-sized segmental bone defects.

2.2 INTRODUCTION

Bone tissue is well known for its remarkable healing abilities, but there are instances in which these mechanisms are insufficient on their own. Large defects or gaps in bone are unable to be bridged without intervention. Allografts and autografts are popular bone grafting methods, accounting for over 2 million procedures per year [1]. However, these procedures are not devoid of complications. Autografts, which are derived from the patient themselves, are the current gold standard, but are the most

difficult to obtain and have the risk of donor site morbidity [2,3]. Allografts, from other individuals of the same species, are more likely to be rejected, require lifelong immunosuppression, and are potential sources of disease transmission [2,4,5]. Due to these issues, there have been numerous attempts to develop new synthetic bone graft substitutes to enhance bone healing.

Bone Morphogenetic Protein 2 (BMP-2) is an osteoinductive growth factor commonly used in bone substitute applications. It usually exists as a homodimer, binding to serine/threonine kinase receptors to initiate endocrine, paracrine, and autocrine effects [6,7]. The recombinant human BMP-2 (rhBMP-2) is FDA-approved and used clinically in combination with a collagen sponge. It has been shown to reduce the rate of secondary intervention and enhance fracture healing and has shown additional benefits for many orthopedic applications [8,9]. Thus, any new modality for treating critically-sized bone defects should undergo a rigorous investigation with comparison to current FDA approved techniques, such as rhBMP-2 on collagen sponge.

Despite its well documented ability to induce bone formation, rhBMP-2 has a very short half-life, leading to the use of supraphysiological doses by clinicians [10,11]. Complications associated with delivery of rhBMP-2 clinically have been reported to include ectopic bone formation, inflammation, and increased cancer rates among patients [12,13]. Additionally, the large amount of recombinant protein required for this approach leads to increased costs compared to alternative treatments [14]. In rats, clinically relevant doses of rhBMP-2 have been shown to induce the formation of structurally abnormal bone, as well as inflammation [15]. These drawbacks could be addressed by using a delivery method with sustained release of a lower dose of BMP-2. One such delivery

system could involve use of constitutive BMP-2 expression via genetically engineered mesenchymal stem cells (MSCs) for BMP-2 delivery (BMP-2 MSC) [16-19].

MSCs are multipotent stromal cells commonly studied and used for their ability to differentiate into bone, cartilage, and adipose tissue [20]. They are attractive as a delivery mechanism due to their ease of collection and expansion from bone marrow, adipose, and umbilical tissue, as well as their immune modulation capabilities and allogeneic tolerability. Osteogenic differentiation can be readily induced in MSCs, even in the absence of BMP-2 and transforming growth factor β1 (TGF-β1) signaling [21]. Our group has previously demonstrated success in creating ectopic bone and regenerating critically-sized defects in rats using BMP-2-expressing MSCs encapsulated in poly-ethylene glycol (PEG) microspheres [22,23]. However, these studies noted a sharp decrease in encapsulated cell viability after 4 days [22]. PEG has been shown to be safe for implantation, but it is not inherently osteoconductive or biodegradable without further modifications [24,25]. In addition, PEG cell encapsulation procedures can be labor intensive, variable, and inefficient [26].

Chondroitin sulfate glycosaminoglycans (CS-GAGs) are found attached to CS proteoglycans in the extracellular matrix of cartilage, bone, and other tissues. They are O-linked glycans consisting of repeating glucuronic acid and N-acetylgalactosamine disaccharides. CS-GAGs are important for bone development as they can support osteogenesis and suppress bone resorption [21,27-30]. Additionally, they regulate both TGF-β1 and BMP signaling in bone and have been shown to retain TGF-β [21,31]. In other studies, sulfated glycosaminoglycans assisted in BMP-2's interaction with its receptor, and oversulfated chondroitin sulfate enhanced osteoblast mineralization in the presence of

BMP-4 [32,33]. These qualities lend themselves to the use of CS-GAGs as a scaffold for the slow release of BMP-2.

In this study, we describe an injectable biologic therapy for large bone defect healing. It consists of human MSCs genetically engineered to overexpress BMP-2, which are then seeded in a CS-GAG hydrogel. To increase retention of the therapeutic within the bone defect, we delivered the hydrogels in electrospun polycaprolactone nanofiber meshes, which have been previously demonstrated by members of our group to enhance hydrogel-mediated BMP-2 delivery [34]. We demonstrated high levels of BMP-2 expression in BMP-2 MSCs, maintained viability post-seeding, and sustained *in vitro* BMP-2 release from this system compared to BMP-2 on collagen sponge. Additionally, we show the formation of comparable bone quantity and quality to the clinical standard in a rigorous rodent critically-sized segmental defect model. These results indicate the potential of this system to be a valuable therapeutic option for healing large bone defects.

2.3 METHODS

Cell Culture and Transduction

Due to differences in MSC behavior due to tissue source, both human umbilical (uMSC) or bone marrow MSCs (bmMSC), (Lifeline Cell Technology, Frederick MD, Sciencell, Carlsbad CA, one donor each) were used [35]. Both MSC types were plated at 5000 cells/cm^2 on tissue culture flasks in complete media Alpha-Minimum Essential Medium (MEM-α), 10% defined fetal bovine serum (Hyclone, South Logan UT), 2 mM L-glutamine, 50 U/mL penicillin, 50 µg/mL streptomycin and allowed to grow to 80-90% confluency (20,000–25,000 cells/cm^2). To transduce, cells were harvested using 0.05% trypsin and plated at 26,000 cells/cm^2 in MEM-α, 10% defined fetal bovine serum, 5

μg/mL Polybrene (Sigma-Aldrich, St. Louis MO), and the appropriate MOI of prEF1a-BMP-2 or prEF1a-RFP lentivirus (Cellecta, Mountain View CA) on tissue culture flasks. The media was changed back to complete media 24 hours post-transduction. All cultures were maintained at 37°C and 5% CO_2. Cells that had undergone up to 20 passages were used in the generation of Figure 1's data, while all subsequent data was generated from cells that had undergone less than 10 passages. All materials were from Invitrogen (Carlsbad CA) unless otherwise stated.

In vitro RFP expression

Following transduction of uMSCs and bmMSCs with the prEF1a-RFP vector in MOIs of 0, 1, 10, and 50 as described above, both phase contrast and fluorescent images were taken. Five images per well and three wells per condition were taken at 24, 48, and 72 hours post-transduction.

In vitro BMP-2 expression

Following transduction of bmMSCs or uMSCs with the prEF1a-BMP-2 vector in MOIs of 10 and 50 as described above, 0.5 mL media samples were collected in triplicate from different sets of wells at 48, 72, 96 and 120 hours post-transduction. BMP-2 concentrations were determined via BMP-2 ELISA (R&D Systems, Minneapolis MN).

Hydrogel Preparation and Characterization

The CS-GAG hydrogels were created as previously described [36]. Briefly, hydrogel mixture was prepared by reconstituting 3% w/v of lyophilized methacrylated chondroitin sulfate and 0.01% 2-hydroxy-4′-(2-hydroxyethoxy)-2-methylpropiophenone (Irgacure-2959, Sigma-Aldrich, St. Louis MO) in PBS. These gels are polyanionic and

have been shown to consist of 86% CS-A (4-sulfated), 6% CS-E (4,6-sulfated), 5% CS-C (6-sulfated), and unsulfated CS [36].

Rheological testing of the hydrogel was performed as described previously [36]. Briefly, 500 µL of the hydrogel mixture was dispensed into a polydimethylsiloxane mold overlaid onto a glass slide, and exposed to 365 nm long-wavelength UV light (160 W BlakRay, UVP, Upland CA) for 3 min to yield hydrogel disks 1 in. in diameter and 6 mm thick. The hydrogels were then overlaid with 1 mL of PBS to swell overnight before rheological testing, which was performed on an ARES rheometer (TA Instruments, New Castle DE), using a parallel plate geometry. Frequency sweep experiments from 0.1 to 100 Hz were performed at 5% strain at 25°C (n=5) and storage modulus (Pa) versus angular frequency (rad/s) was plotted. Similarly, the dynamic viscosity and shear stress of the hydrogels was measured and Viscosity (Pa·s) and Shear Stress (Pa) versus shear rate (S^{-1}) were plotted.

Morphology of gold coated lyophilized hydrogel samples was examined as described previously using a Zeiss 1450EP SEM scanning electron microscope (Carl Zeiss, Oberkochen Germany) [36]. Briefly, hydrogels were flash frozen in liquid nitrogen and lyophilized. We have not observed any discernible difference in structure and porosity of lyophilized snap frozen CS-GAG hydrogels reported in this study to hydrogels frozen overnight at -80C as reported by us previously [36,37]. They were then mounted on 10 mm SEM stubs and sputter coated (Structure Probe Inc., West Chester PA) with gold for 30 s, and imaged under an accelerated voltage of 5 kV. Images were acquired at 165x and 500x to observe the porosity and microstructure of the hydrogels.

Cell Seeding

Following casting as described above, 500 µL gels were frozen overnight at -80°C, after which they were lyophilized for 24 hours (Fig. 3A). To rehydrate them, the lyophilized hydrogels were overlaid with either a $6.66x10^6$/mL cell suspension (GAG+MSC or GAG+BMP-2 MSC) or 33.3 µg/mL rhBMP-2 (GAG+rhBMP-2) of equal volume to the gel in MEM-α and allowed to incubate at 37°C and 5 % CO_2 until all free liquid was absorbed into the gel. The hydrogel was then transferred to a sterile 1mL syringe, pulse centrifuged to remove air pockets and injected/ejected with a sterile 22G needle.

Viability and Distribution

24 hours after transduction with the prEF1a-RFP vector at MOI 10, uMSCs were seeded in CS-GAG hydrogels and overlaid with 2 µM Calcein in PBS (n=5). Non fluorescent calcein AM was hydrolyzed to fluorescent calcein in live cells by the action of intracellular esterases. Cells were imaged using FITC and TRITC fluorescent filters 3 hours after seeding. Viability of transduced cells was determined by quantifying the degree of fluorescence overlap of RFP and Calcein using the Mander's overlap co-efficient parameters in Volocity (PerkinElmer, Waltham MA) as described previously [37].

Nanofiber mesh fabrication

Perforated nanofiber mesh tubes were fabricated as described previously [34]. A 12% (w/v) solution of poly(ε-caprolactone) (PCL) was made by dissolving PCL (Sigma-Aldrich, St. Louis MO) in a 90:10 mixture of hexafluoro-2-propanol:dimethylformamide (Sigma-Aldrich, St. Louis MO). The solution (~4mL) was electrospun onto a static collector plate to obtain PCL sheets. Rectangular sections (12x19 mm) containing twenty three 1-mm-diameter circular holes were then cut using a VLS3.50 laser cutter

(Universal Laser Systems, Scottsdale AZ). Each rectangular piece was then rolled up into a cylindrical tube (5 mm diameter, 12 mm in length) and glued using medical grade UV-curable adhesive (Dymax, Torrington CT). Meshes were sterilized by ethanol evaporation, washed and stored in PBS, and then transferred to MEM-α and stored at 4°C prior to use.

Preparation of GAG treatment groups

One day prior to surgery/experiment, uMSCs were either left non-transduced or transduced at 10 MOI and seeded in CS-GAG hydrogels 24 hours after transduction as described above. On the day of surgery/experiment, rhBMP-2 (R&D Systems, Minneapolis MN) was reconstituted according to the manufacturer's instructions, diluted to 33.3 ug/mL in MEM-α, and used to rehydrate lyophilized CS-GAG hydrogel as described above. This rhBMP-2 dose, equating to 5 µg/gel, has previously been demonstrated to be the ideal minimum does for defect bridging in this defect model with low risk of complications [38].

Collagen sponge preparation

The day before each surgery/experiment, rhBMP-2 (Pfizer Inc., New York, NY) in 0.1% rat serum albumin (Sigma-Aldrich, St. Louis MO) in 4 mM HCl solution was made up to a concentration of 33.3 ug/mL and then stored at 4°C overnight. Collagen sponge cylinders ~5mm in diameter and 10mm in length were created by biopsy punching out from a sheet of bovine collagen sponge (Kensey Nash/DSM, Exton PA). All collagen sponge cylinders were sterilized by ethylene oxide. Prior to the start of the surgery/experiment, the collagen sponge cylinders were transferred to a 24-well plate, and then 150 µl of the rhBMP-2 solution was slowly loaded onto each cylinder. The

sponges were left to sit for ~10 minutes to soak up any residual rhBMP-2 solution in the well before being carefully transferred to another well plate for *in vitro* release characterization or press-fit into the bone defect for *in vivo* studies

Hydrogel BMP-2 Release

Experimental groups were prepared as follows: CS-GAG hydrogels were rehydrated with $6.67x10^6$ cells/mL non-transduced uMSCs (GAG+MSC), transduced uMSCs (GAG+BMP-2 MSC), or 33.3 µg/mL rhBMP-2 (GAG+rhBMP-2), and 150 µL of each rehydrated gel was injected into polycaprolactone (PCL) nanofiber meshes and placed into individual wells of an ultra-low adhesion 24-well plate (Nunclon Sphera, ThermoFisher, Waltham MA). For the collagen sponge group (Col+rhBMP-2), 150 µL of 3.33µg/mL rhBMP-2 solution was loaded onto each sponge and each sponge was then placed into an individual well of the 24-well plate (without any PCL mesh).

For the release experiment, 1 mL of MEM-α only were added to each well (n=3-4). All scaffolds were then allowed to incubate at 37°C and 5 % CO_2. At 3 h, 12 h, 1, 2, 3, 5, 7, 9, 11, and 13 days, the overlaid media were collected and immediately stored at -80°C, and the extracted media was replaced with 1 ml of fresh media. On day 15, media were collected and then replaced with 1 ml of digest solution. The CS-GAG hydrogels were digested with 1 ml media containing 20 mU of chondroitinase ABC (Sigma-Aldrich, St. Louis MO) while the collagen sponges were digested with 1 mg/ml collagenase type I (Sigma-Aldrich, St. Louis MO). Digestion occurred for 24 hours at 37°C before collection and storage at -80°C as before. BMP-2 ELISA was performed on the collected media to determine the amount of BMP-2 released from the scaffolds at each timepoint.

Segmental defect surgery

All surgical procedures were approved by the Georgia Institute of Technology Institutional Animal Care and Use Committee and NIH standards for animal care were followed. This surgical procedure has been described previously [39]. Prior to surgery, all animals were given a subcutaneous injection of slow-release buprenorphine (ZooPharm, Windsor CO) for analgesia and anesthesia was induced and maintained using isoflurane (Henry Schein Animal Health, Dublin OH) inhalation. Briefly, an anterolateral skin incision was made in the leg, and then blunt dissection was performed to allow for placement of a polysulfone fixation plate. Critically-sized 8 mm defects were created in the mid-diaphysis of the femur using an oscillating saw. The desired therapeutic was then delivered to the defect site, and finally the muscle and skin were closed using 4-0 vicryl suture (Ethicon, Somerville NJ) and wound clips, respectively. While the collagen sponge was pressed fit in the defect space, for the rest of the groups the PCL scaffold was first fitted over the ends of the femur, followed by injection of the hydrogel. For all experiments, 14-week-old female RNU Nude rats (Charles River Laboratories, Wilmington MA) were used. A total of 15 rats were used, which allowed for 30 total bone defects (bilateral femurs). The sample sizes for each group were as follows: GAG+MSC (n=7), GAG+BMP-2 MSC (n=7), GAG+rhBMP-2 (n=8), Col+rhBMP-2 (n=8).

Radiography and microcomputed tomography

To qualitatively assess longitudinal bone regeneration, 2D in vivo radiographs were taken using the MX-20 digital machine (Faxitron X-ray Corp, Tucson AZ) at 2, 4, 8, and 12 weeks post-surgery. Radiographs were acquired using an exposure time of 15

seconds and energy at 25 kV. Bridging scores were assigned to each radiograph by two blinded investigators where bridging was defined as contiguous bone spanning the entire defect space (connecting at least one cortex from each bone end). In instances of disagreement, a third blinded investigator served as tiebreaker.

New bone formation was quantitatively evaluated using 3D microcomputed tomography (μCT) at 12 weeks post-surgery. Scans were performed using the vivaCT40 (Scanco Medical, Brüttisellen Switzerland). Ex vivo scans were performed at a 21 μm voxel size, 55 kVp voltage, and a 145 μA current. The volume of interest (VOI) consisted of the central 6.36 mm (303 slices) of the defect. A threshold corresponding to 50% of native cortical bone density was applied to segment bone mineral [40].

Mechanical testing

Torsional testing to failure was performed as previously described [39]. Animals were euthanized by CO_2 inhalation at 12 weeks post-surgery. Femurs were then excised, wrapped in PBS-soaked gauze, and stored at -20°C until testing could be performed. On the day of testing, samples were thawed in a beaker of tap water, the surrounding soft tissues were excised, and the fixation plate was removed so that the native bone ends could be potted in Wood's metal (Alfa Aesar, Haverhill MA). Potted femurs were then rotated at a rate of 3 degrees per second until failure using the EnduraTEC ELF3200 axial/torsion testing system (Bose, Framingham MA). Failure strength was determined by locating the failure (peak) torque within the first 60° of rotation. Torsional stiffness was calculated by finding the slope of the linear region before failure in the torque-rotation plot.

Statistical Analysis

Unless otherwise noted, all data were analyzed via nonparametric Kruskal-Wallis test with multiple comparisons made by Dunn's post-tests as appropriate using GraphPad Prism software. Significance was determined as $p < 0.05$.

2.4 RESULTS

MSC transduction

Fluorescence microscopy of pr-EF1a-RFP lentivirus transduced uMSCs qualitatively showed transduction efficiency at 24, 48, and 72 hours post-transduction. Visual transduction efficiency approached 100% at 10 and 50 MOI (Fig. 1A). BMP-2 ELISA of media collected from pr-EF1a-BMP2 lentivirus transduced MSCs at 48, 72, 96, and 120 hours post-transduction assessed rhBMP-2 production in both uMSCs and bmMSCs at 10 and 50 MOI (Fig. 1B). Non-transduced MSCs expressed BMP-2 below the detection threshold of the ELISA kit used and are not shown. All transductions resulted in greater amounts of rhBMP-2 released over time. By 96 and 120 hours post-transduction, significantly more BMP-2/cell was produced at both 10 and 50 MOI in uMSC than bmMSC. However, there was no significant difference between 10 and 50 MOI for either cell type.

CS hydrogel characterization

The 3% CS hydrogels were transparent and porous (Fig. 2A), with pores ranging between 20-100 μm in diameter. The hydrogel storage modulus ranged between 350 and 450 Pa, increased at higher frequencies indicating strain hardening, and demonstrated nonlinear elasticity that is typical of biological materials (Fig. 2B) (6). Measurement of dynamic viscosity indicated a decrease in viscosity with increasing shear rate, reflecting shear-thinning and pseudoplastic material properties that are

characteristic of shear rate dependent breakage of interchain linkages in hydrogels (Fig 2C). The shear stress versus shear rate plot indicates a dependence of shear stress on shear rate, especially at higher shear rate values suggesting that the hydrogel exhibits partially viscoplastic properties (Fig 2D).

Transduced MSC Viability and Distribution in CS hydrogels

Viable transduced MSCs were identified via colocalization of RFP and Calcein AM. Seeded MSCs were distributed homogeneously, and showed colocalization of RFP and Calcein in the cytoplasm. Ejection from the syringe had no effect on the viability of MSCs encapsulated within the gel (data not shown). Mean values and standard error of Pearson's Correlation and Colocalization Coefficients M1 and M2 were 0.88± 0.01, 0.94 ± 0.01, and 0.85 ± 0.02, respectively, indicating approximately 85-88% viability in seeded cells (Fig 3B).

Quantification of BMP-2 release

BMP-2 MSC in GAG hydrogel secreted over 7 µg of BMP-2 cumulatively over the course of 16 days *in vitro*, which was over 1000x higher than the release from non-transduced MSCs in GAG in the same time period (Fig. 3C). Furthermore, comparison of the release kinetics to exogenous delivery of rhBMP-2 revealed that Col+rhBMP-2 had the highest initial burst release of BMP-2, followed by GAG+rhBMP-2, and GAG+BMP-2 MSC having the slowest BMP-2 release profile (Fig. 3D). The time taken to release 50% of the total BMP-2, was approximately Day 1.5, Day 5, and Day 9 for Col+rhBMP-2, GAG+rhBMP-2, and GAG+BMP-2 MSC, respectively.

Bone defect bridging

Radiographs qualitatively showed progressive mineralization from 4 to 12 weeks in the GAG+BMP-2 MSC, GAG+rhBMP-2, and Col+rhBMP-2 groups (Fig. 4B). Defect bridging was determined from the radiographs after 12 weeks, and the bridging scores for each group were 0/7 for GAG+MSC, 4/7 for GAG+BMP-2 MSC, 6/8 for GAG+rhBMP-2, and 7/8 for Col+rhBMP-2. These two-dimensional assessments of defect bridging were verified using three-dimensional μCT reconstructions as well (Fig. 4C).

Bone formation quantification

μCT analysis showed mean total bone volumes of 2.81, 42.91, 44.52 and 39.70 mm^3, respectively, in the GAG+MSC, GAG+BMP-2 MSC, GAG+rhBMP-2, and Col+rhBMP-2 groups at 12 weeks (Fig. 5A). Bone volumes in the GAG+MSC group were significantly lower than that of the other three groups. There were no significant differences in bone volume among GAG+BMP-2 MSC, GAG+rhBMP-2, and Col+rhBMP-2. Interestingly, when polar moment of inertia (pMOI) was calculated to assess the spatial distribution of the newly formed bone (Fig. 5B), both GAG+BMP-2 MSC and GAG+rhBMP-2 groups had significantly higher average pMOI compared to GAG+MSC, while Col+rhBMP-2 did not.

Biomechanical testing

The mean failure torques were 0.0066, 0.1250, 0.1465 and 0.1774 N-m, respectively, in the GAG+MSC, GAG+BMP-2 MSC, GAG+rhBMP-2, and Col+rhBMP-2 groups at 12 weeks (Fig. 5C). The mean torsional stiffnesses were 0.00009, 0.0149, 0.0159 and 0.0197 N-m/deg, respectively, in the GAG+MSC, GAG+BMP-2 MSC, GAG+rhBMP-2, and Col+rhBMP-2 groups (Fig. 5D). For both parameters, only the

GAG+rhBMP-2 and Col+rhBMP-2 groups had significantly higher values compared to GAG+MSC. However, there were no significant differences among GAG+BMP-2 MSC, GAG+rhBMP-2, and Col+rhBMP-2 groups.

Histology

H&E staining demonstrated clear morphological differences between the three BMP-2 groups and the GAG+MSC group (Fig. 6A). In the GAG+MSC samples, there was very little new bone formation and instead, the defect was filled with mostly soft, fibrous-like tissue with extensive cell infiltrate. In contrast, the GAG+BMP-2 MSC, GAG+rhBMP-2, and Col+rhBMP-2 groups all showed distinct islands of new bone formation that were surrounded by marrow-like material. In the Col+rhBMP-2 group in particular, this marrow-like material appeared less dense and much more disperse. When viewed under polarized light (Fig. 6B), the collagen of the new bone in the Col+rhBMP-2 group appeared much more aligned (bright pink), indicative of lamellar structure, whereas the new bone in both GAG+BMP-2 MSC and GAG+rhBMP-2 groups had more disorganized collagen, suggestive of woven bone morphology.

2.5 DISCUSSION

The complex milieu of cells, soluble factors and extracellular matrix at the bone defect site is largely unexplored. However, treatment with substantial doses of rhBMP-2 at orthotopic sites can lead to robust bone healing. Given the complications that can arise from high dose bolus rhBMP-2 treatment, alternative controlled delivery strategies have been sought, comprising cell and gene-based therapies within biomaterial carriers. Indeed rhBMP-2 genetically-engineered MSCs have been shown to promote bone regeneration in a rat calvarial bone defect [41] and in mandible distraction surgery in dogs

[42]. In previous studies, polymer scaffolds coated with adeno-associated viral vector encoding rhBMP-2 successfully bridged about 50% of rat femoral defects at 12 weeks without ectopic bone formation [43], and low dose sustained rhBMP-2 expression was achieved by PEG-encapsulated rhBMP-2 expressing MSCs [23]. In the latter case, the use of a CS-GAG hydrogel could present additional advantages with sulfated CS-GAGs promoting rhBMP-2 stabilization as demonstrated previously [32], and as discussed in our findings here.

In this study, we compared the collagen sponge clinical standard to CS-GAG as a delivery vehicle for recombinant human BMP-2 (rhBMP-2) and rhBMP-2 expression via rhBMP-2 gene inserted into mesenchymal stem cells (BMP-2 MSC). Since the lentiviral system is able to integrate into the host cell genome, MSCs were transduced with a lentiviral vector to express high levels of rhBMP-2, with MSCs sourced from umbilical tissue expressing at a higher level than those from bone marrow. The uMSCs were therefore used in the subsequent experiments. Most previous studies have used bone marrow MSCs, but Mizrahi et al showed similar efficiency of BMP overexpression between bone and adipose-derived MSCs [18,44-46]. However, given that this study only used one donor from each cell type, any differences seen here should be attributed to differences between cell lines, rather than tissue sources. Alternatively, uMSCs have a higher proliferative potential than bmMSCs, together with differences in gene expression and secretome and a more optimal tissue source for BMP-2 overexpression[47]. Compared to previous studies using adenovirus or nucleofection, lentiviral transduction induced a higher expression of BMP, and greater bone formation *in vivo* [23,48,49]. Our comparisons between adeno- and lentiviral transduction within the

same MSC population (not shown) corroborate these findings, prompting us to implant far fewer cells (only 1 million BMP-2 MSCs per defect) than similar studies.

The characterization of the *in vitro* rhBMP-2 release profiles permitted greater insights into the potential differences in bone regeneration *in vivo*. Of the three rhBMP-2 treatment groups tested (GAG+BMP-2 MSC, GAG+rhBMP-2, and Col+rhBMP-2), Col+rhBMP-2 demonstrated the fastest initial burst release while GAG+BMP-2 MSC exhibited the slowest, most sustained release. We expect the CS-GAG to be degraded over the course of two weeks, while the collagen sponge will persist for longer [36]. However, given the very short half-life of BMP-2 in vivo, we expect that this shorter degradation time for CS-GAG will not have much bearing on the release of active BMP-2 [50]. These *in vitro* observations were partially reflected in the spatial distribution of newly formed bone *in vivo,* as the GAG+BMP-2 MSC group had the highest average pMOI, indicative of bone formation that is more disperse and peripheral. These results are in-line with findings from other groups, which have shown that the timing of rhBMP-2 expression/release greatly influences the distribution and quality of new bone formation. In particular, Koh et al. demonstrated that using a rapamycin-inducible system to generate more sustained rhBMP-2 release from delivered fibroblasts results in better mineralization compared to uncontrolled constitutive expression of rhBMP-2 [51]. Furthermore, histological characterization in our study revealed that the new bone formed in the Col+rhBMP-2 group had a lamellar-like structure, indicative of mature bone. This may suggest that the bone observed in the histological sections from the other two rhBMP-2 groups (GAG+BMP-2 MSC and GAG+rhBMP-2) had been deposited more recently and was possibly still actively (re)modeling at the 12-week time

point. Interestingly, these observed differences in bone maturity and spatial distribution did not translate into functional differences between the three groups, in terms of the mechanical strength and stiffness of the regenerated femurs. A longer-term study may enable newly formed bone in all groups to progress to a similar stage of maturation and consequently result in quantifiable mechanical differences. Overall, these results suggest that GAG+BMP-2 MSC delivery remains a viable treatment strategy which is comparable to delivery of rhBMP-2 in collagen sponge in this pre-clinical model.

Although GAG+BMP-2 MSC did not perform significantly better than Col+rhBMP-2 in this study, it is still remarkable that sufficient rhBMP-2 was released to induce healing that was comparable to the 5 μg rhBMP-2 delivered on collagen sponge. The 5 μg dose was chosen because previous work from our group has demonstrated this to be the optimal healing dose in this rat segmental defect model [52]. However, we should acknowledge that this level of dosing is not reflective of clinical doses, which is often orders of magnitude higher (even after accounting for dose per weight) [53]. The cell suspension is capable of producing up to 7 ug BMP-2 over 16 days in culture (Fig. 3C) but this is assuming that all cells survive implantation. In vivo release of BMP-2 by these cells is an unknown. Recent work has shown that using higher doses of rhBMP-2 on collagen sponge in this model results in substantial ectopic bone formation [54], recapitulating one of the main adverse events associated with high dose rhBMP-2 use clinically. It remains to be seen whether this GAG gel system, which we demonstrated here to exhibit more sustained release compared to collagen sponge, would perform better at higher, more clinically-relevant doses of rhBMP-2.

These results add to a growing body of evidence concerning the importance of CS-GAG to bone formation and BMP-2 signaling. While there has been some disagreement on the role of glycosaminoglycans in BMP-2 release, the sustained BMP-2 release profile from CS-GAG as compared to collagen may be explained by CS-GAG sulfation [55,56]. Wang et al. found that CS-modified collagen scaffolds were more hydrophilic and had greater surface energy than their unmodified counterparts, which they postulated contributed to higher initial release of rhBMP-2 in the first 8 hours [57]. This contrasts somewhat with the *in vitro* release we observed but may indicate that sulfated GAGs play a role in rhBMP-2 stabilization. The importance of GAG sulfation is further reinforced by Hintze et al, who showed that CS with a higher degree of sulfation interacted with rhBMP-2 more strongly than their less sulfated counterparts for the same concentration [32], indicating that GAGs contributed to conformational and thermodynamic stabilization of rhBMP-2 and as a result, enhanced rhBMP-2 signaling. This enhanced rhBMP-2 stabilization and signaling could help explain the presence of woven bone in defects treated with either CS-GAG group in our study.

To our knowledge, this is the first study to investigate the suitability of CS-GAG hydrogels for rhBMP-2 delivery, and to mediate the regeneration of a critically-sized bone defect. Beyond the collagen scaffolds used clinically, there are a host of scaffold materials under development for BMP delivery [58]. Members of our group have previously demonstrated similar success in this same model with an alginate hydrogel [59]. In a study comparing rhBMP-2 delivery by chitosan and hyaluronic acid hydrogels, Luca et al showed greater bone formation by volume using hyaluronic acid, while the chitosan scaffold led to more mature bone [60]. While both materials are polysaccharides,

chitosan is positively charged and hyaluronic acid is negatively charged – likely influencing their interactions with the positively charged rhBMP-2. Of these materials, hyaluronic acid is the most chemically similar to CS-GAG, with one of its key differences being a lack of sulfation. In a study examining rhBMP-2 release kinetics from hyaluronic acid, 100% of the protein was eluted within 1 week from a relatively slowly degrading gel [61], which reinforces CS-GAG's advantages as scaffold for slow release of rhBMP-2.

Our *in vitro* results demonstrated that the GAG+BMP-2 MSC system resulted in slower release compared to Col+rhBMP-2. Future studies could assess cumulative release at higher rhBMP-2 doses and more importantly, whether sustained release at higher doses is actually beneficial. In addition, one of the main concerns associated with rhBMP-2 use clinically is a heightened and uncontrolled inflammatory response [12,62]. While this was not directly investigated in this study, MSC delivery may mitigate these risks, given MSCs have extensive immunomodulatory capabilities and can influence multiple immune cell types [63-66]. Future work exploring how MSC therapy may improve rhBMP-2-mediated bone healing by limiting adverse effects could be impactful for clinicians.

Finally, this GAG+BMP-2 MSC system could potentially be enhanced further through incorporation of cell-adhesive ligands. In the context of bone repair, the fibronectin motif RGD [34] and the collagen-mimetic peptide GFOGER [67] have been shown to be effective in promoting new bone formation. These studies have demonstrated that including cell adhesion ligands in the biomaterial scaffold can improve healing for both rhBMP-2 delivery as well as cell delivery approaches. Shekaran et al. showed that GFOGER delivered with a low dose of rhBMP-2 actually

increased recruitment of CD45-/CD90+ osteoprogenitor cells to a radial defect compared to collagen sponge with rhBMP-2 [68]. In addition, Moshaverinia et al. demonstrated that osteogenic differentiation of multiple types of MSCs was enhanced when the cells were encapsulated in RGD alginate microspheres compared to non-functionalized alginate [69]. For our study, we tested both rhBMP-2 and MSC delivery approaches with a non-functionalized GAG gel and observed comparable healing to collagen sponge with rhBMP-2. Based on these findings from other labs, it seems plausible that functionalizing our GAG gel with RGD or GFOGER in the future could potentially result in even better outcomes.

REFERENCES

1. Greenwald AS, Boden SD, Goldberg VM, et al. Bone-graft substitutes: facts, fictions, and applications. *J Bone Joint Surg Am.* 2001;83-A Suppl 2 Pt 2(0021-9355 (Print)):98-103.
2. Toolan BC. Current Concepts Review: Orthobiologics. *Foot and ankle international.* 2006;27(7).
3. De Long WG ET, Koval K. Current concepts review: Bone grafts and bone graft substitutes in orthopaedic trauma surgery. *Journal of Bone and Joint Surgery American Edition.* 2007;89:649-658.
4. Laurencin C, Khan Y, El-Amin SF. Bone graft substitutes. *Expert Rev Med Devices.* 2006;3(1):49-57.
5. Desai BM. Osteobiologics. *Am J Orthop (Belle Mead NJ).* 2007;36(4 Suppl):8-11.
6. Rahman MS, Akhtar N, Jamil HM, Banik RS, Asaduzzaman SM. TGF-beta/BMP signaling and other molecular events: regulation of osteoblastogenesis and bone formation. *Bone Res.* 2015;3:15005.

7. Balboni AL, Hutchinson JA, DeCastro AJ, et al. ΔNp63α-Mediated Activation of Bone Morphogenetic Protein Signaling Governs Stem Cell Activity and Plasticity in Normal and Malignant Mammary Epithelial Cells. *Cancer Research.* 2013;73:1020-1030.

8. Govender S CC, Genant HK, Valentin-Opran A, Amit Y, Arbel R, Aro H, Atar D, Bishay M, Borner MG, Chiron P, Choong P, Cinats J, Courtenay B, Feibel R, Geulette B, Gravel C, Haas N, Raschke M, Hammacher E, van der Velde D, Hardy P, Holt M, Josten C, Ketterl RL, Lindeque B, Lob G, Mathevon H, McCoy G, Marsh D, Miller R, Munting E, Oevre S, Nordsletten L, Patel A, Pohl A, Rennie W, Reynders P, Rommens PM, Rondia J, Rossouw WC, Daneel PJ, Ruff S, Ruter A, Santavirta S, Schildhauer TA, Gekle C, Schnettler R, Segal D, Seiler H, Snowdowne RB, Stapert J, Taglang G, Verdonk R, Vogels L, Weckbach A, Wentzensen A, Wisniewski T. Recombinant human bone morphogenetic protein-2 for treatment of open tibial fractures: a prospective, controlled, randomized study of four hundred and fifty patients. *Journal of Bone and Joint Surgery American Edition.* 2002;84:2123-2134.

9. D. Gothard ELS, J.M. Kanczler, H. Rashidi, O. Qutachi, J. Henstock, M. Rotherham, A. El Haj, K.M. Shakesheff, R.O.C. Oreffo. Tissue engineered bone using select growth factors: A comprehensive review of animal studies and clinical translation studies in man. *European Cells and Materials.* 2014;28:166-208.

10. Jones AL BR, Bosse MJ, Mirza SK, Lyon TR, Webb LX, Pollak AN, Golden JD, Valentin-Opran A. Recombinant human BMP-2 and allograft compared with autogenous bone graft for reconstruction of diaphyseal tibial fractures with cortical defects. *Journal of Bone and Joint Surgery American Edition.* 2006;88:1431-1441.

11. Zhao B KT, Toyoda H, Takada T, Yanai T, Fukuda T, Chung UI, Koike T, Takaoka K, Kamijo R. Heparin potentiates the in vivo ectopic bone formation induced by bone morphogenetic protein-2. *J Biol Chem.* 2006;281(32):23246-23253.

12. Tannoury CA, An HS. Complications with the use of bone morphogenetic protein 2 (BMP-2) in spine surgery. *Spine J.* 2014;14(3):552-559.

13. Valdes MA, Thakur NA, Namdari S, Ciombor DM, Palumbo M. Recombinant bone morphogenic protein-2 in orthopaedic surgery: a review. *Arch Orthop Trauma Surg.* 2009;129(12):1651-1657.

14. Daniel S. Mulconrey M, Keith H. Bridwell, MD, Jennifer Flynn, BS, Geoffrey A. Cronen, MD, and Peter S. Rose, MD. Bone Morphogenetic Protein (RhBMP-2) as a Substitute for Iliac Crest Bone Graft in Multilevel Adult Spinal Deformity Surgery. *Spine J.* 2008;33(20):2153-2159.

15. Zara JN, Siu RK, Zhang X, et al. High doses of bone morphogenetic protein 2 induce structurally abnormal bone and inflammation in vivo. *Tissue engineering Part A.* 2011;17(9-10):1389-1399.

16. K. D. Riew NMW, S.-L. Cheng, L. V. Avioli, J. Lou. Induction of Bone Formation Using a Recombinant Adenoviral Vector Carrying the Human BMP-2 Gene in a Rabbit Spinal Fusion Model. *Calcified Tissue International.* 1998;63:357-360.

17. Jay Lieberman AD, Sharon Stevenson, Lily Wu, Paula McAllister, Yu Po Lee, Michael Kabo, Gerald Finerman, Arnold Berk, Owen Wite. The effect of regional gene therapy with bone morphogenetic protein-2-producing bone-marrow cells on the repair of segmental femoral defects in rats. *Journal of Bone and Joint Surgery.* 1999;81-A(7).

18. S-L Cheng JL, N. M. Wright, C.-F. Lai, L. V. Avioli, K. D. Riew. In Vitro and In Vivo Induction of Bone Formation Using a Recombinant Adenoviral Vector Carrying the Human BMP-2 Gene. *Calcified Tissue International.* 2001;68:87-94.

19. Hiroyuki Tsuchida JH, Eric Crawford, Paul Manske, Jueren Lou. Engineered allogeneic mesenchymal stem cells repair femoral segmental defect in rats. *Journal of Orthopaedic Research.* 2003;21:44-53.

20. Campana V, Milano G, Pagano E, et al. Bone substitutes in orthopaedic surgery: from basic science to clinical practice. *J Mater Sci Mater Med.* 2014;25(10):2445-2461.

21. Buttner M, Moller S, Keller M, et al. Over-sulfated chondroitin sulfate derivatives induce osteogenic differentiation of hMSC independent of BMP-2 and TGF-beta1 signalling. *J Cell Physiol.* 2013;228(2):330-340.

22. Mumaw J, Jordan ET, Sonnet C, et al. Rapid Heterotrophic Ossification with Cryopreserved Poly(ethylene glycol-) Microencapsulated BMP2-Expressing MSCs. *International journal of biomaterials.* 2012;2012:861794.

23. Sonnet C, Simpson CL, Olabisi RM, et al. Rapid healing of femoral defects in rats with low dose sustained BMP2 expression from PEGDA hydrogel microspheres. *J Orthop Res.* 2013;31(10):1597-1604.

24. Nuttelman CR, Tripodi MC, Anseth KS. Synthetic hydrogel niches that promote hMSC viability. *Matrix Biol.* 2005;24(3):208-218.

25. Lutolf MP, Lauer-Fields JL, Schmoekel HG, et al. Synthetic matrix metalloproteinase-sensitive hydrogels for the conduction of tissue regeneration: engineering cell-invasion characteristics. *Proc Natl Acad Sci U S A.* 2003;100(9):5413-5418.

26. Olabisi RM. Cell microencapsulation with synthetic polymers. *Journal of Biomedical Materials Research Part a.* 2015;103(2):846-859.

27. Salbach-Hirsch J, Ziegler N, Thiele S, et al. Sulfated glycosaminoglycans support osteoblast functions and concurrently suppress osteoclasts. *J Cell Biochem.* 2014;115(6):1101-1111.

28. Koike T, Izumikawa T, Tamura J, Kitagawa H. Chondroitin sulfate-E fine-tunes osteoblast differentiation via ERK1/2, Smad3 and Smad1/5/8 signaling by binding to N-cadherin and cadherin-11. *Biochem Biophys Res Commun.* 2012;420(3):523-529.

29. Gualeni B, de Vernejoul MC, Marty-Morieux C, et al. Alteration of proteoglycan sulfation affects bone growth and remodeling. *Bone.* 2013;54(1):83-91.

30. Cortes M, Baria AT, Schwartz NB. Sulfation of chondroitin sulfate proteoglycans is necessary for proper Indian hedgehog signaling in the developing growth plate. *Development.* 2009;136(10):1697-1706.

31. Lim JJ, Temenoff JS. The effect of desulfation of chondroitin sulfate on interactions with positively charged growth factors and upregulation of cartilaginous markers in encapsulated MSCs. *Biomaterials.* 2013;34(21):5007-5018.

32. Hintze V, Samsonov SA, Anselmi M, et al. Sulfated Glycosaminoglycans Exploit the Conformational Plasticity of Bone Morphogenetic Protein-2 (BMP-2) and Alter the Interaction Profile with Its Receptor. *Biomacromolecules.* 2014;15(8):3083-3092.

33. Miyazaki T, Miyauchi S, Tawada A, Anada T, Matsuzaka S, Suzuki O. Oversulfated chondroitin sulfate-E binds to BMP-4 and enhances osteoblast differentiation. *Journal of Cellular Physiology.* 2008;217(3):769-777.

34. Kolambkar YM, Dupont KM, Boerckel JD, et al. An alginate-based hybrid system for growth factor delivery in the functional repair of large bone defects. *Biomaterials.* 2011;32(1):65-74.

35. Hass R, Kasper C, Böhm S, Jacobs R. Different populations and sources of human mesenchymal stem cells (MSC): A comparison of adult and neonatal tissue-derived MSC. *Cell Communication and Signaling : CCS.* 2011;9:12-12.

36. Karumbaiah L, Enam SF, Brown AC, et al. Chondroitin Sulfate Glycosaminoglycan Hydrogels Create Endogenous Niches for Neural Stem Cells. *Bioconjug Chem.* 2015;26(12):2336-2349.

37. Logun MT, Bisel NS, Tanasse EA, et al. Glioma Cell Invasion is Significantly Enhanced in Composite Hydrogel Matrices Composed of Chondroitin 4- and 4,6-Sulfated Glycosaminoglycans. *Journal of materials chemistry B.* 2016;4(36):6052-6064.

38. Boerckel JD, Kolambkar YM, Dupont KM, et al. Effects of protein dose and delivery system on BMP-mediated bone regeneration. *Biomaterials.* 2011;32(22):5241-5251.

39. Oest ME, Dupont KM, Kong HJ, Mooney DJ, Guldberg RE. Quantitative assessment of scaffold and growth factor-mediated repair of critically sized bone defects. *J Orthop Res.* 2007;25(7):941-950.

40. Duvall CL, Taylor WR, Weiss D, Wojtowicz AM, Guldberg RE. Impaired angiogenesis, early callus formation, and late stage remodeling in fracture healing of osteopontin-deficient mice. *J Bone Miner Res.* 2007;22(2):286-297.

41. He X, Dziak R, Yuan X, et al. BMP2 genetically engineered MSCs and EPCs promote vascularized bone regeneration in rat critical-sized calvarial bone defects. *PLoS One.* 2013;8(4):e60473.

42. Castro-Govea Y, Cervantes-Kardasch VH, Borrego-Soto G, et al. Human bone morphogenetic protein 2-transduced mesenchymal stem cells improve bone regeneration in a model of mandible distraction surgery. *J Craniofac Surg.* 2012;23(2):392-396.

43. Dupont KM, Boerckel JD, Stevens HY, et al. Synthetic scaffold coating with adeno-associated virus encoding BMP2 to promote endogenous bone repair. *Cell Tissue Res.* 2012;347(3):575-588.

44. Mizrahi O, Sheyn D, Tawackoli W, et al. BMP-6 is more efficient in bone formation than BMP-2 when overexpressed in mesenchymal stem cells. *Gene Ther.* 2013;20(4):370-377.

45. Lieberman JR DA, Stevenson S, Wu L, McAllister P, Lee YP, Kabo JM, Finerman GAM, Berk A, Witte ON. The effect of regional gene therapy with bone morphogenetic protein-2-producing bone-marrow cells on the repair of segmental femoral defects in rats. *Journal of Bone and Joint Surgery.* 1999;81(7):905.

46. Chang SC, Chung HY, Tai CL, Chen PK, Lin TM, Jeng LB. Repair of large cranial defects by hBMP-2 expressing bone marrow stromal cells: comparison between alginate and collagen type I systems. *J Biomed Mater Res A.* 2010;94(2):433-441.

47. Arutyunyan I, Elchaninov A, Makarov A, Fatkhudinov T. Umbilical Cord as Prospective Source for Mesenchymal Stem Cell-Based Therapy. *Stem Cells Int.* 2016;2016:6901286.

48. Pelled G, Sheyn D, Tawackoli W, et al. BMP6-Engineered MSCs Induce Vertebral Bone Repair in a Pig Model: A Pilot Study. *Stem Cells Int.* 2016;2016:6530624.

49. Miyazaki T, Miyauchi S, Tawada A, Anada T, Matsuzaka S, Suzuki O. Oversulfated chondroitin sulfate-E binds to BMP-4 and enhances osteoblast differentiation. *J Cell Physiol.* 2008;217(3):769-777.

50. Zhao B, Katagiri T Fau - Toyoda H, Toyoda H Fau - Takada T, et al. Heparin potentiates the in vivo ectopic bone formation induced by bone morphogenetic protein-2. 2006(0021-9258 (Print)).

51. Koh JT, Ge C, Zhao M, et al. Use of a stringent dimerizer-regulated gene expression system for controlled BMP2 delivery. *Mol Ther.* 2006;14(5):684-691.

52. Kolambkar YM, Boerckel JD, Dupont KM, et al. Spatiotemporal delivery of bone morphogenetic protein enhances functional repair of segmental bone defects. *Bone.* 2011;49(3):485-492.

53. Fu R, Selph S, McDonagh M, et al. Effectiveness and harms of recombinant human bone morphogenetic protein-2 in spine fusion: a systematic review and meta-analysis. *Ann Intern Med.* 2013;158(12):890-902.

54. Krishnan L, Priddy LB, Esancy C, et al. Delivery vehicle effects on bone regeneration and heterotopic ossification induced by high dose BMP-2. *Acta Biomater.* 2017;49:101-112.

55. Jiao X, Billings PC, O'Connell MP, Kaplan FS, Shore EM, Glaser DL. Heparan sulfate proteoglycans (HSPGs) modulate BMP2 osteogenic bioactivity in C2C12 cells. *J Biol Chem.* 2007;282(2):1080-1086.

56. Takada T, Katagiri T, Ifuku M, et al. *Sulfated polysaccharides enhance the biological activities of bone morphogenetic proteins.* Vol 2782003.

57. Wang Y, Zhang L, Hu M, Wen W, Xiao H, Niu Y. Effect of chondroitin sulfate modification on rhBMP-2 release kinetics from collagen delivery system. *J Biomed Mater Res A.* 2010;92(2):693-701.

58. Blackwood KA, Bock N, Dargaville TR, Ann Woodruff M. Scaffolds for Growth Factor Delivery as Applied to Bone Tissue Engineering. *International Journal of Polymer Science.* 2012;2012:1-25.

59. Krishnan L, Priddy LB, Esancy C, et al. Hydrogel-based Delivery of rhBMP-2 Improves Healing of Large Bone Defects Compared With Autograft. *Clin Orthop Relat Res.* 2015;473(9):2885-2897.

60. Luca L, Rougemont AL, Walpoth BH, Gurny R, Jordan O. The effects of carrier nature and pH on rhBMP-2-induced ectopic bone formation. *Journal of controlled release : official journal of the Controlled Release Society.* 2010;147(1):38-44.

61. Patterson J, Siew R, Herring SW, Lin AS, Guldberg R, Stayton PS. Hyaluronic acid hydrogels with controlled degradation properties for oriented bone regeneration. *Biomaterials.* 2010;31(26):6772-6781.

62. Ritting AW, Weber EW, Lee MC. Exaggerated inflammatory response and bony resorption from BMP-2 use in a pediatric forearm nonunion. *J Hand Surg Am.* 2012;37(2):316-321.

63. Chiesa S, Morbelli S, Morando S, et al. Mesenchymal stem cells impair in vivo T-cell priming by dendritic cells. *Proc Natl Acad Sci U S A.* 2011;108(42):17384-17389.

64. Corcione A, Benvenuto F, Ferretti E, et al. Human mesenchymal stem cells modulate B-cell functions. *Blood.* 2006;107(1):367-372.

65. English K. Mechanisms of mesenchymal stromal cell immunomodulation. *Immunol Cell Biol.* 2013;91(1):19-26.

66. Maggini J, Mirkin G, Bognanni I, et al. Mouse bone marrow-derived mesenchymal stromal cells turn activated macrophages into a regulatory-like profile. *PLoS One.* 2010;5(2):e9252.

67. Wojtowicz AM, Shekaran A, Oest ME, et al. Coating of biomaterial scaffolds with the collagen-mimetic peptide GFOGER for bone defect repair. *Biomaterials.* 2010;31(9):2574-2582.

68. Shekaran A, Garcia JR, Clark AY, et al. Bone regeneration using an alpha 2 beta 1 integrin-specific hydrogel as a BMP-2 delivery vehicle. *Biomaterials.* 2014;35(21):5453-5461.

69. Moshaverinia A, Chen C, Xu X, et al. Bone regeneration potential of stem cells derived from periodontal ligament or gingival tissue sources encapsulated in RGD-modified alginate scaffold. *Tissue engineering Part A.* 2014;20(3-4):611-621.

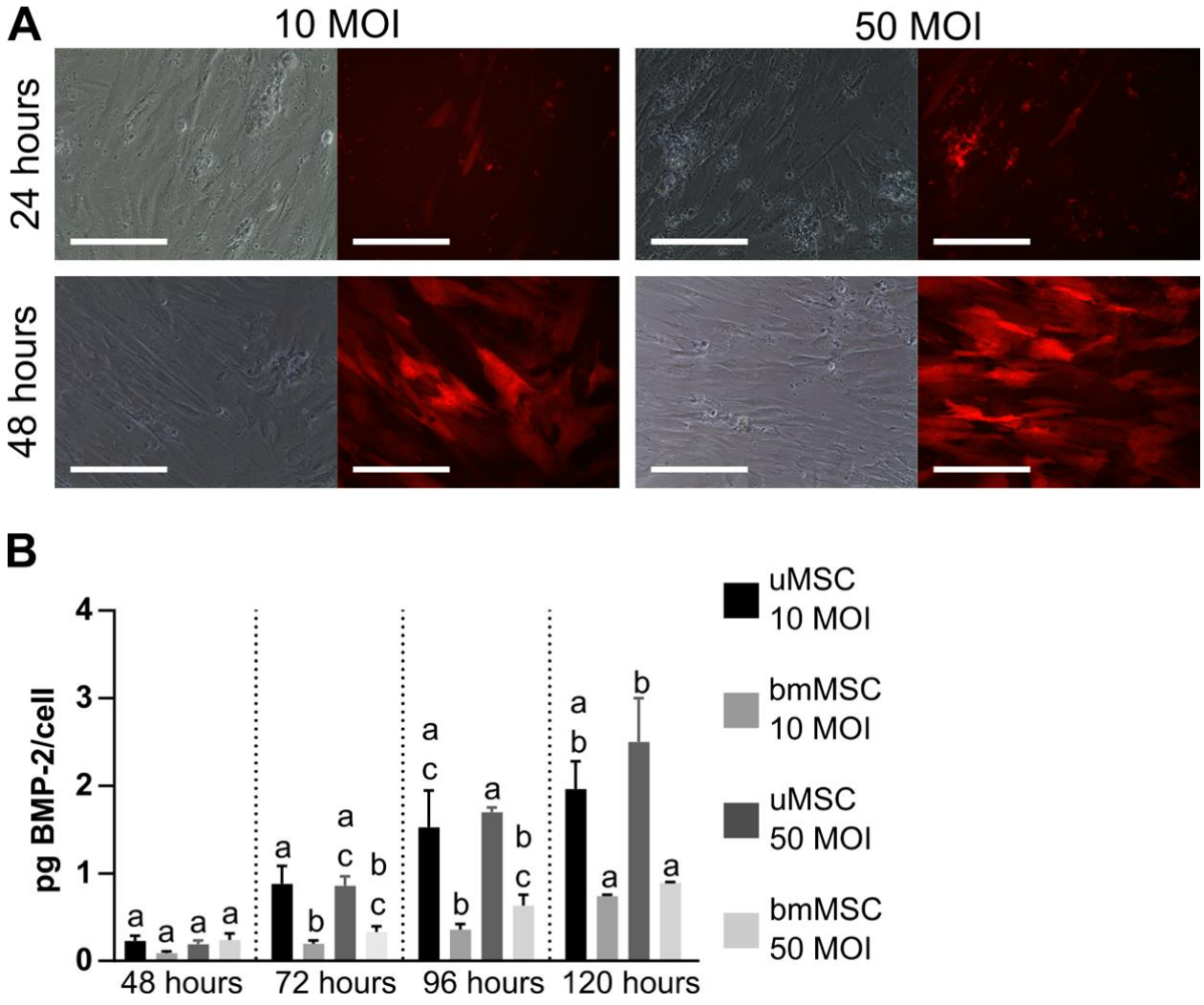

Figure 2.1: Efficient transduction of MSCs with a lentiviral vector at 10 MOI. (A) Images of uMSC over 72 hours after transducing with prEF1a-RFP at 10 and 50 MOI under phase contrast and RFP filter to evaluate transduction efficiency. Scale bars indicate 200 µm. N = 15. (B) Mean BMP-2 expression in uMSCs and bmMSCs at 48, 72, 96, and 120 hours after transducing with prEF1a-BMP2 at 10, and 50 MOI, comparing expression over cell type and MOI within each time point. Transductions at 0 MOI did not result in BMP-2 expression detectable by BMP-2 ELISA. Groups with differing letters are significantly different from each other within a timepoint at $p<0.05$. Error bars indicate standard error. Two-way ANOVA with Tukey's multiple comparison test (n=5-6).

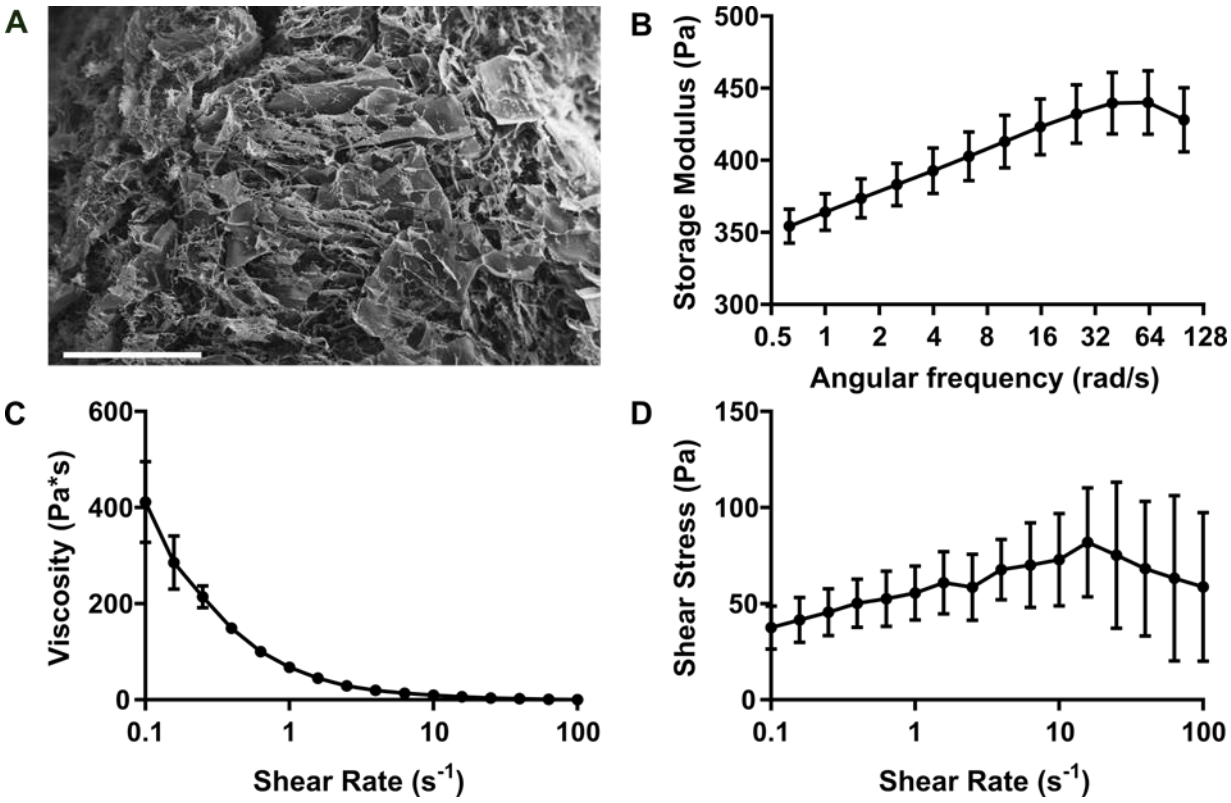

Figure 2.2: CS-GAG hydrogel is porous with stable rheology. (A) Scanning electron microscopy of CS gel surface at 165x magnification. Pore sizes are about 20-100 µm. Scale bar indicates 500 µm. (B) Rheology of CS-GAG gel. Data indicate stable rheological properties across a range of frequencies. Error bars indicate standard error (n=5).

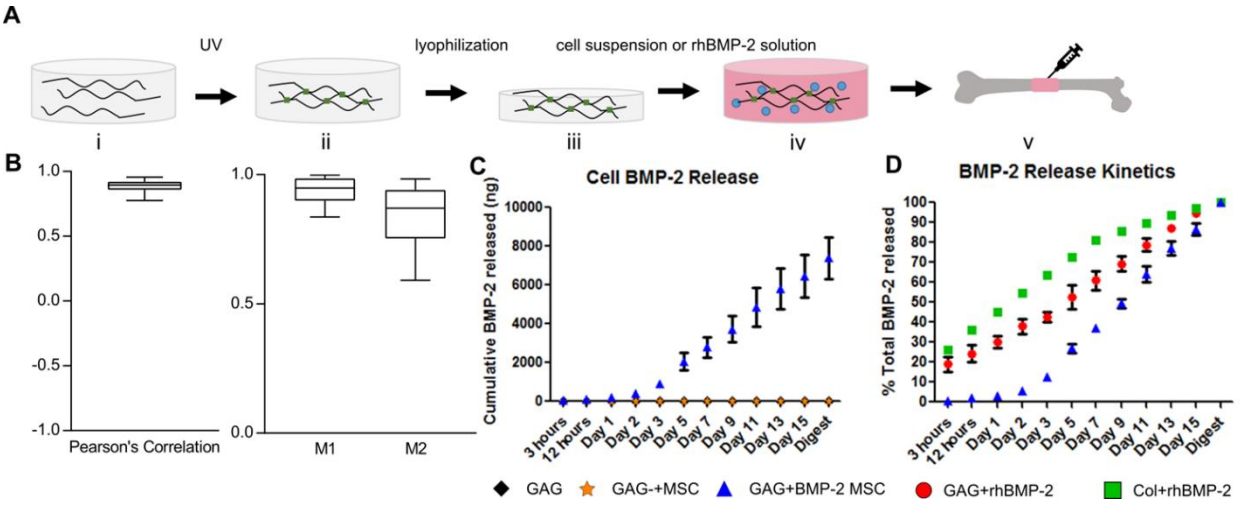

Figure 2.3: Preparation of CS-GAG hydrogel and interactions with transduced MSCs. (A) Casting of 3% GAG hydrogel (i) followed by photo crosslinking under UV light (ii). The hydrogel is lyophilized for 24 hours (iii) before it is rehydrated with a cell suspension in basal media (iv). (B) Measures of colocalization for calcein and RFP: Pearsons Correlation, describing the extent of overlap between RFP and calcein images, and Colocalization Coefficients M1/M2, describing the fraction of RFP colocalizing with calcein, and the fraction of calcein localizing with RFP, respectively (n=5). (C) Cumulative BMP-2 release over 15 days from empty GAG gels, GAG gels loaded with 1 million non-transduced MSCs, and GAG gels loaded with 1 million BMP-2 MSCs (n=3-4). (D) BMP-2 release kinetics shown as percentage of the total amount released for GAG gels loaded with BMP-2 MSCs, as well as GAG gels and collagen sponges loaded with rhBMP-2 (n=3-4).

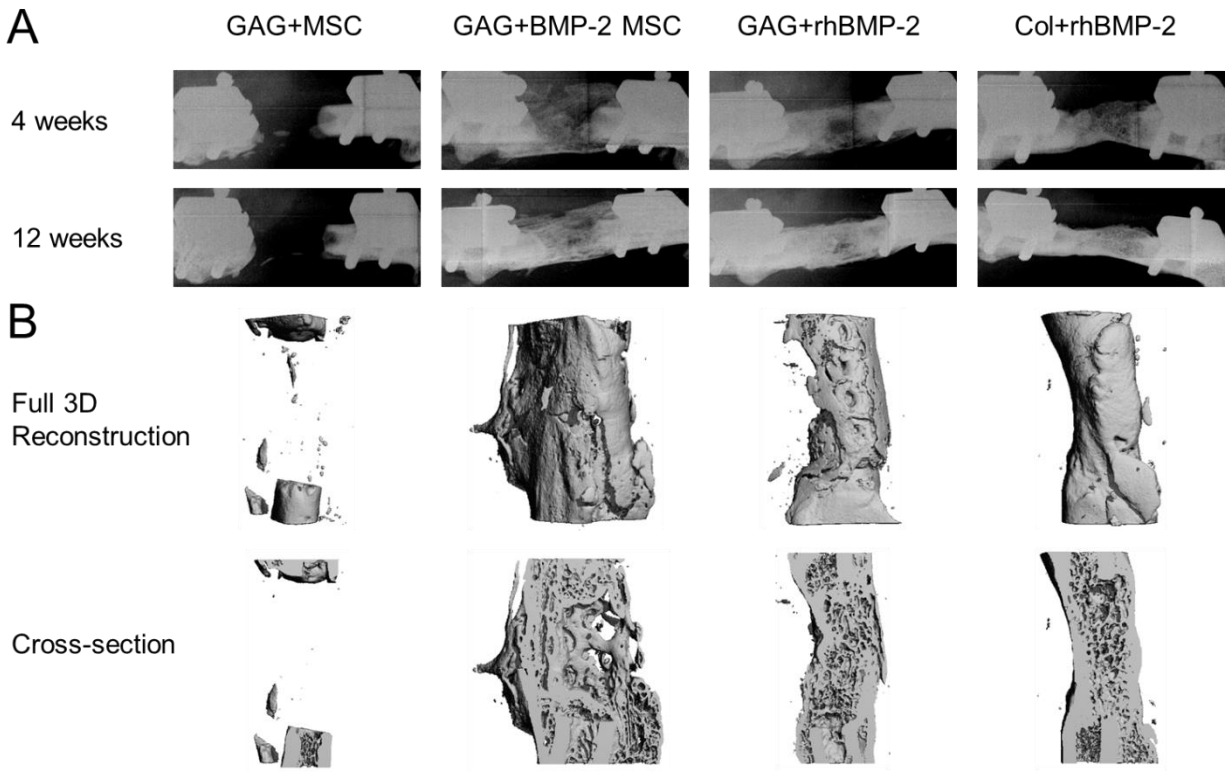

Figure 2.4: Defects bridge when treated with rhBMP-2 or BMP-2 MSCs. (A) Representative longitudinal radiographs at 4 and 12 weeks post-surgery. Defects were treated with 1 million non-transduced uMSCs in 150 µLCS-GAG gel, 1 million BMP-2 uMSCs in 150 µLCS-GAG gel, 150 µL CS-GAG hydrogel loaded with 5 µg rhBMP-2, or 150 µL collagen sponge loaded with 5 µg rhBMP-2. (B) 12-week µCT reconstructions of the same bone defects shown in the radiographs.

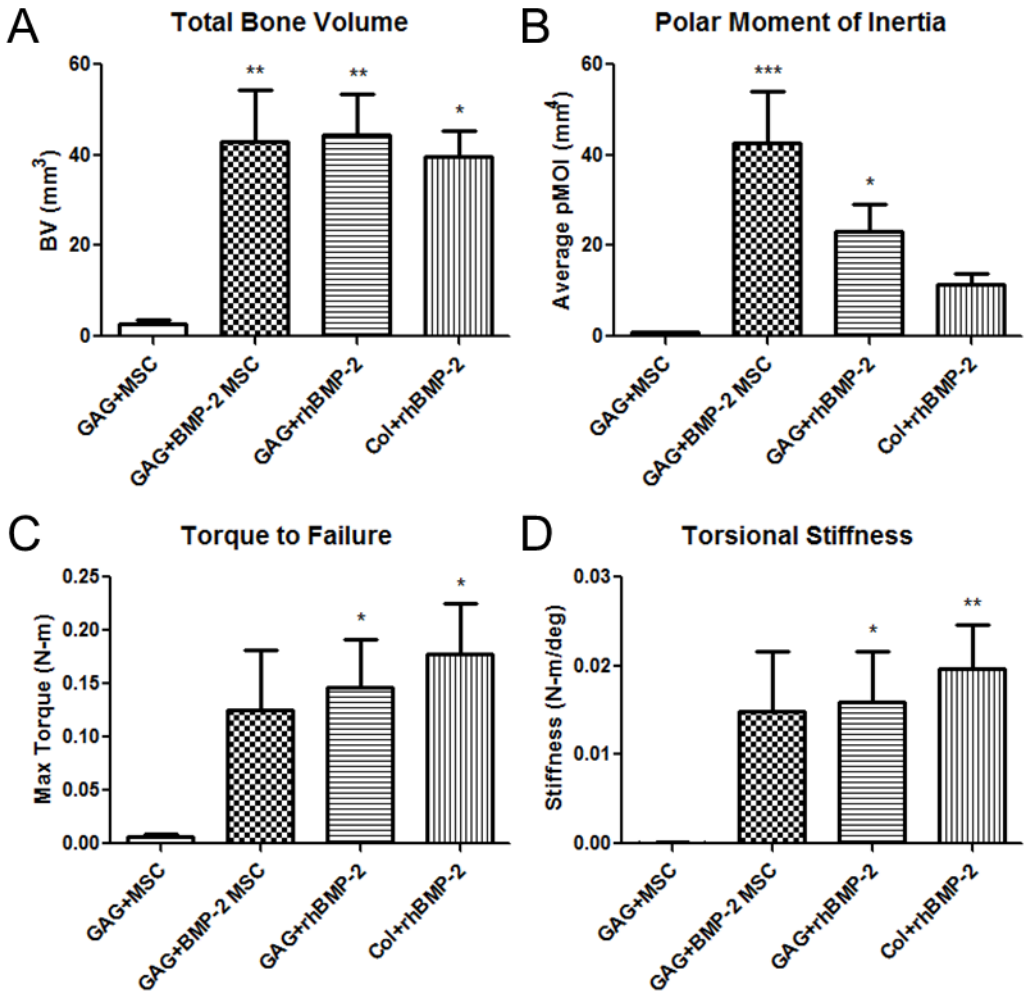

Figure 2.5: Newly formed bone similar between rhBMP-2 and BMP-2 MSC groups. µCT characterization and mechanical testing of regenerated femurs at 12 weeks. (A) Quantification of new bone revealed GAG+BMP-2 MSC, GAG+rhBMP-2, and Col+rhBMP-2 all demonstrated greater total bone volumes than GAG+MSC. (B) Calculated average polar moment of inertia (pMOI) showed both GAG+BMP-2 MSC and GAG+rhBMP-2 groups had significantly higher pMOI compared to GAG+MSC. (C) Torque to failure and (D) torsional stiffness measured from testing regenerated femurs to failure at 12 weeks. Both GAG+rhBMP-2 and Col+rhBMP-2 groups had significantly higher torque to failure and torsional stiffness compared to GAG+MSC. There were no

significant differences between GAG+BMP-2 MSC, GAG+rhBMP-2, and Col+rhBMP-2 for any of these metrics. Error bars indicate standard error (n=7-8/group). Nonparametric Kruskal-Wallis test with multiple comparisons made by Dunn's post-tests.

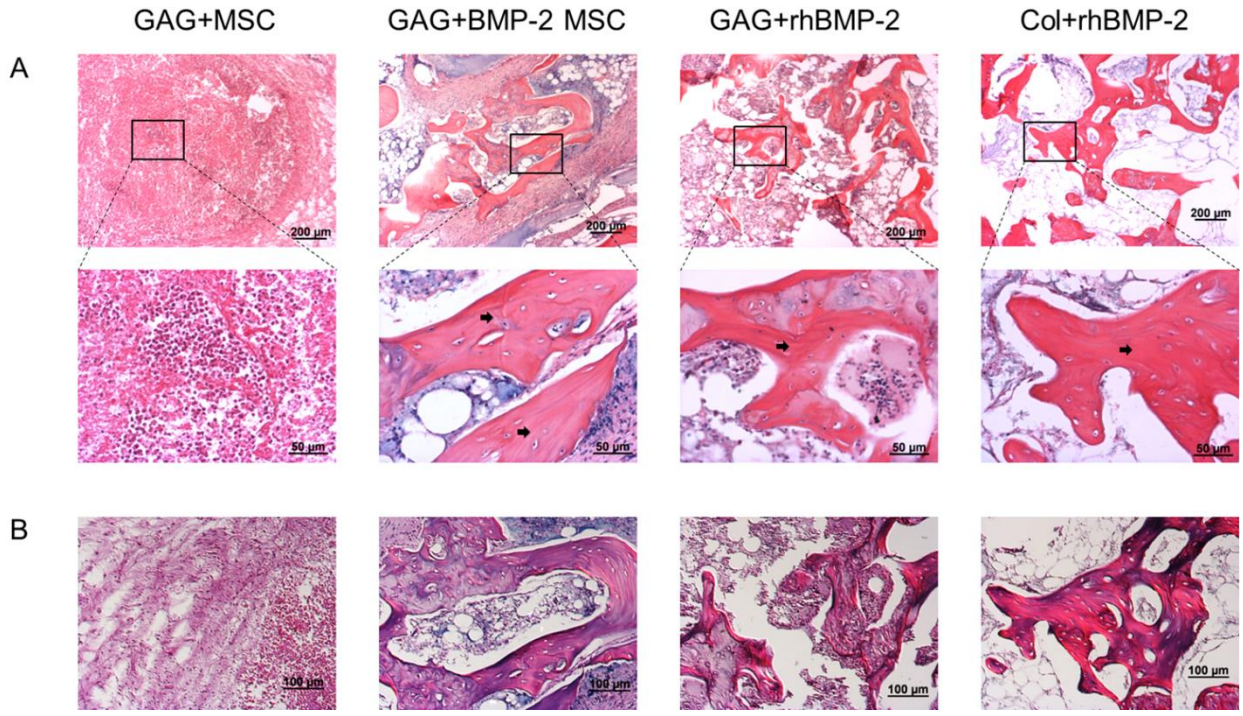

Figure 2.6: Histology reveals qualitative differences in bone maturity. Representative H&E images of defect tissue at 12 weeks post-surgery. (A) All BMP-2 groups exhibited islands of new bone formation while GAG+MSC did not. New bone is denoted by the black arrows in the higher magnification inset. (B) Furthermore, upon inspection under polarized light to assess collagen alignment, the bone in the Col+rhBMP-2 group appeared to be predominantly lamellar in structure whereas both GAG+BMP-2 MSC and GAG+rhBMP-2 had material resembling woven bone. All images were taken in the middle of the bone defect.

CHAPTER 3

OVEREXPRESSION OF BMP-2 IN MESENCHYMAL STEM CELLS WITH AMPLIFYING VIRUS-LIKE PARTICLES[2]

[2] Seth Andrews, Huiling Wei, Christina Elling, Biao He, Steve Stice. Accepted by the International Journal of Regenerative Medicine. Reprinted here with permission of publisher.

3.1 ABSTRACT

There are numerous strategies under development to supplement or replace bone grafts. Among these synthetic options, growth factors such as bone morphogenetic protein (BMP-2) are often used. However, current burst delivery strategies have been associated with a number of complications. Transplanting cells engineered to over-express osteoinductive proteins over a longer period of time is a possible solution to this problem. In this study, we demonstrated the use of a parainfluenza virus 5 (PIV-5) vector (amplifying virus-like particles, AVLP) to induce expression of exogenous proteins in mesenchymal stem cells (MSC). We obtained extended expression of enhanced green fluorescent protein eGFP in transduced MSCs, as well as selection and maintenance of eGFP+ cells. We also attained expression of BMP-2 on a shorter timescale using this method. We conclude that AVLP is a promising tool for genetic engineering, both in regenerative medicine and other applications.

3.2 INTRODUCTION

Bone tissue is well known for its remarkable healing abilities, but there are instances in which these mechanisms are not sufficient to bridge large defects or gaps naturally. Historically, bone grafts have been used to aid in bone regeneration when needed. Allografts and autografts are the most popular bone grafts used, accounting for over 2 million procedures per year (Giannoudis, Dinopoulos, & Tsiridis, 2005). Allografts, derived from other individuals of the same species, are potential sources of disease transmission and can fail to integrate with the host's existing bone (BC, 2006; Laurencin, Khan, & El-Amin, 2006). Autografts, which are derived from the patient themselves, are the current gold standard, but are the most difficult to obtain and have the risk of donor

site morbidity (BC, 2006; De Long WG, 2007). To overcome the challenges associated with allografts and autografts there have been numerous attempts to develop synthetic bone graft substitutes. One of the most widespread strategies in developing these substitutes is the incorporation of growth factors and cells that encourage bone formation (Campana et al., 2014; Gomez-Barrena et al., 2015).

Bone morphogenetic protein 2 (BMP-2) is an osteoinductive growth factor commonly used in bone substitute applications. The recombinant human protein (rhBMP-2) is FDA-approved and used clinically in combination with a collagen sponge for spinal fusions and tibial shaft fractures (McKay, Peckham, & Badura, 2007). BMP-2 has reduced the rate of secondary intervention and enhanced fracture healing in many orthopedic applications, including facial reconstruction, maxillary sinus floor augmentation, long bone non-unions, tibial fractures, and lumbar fusions (D. Gothard, 2014; Govender S, 2002). Despite its efficacy, rhBMP-2 has a very short half-life requiring a high dose for efficacy (Jones AL, 2006; Zhao B, 2006). Clinically relevant doses of BMP-2 in rats induced the formation of structurally abnormal bone as well as inflammation (Zara et al., 2011). In humans, this amount of BMP-2 has been associated with ectopic bone formation and increased cancer rates (Tannoury & An, 2014; Valdes, Thakur, Namdari, Ciombor, & Palumbo, 2009). Additionally, rhBMP-2 is often an expensive therapeutic option, costing upwards of $3500 per kit, of which several may be used per patient (Obremskey et al., 2007).

To reduce comorbidities and cost associated with BMP-2 treatment, numerous groups have investigated the transplantation of BMP-expressing cells as an alternative to this treatment (Jay Lieberman, 1999). Our group has demonstrated comparable bone

growth in a rat femoral defect model between the collagen sponge delivery method and mesenchymal stem cells (MSCs) transduced to overexpress BMP-2 using a lentiviral vector (Chapter 1). Despite BMP expression in lentiviral and adenoviral vector-transduced MSCs, technical drawbacks associated with these gene therapy delivery systems reduce the likelihood that this treatment option would advance to clinical use for bone regeneration (for review see (Waehler, Russell, & Curiel, 2007)). For example, commonly used techniques for lentiviral transduction inhibit proliferation of the transduced cells thus negating the possibility of subculture, while the vector's expense precludes transducing each new lot (Paul Lin, Correa, Lin, & Caplan, 2011; Milone & O'Doherty, 2018). Additionally, lentiviral vectors have been subject to a number of safety concerns regarding the possibility of off-target effects and oncogene activation (Williams & Thrasher, 2014). While adenoviral vectors do not have the safety issues associated with lentiviral ones, when applied to BMP-2 expression their protein yield is comparatively low (Mumaw et al., 2012; Sonnet et al., 2013). Therefore, a safer and lower-cost vector that allows for cell proliferation while inducing BMP-2 expression comparable to the lentiviral vector would make for a more viable therapy.

Parainfluenza virus 5 (PIV-5) is a paramyxovirus with negative-sense single stranded RNA (Yang et al., 2015). It is a 150-300 nm diameter spherical, enveloped virus 150-300 nm in diameter that is rarely pathogenic in immune-competent individuals despite infecting a wide variety of cells and species (Hsiung, 1972; McCandlish IA, 1978). Rather than integrating into the host genome, PIV-5 creates an RNA episome within the host cell's cytoplasm. Amplifying virus-like particles (AVLP) have been developed from PIV-5 by our group to express viral proteins in transduced cells (Chen et al., 2015; Huang,

Chen, Huang, Fu, & He, 2015; Li et al., 2013; Wei et al., 2017). This prior success indicates that AVLP may be able to find wider use as a viral vector.

Musculoskeletal gene therapy will benefit from more efficient vectors that generate fewer off target effects. We addressed this need by initially testing AVLP technology and determining whether an AVLP-BMP vector would induce comparable or greater BMP-2 expression in MSCs compared to other vectors, while allowing for selection and maintenance of BMP-2 overexpressing cells. We found that AVLP can be used to reliably express eGFP at high levels over time in MSCs, and can also be used to express BMP-2 over shorter periods of time.

3.3 METHODS

AVLP generation

Generation of amplifying virus-like particles (AVLP) from PIV5 was performed as described by Wei et al. (Wei et al., 2017). Briefly, a plasmid with the full-length genome of PIV-5 was used to construct the PIV5 AVLP vector (pAVLP) (Fig 1A). The AVLP vector contains the nucleoprotein, phosphoprotein, V protein, and L RNA-dependent RNA polymerase of PIV-5 (Fig. 1A). Genes for either eGFP or BMP-2 were inserted into pAVLP between the V/P and hygromycin genes, creating AVLP–eGFP or AVLP–BMP2.

Cell Culture and Transduction

Human umbilical MSCs (huMSC, Lifeline Cell Technology, Frederick MD, Sciencell, Carlsbad CA) were plated at 5000 cells/cm^2 on tissue culture flasks in complete medium and allowed to grow to 80-90% confluency (20,000–25,000 cells/cm^2) in 5% CO_2 at 37C. One day prior to infection with AVLP, the cells were removed from the plate using 0.05% Trypsin-EDTA (Gibco) then counted with a TC20 automated cell counter (Bio-Rad

Laboratories) using Trypan Blue according to the manufacturer's instructions. Viability of the cell population was determined as the fraction of cells unstained by Trypan Blue to the total number of cells. They were then plated at 26,000 cells/cm^2 in complete growth medium and incubated overnight at 37C and 5% CO2. Next, the cells were infected at 5 MOI with either AVLP-eGFP or AVLP-BMP2 in 0.25 mL of complete medium per cm^2 of growth area and incubated for 24 hours in 5% CO_2 at 37C. Finally, the infection medium was changed and replaced with fresh complete medium, after which the cells were used according to the particular experiment.

BMP-2 Expression

Conditioned culture medium was collected from separate wells at 48, 72, 96, and 120 hours post-transduction and frozen at -80C. The collected medium was later analyzed for BMP-2 by ELISA (R&D Systems).

AVLP-hygro-eGFP selection

At 24 hours post-transduction, two wells per group of huMSC (AVLP-eGFP) received either complete medium or selection medium (complete medium with 50 µg/mL hygromycin B), as did two wells per group of huMSC (n=3). Additionally, two wells per group of either huMSC (AVLP-eGFP) or huMSC were harvested and analyzed for GFP expression by flow cytometry.

Subsequently, cells were maintained in culture for 1 week with medium changed every 2 days using either growth or selection medium. At 8 days post-transduction, all cells were harvested, with a portion of each group being subcultured at 5000 cells/cm^2 and the rest being analyzed for eGFP expression via flow cytometry. The subcultured cells were propagated in either selection or growth medium. Upon reaching 80%

confluence, they were again harvested and some were subcultured and the rest analyzed using flow cytometry. This was repeated until all cells had been subcultured 5 times after transduction.

Flow cytometry

All flow analysis was performed using a CyAn ADP (Beckman Coulter, Hialeah, Florida) flow cytometer. Cell suspensions were gated by forward and side scatter to exclude small debris. Gates for eGFP were set such that huMSC cultured in parallel with huMSC (AVLP-eGFP) were 1% positive (Figure 2). FlowJo software (Treestar, Inc., Ashland, Oregon) was used in flow data analysis.

AVLP-BMP2 selection

At 24 hours post-transduction, two wells per group of huMSC (AVLP-BMP2) received either complete medium or selection medium (complete medium with 50 µg/mL hygromycin B), as did two wells per group of huMSC (n=3). Also at 24 hours post-transduction, the medium of two wells per group of either huMSC (AVLP-BMP2) or huMSC was collected and stored at -80C.

Subsequently, cells were cultured for 1 week with media changes every 2 days using the appropriate medium. After this, all cells were harvested, with a portion of each group being subcultured at 5000 cells/cm2 and another portion subcultured at 26000 cells/cm^2. The cells plated at 26000 cells/cm^2 were incubated for 24 hours, after which their medium was collected and stored at -80C. The cells plated at 5000 cells/cm^2 grew in either selection or growth medium until reaching 80% confluence when they were again harvested, counted, and split into continued culture and media collection. This was

repeated until all cells had been subcultured 5 times after transduction. All collected media was assayed for BMP-2 expression via BMP-2 ELISA.

Statistics and Calculations

Population doubling level (PDL) was calculated as described by Kruse et al and its equation shown in Equation 1 (Kruse & Patterson, 1973). The difference in population doubling levels between passages is referred to as population doublings and was used to describe cell growth.

Unless otherwise noted, all data were analyzed via two-way ANOVA with Bonferroni's test as appropriate using GraphPad Prism software. Significance was determined as $p < 0.05$.

3.4 RESULTS

At 48 hours post-transduction with 5 MOI AVLP-eGFP, huMSC (AVLP-eGFP) were positive for eGFP (Figure 1B). BMP-2 ELISA of media collected from AVLP-BMP2 transduced MSCs at 48, 72, 96, and 120 hours post-transduction assessed rhBMP-2 production in huMSCs at 5 MOI (Figure 1C). Non-transduced cells expressed BMP-2 below the detection threshold of the ELISA kit used and are not shown. Cells had low initial expression of BMP-2 which increased over time. BMP-2 mean expression was 0.488 pg BMP-2/cell 120 hours post-transduction but was highly variable between replicates, with a standard error of 0.358 pg/cell.

At each passage, the cells were counted and their viability assessed with Trypan Blue (Figure 3A). Viability of all groups was close to 100% across passages. There was a slight initial decrease in viability ($p=0.0415$) in the huMSC (AVLP-eGFP) group receiving complete medium after transduction compared to huMSCs, but this difference was not

significant after one passage. Viability of huMSC (AVLP-eGFP) group that underwent hygromycin selection did not differ from that of the huMSCs. There were no significant differences between the growth rate of any of the groups as measured by doublings per day, with all groups maintaining a proliferation rate of approximately 1.0-1.5 doublings per day (Figure 3B).

A portion of the MSCs harvested at each passage were used in flow cytometry analysis for eGFP expression. The initial transduction efficiency with AVLP-GFP was roughly 60%. Selection improved the percentage of GFP+ cells to near 90% across multiple passages, while subculturing cells in growth medium saw a steady decrease in the percentage of GFP+ cells to under 10% (Fig 3C). However, when comparing the mean fluorescence intensity of GFP+ cells (Figure 3D), a significant decrease from post-selection to P5 can be seen for huMSC (AVLP-eGFP) in both selection ($p<0.0001$) and growth media ($p<0.0001$).

Viability of huMSC (AVLP-BMP2) ranged from 75% to 95% across three passages (Figure 4a). The viability of the transduced cells in selection medium trended somewhat lower than that of the transduced cells in growth medium, but there were no significant differences between them. The proliferation rate of huMSC (AVLP-BMP2) was 1.02-1.24 doublings/day in growth medium and 0.96-1.20 doublings/day in selection medium (Figure 4b). There were no significant differences between the proliferation rate of huMSC (AVLP-BMP2) in selection or growth medium. Hygromycin-B selection of cells transduced with AVLP-BMP2 did not alter BMP-2 production (Figure 4c). There was a low level of BMP-2 secretion pre-selection, which was not improved post-selection and post-passaging, and levels varied throughout.

3.5 DISCUSSION

The cost and morbidity associated with conventional bone grafts has led to interest in the development of osteogenic gene therapy. The two most-used viral systems to accomplish this are adenoviruses and lentiviruses, each with advantages and disadvantages (Balmayor 2015 - Park 2003, Tsuda 2003). Adenoviral vectors are highly efficient for short-term expression, but wane over the long term and may induce an immune response (Shayakhmetov, 2010; Waehler et al., 2007). This has been shown to interfere with bone formation (Balmayor & van Griensven, 2015; Xu et al., 2005). Conversely, lentiviruses permanently integrate into the host genome, but in doing so incur significant risk of insertional mutagenesis as seen in clinical trials (Hacein-Bey-Abina et al., 2003; Kohn & Candotti, 2009).

In this study, we investigated the use of AVLP as a vector for inducing expression of BMP-2 in mesenchymal stem cells due to its lack of cytopathic effect or immune response despite infecting many different cell types. Cells were transduced with AVLP to produce BMP-2 in quantities approaching 3 pg/cell at 96 hours post-transduction in some cases. Our group has previously attained BMP-2 expression of 0.7 pg/cell in adenvirus-transduced MSCs, and 1.5 pg/cell in lentivirus-transduced MSCs {Andrews, 2019 #493}{Mumaw, 2012 #15}. Adenovirus-transduced MSCs successfully induced heterotopic bone formation in rats, while the lentivirus-transduced MSCs successfully bridged a rat femur model of a critical-sized defect.

There have been several other attempts to create a stable line of MSCs expressing an exogenous protein using viral and non-viral vectors. For example, Sweeney et al successfully used a foamy virus vector to maintain high expression of GFP in MSCs over

10 passages as measured by both percent GFP positive cells and MFI (Sweeney et al., 2016). However, as a retrovirus, the foamy virus will face safety concerns due to its integration into the host genome. In this study, AVLP induced exogenous gene expression in MSCs. Importantly, AVLP-transduced cells were selected for and propagated without loss of viability or growth potential, and huMSC (AVLP-eGFP) were maintained at high purity over multiple passages for at least 30 days. This duration of expression is consistent with previous experiments on AVLP-eGFP expression in epithelial cells, which maintained eGFP expression for 42 days without passaging and selection (Wei et al., 2017). However, we were unable to create cells that consistently expressed high amounts of BMP-2 using AVLP-BMP2. This may be explained by the median fluorescence intensity (MFI) data of huMSC (AVLP-eGFP) (Figure 3D). These cells survived selection and were approximately 90% positive for eGFP over several passages. However, the MFI of those same cells, roughly correlated with the amount of eGFP produced, drops steeply with passaging. This suggests that the level of expression or copy number of the AVLP-eGFP genome required for a cell to survive selection is quite low, which limits AVLP's usefulness in synthetic bone grafts. In another study involving genetic engineering of MSCs, electroporation of a plasmid containing eGFP and neomycin phosphotransferase with human MSCs produced cells that, after selection, were highly positive for eGFP, even over many passages. However, similar to our findings, the eGFP MFI decreased over many passages in selection (Peister, Mellad, Wang, Tucker, & Prockop, 2004).

AVLP-eGFP was able to induce consistent, high, and sustained expression of eGFP in MSCs. There are several options for improving the ability of AVLP to consistently

induce high BMP-2 expression. It may be possible to infect cells at a high MOI without a cytopathic effect. This is associated with an increased copy number per cell which could lead to increased protein expression (Ellis & Delbruck, 1939). Additionally, transfection aids such as Polybrene or protamine sulfate can be used to increase initial transduction efficiency by reducing charge repulsion between cells and the virus (P. Lin et al., 2012). Different strategies for encouraging packaging, assembling, and budding of the construct may increase the efficiency and consistency of AVLP-BMP2. For example, the F protein, which mediates fusion with host cells, can be modified to increase its efficiency (Waning, Schmitt, Leser, & Lamb, 2002). Finally, a different selection marker could be used to select for higher-expressing cells. The bleomycin analogue Zeocin™ has been shown to outperform hygromycin-B in selection efficiency (Lanza, Kim, & Alper, 2013). In summary, there are numerous avenues for future work to enhance AVLP for use in gene therapy.

Additionally, AVLP could be useful in several applications beyond secretion of BMP-2. As mentioned above, AVLP has been used successfully in vaccines which induce expression of specific adhesion markers (Wei et al., 2017). AVLP could be used for other cell surface modifications, including generation of CAR-T cells for cancer therapy, cell tracking, and labelling or modifying extracellular vesicles such as exosomes. Further work is needed to realize the full potential of the AVLP vector.

REFERENCES

Balmayor, E. R., & van Griensven, M. (2015). Gene therapy for bone engineering. *Front Bioeng Biotechnol, 3*, 9. doi:10.3389/fbioe.2015.00009

BC, T. (2006). Current concepts review: Orthobiologics. *Foot and Ankle International, 27*, 561-566.

Campana, V., Milano, G., Pagano, E., Barba, M., Cicione, C., Salonna, G., . . . Logroscino, G. (2014). Bone substitutes in orthopaedic surgery: from basic science to clinical practice. *J Mater Sci Mater Med, 25*(10), 2445-2461. doi:10.1007/s10856-014-5240-2

Chen, Z., Gupta, T., Xu, P., Phan, S., Pickar, A., Yau, W., . . . He, B. (2015). Efficacy of parainfluenza virus 5 (PIV5)-based tuberculosis vaccines in mice. *Vaccine, 33*(51), 7217-7224. doi:10.1016/j.vaccine.2015.10.124

D. Gothard, E. L. S., J.M. Kanczler, H. Rashidi, O. Qutachi, J. Henstock, M. Rotherham, A. El Haj, K.M. Shakesheff, R.O.C. Oreffo. (2014). Tissue engineered bone using select growth factors: A comprehensive review of animal studies and clinical translation studies in man. *European Cells and Materials, 28*, 166-208.

De Long WG, E. T., Koval K. (2007). Current concepts review: Bone grafts and bone graft substitutes in orthopaedic trauma surgery. *Journal of Bone and Joint Surgery American Edition, 89*, 649-658.

Ellis, E. L., & Delbruck, M. (1939). THE GROWTH OF BACTERIOPHAGE. *J Gen Physiol, 22*(3), 365-384.

Giannoudis, P. V., Dinopoulos, H., & Tsiridis, E. (2005). Bone substitutes: An update. *Injury-International Journal of the Care of the Injured, 36*, 20-27. doi:10.1016/j.injury.2005.07.029

Gomez-Barrena, E., Rosset, P., Lozano, D., Stanovici, J., Ermthaller, C., & Gerbhard, F. (2015). Bone fracture healing: cell therapy in delayed unions and nonunions. *Bone, 70*, 93-101. doi:10.1016/j.bone.2014.07.033

Govender S, C. C., Genant HK, Valentin-Opran A, Amit Y, Arbel R, Aro H, Atar D, Bishay M, Borner MG, Chiron P, Choong P, Cinats J, Courtenay B, Feibel R, Geulette B, Gravel C, Haas N, Raschke M, Hammacher E, van der Velde D, Hardy P, Holt M, Josten C, Ketterl RL, Lindeque B, Lob G, Mathevon H, McCoy G, Marsh D, Miller R, Munting E, Oevre S, Nordsletten L, Patel A, Pohl A, Rennie W, Reynders P, Rommens PM, Rondia J,

Rossouw WC, Daneel PJ, Ruff S, Ruter A, Santavirta S, Schildhauer TA, Gekle C, Schnettler R, Segal D, Seiler H, Snowdowne RB, Stapert J, Taglang G, Verdonk R, Vogels L, Weckbach A, Wentzensen A, Wisniewski T. (2002). Recombinant human bone morphogenetic protein-2 for treatment of open tibial fractures: a prospective, controlled, randomized study of four hundred and fifty patients. *Journal of Bone and Joint Surgery American Edition, 84*, 2123-2134.

Hacein-Bey-Abina, S., Von Kalle, C., Schmidt, M., McCormack, M. P., Wulffraat, N., Leboulch, P., . . . Cavazzana-Calvo, M. (2003). LMO2-associated clonal T cell proliferation in two patients after gene therapy for SCID-X1. *Science, 302*(5644), 415-419. doi:10.1126/science.1088547

Hsiung, G. (1972). Parainfluenza-5 virus. Infection of man and animal. *Prog Med Virol, 14*, 241-274.

Huang, Y., Chen, Z., Huang, J., Fu, Z., & He, B. (2015). Parainfluenza virus 5 expressing the G protein of rabies virus protects mice after rabies virus infection. *J Virol, 89*(6), 3427-3429. doi:10.1128/JVI.03656-14

Jay Lieberman, A. D., Sharon Stevenson, Lily Wu, Paula McAllister, Yu Po Lee, Michael Kabo, Gerald Finerman, Arnold Berk, Owen Wite. (1999). The effect of regional gene therapy with bone morphogenetic protein-2-producing bone-marrow cells on the repair of segmental femoral defects in rats. *Journal of Bone and Joint Surgery, 81-A*(7).

Jones AL, B. R., Bosse MJ, Mirza SK, Lyon TR, Webb LX, Pollak AN, Golden JD, Valentin-Opran A. (2006). Recombinant human BMP-2 and allograft compared with autogenous bone graft for reconstruction of diaphyseal tibial fractures with cortical defects. *Journal of Bone and Joint Surgery American Edition, 88*, 1431-1441.

Kohn, D. B., & Candotti, F. (2009). Gene therapy fulfilling its promise. *N Engl J Med, 360*(5), 518-521. doi:10.1056/NEJMe0809614

Kruse, P. F., & Patterson, M. K. (1973). *Tissue culture: methods and applications*: New York, Academic Press, 1973.

Lanza, A. M., Kim, D. S., & Alper, H. S. (2013). Evaluating the influence of selection markers on obtaining selected pools and stable cell lines in human cells. *Biotechnol J, 8*(7), 811-821. doi:10.1002/biot.201200364

Laurencin, C., Khan, Y., & El-Amin, S. F. (2006). Bone graft substitutes. *Expert Review of Medical Devices, 3*(1), 49-57. doi:10.1586/17434440.3.1.49

Li, Z., Mooney, A. J., Gabbard, J. D., Gao, X., Xu, P., Place, R. J., . . . He, B. (2013). Recombinant parainfluenza virus 5 expressing hemagglutinin of influenza A virus H5N1 protected mice against lethal highly pathogenic avian influenza virus H5N1 challenge. *J Virol, 87*(1), 354-362. doi:10.1128/JVI.02321-12

Lin, P., Correa, D., Lin, Y., & Caplan, A. I. (2011). Polybrene Inhibits Human Mesenchymal Stem Cell Proliferation during Lentiviral Transduction. *PLoS One, 6*(8), e23891. doi:10.1371/journal.pone.0023891

Lin, P., Lin, Y., Lennon, D. P., Correa, D., Schluchter, M., & Caplan, A. I. (2012). Efficient lentiviral transduction of human mesenchymal stem cells that preserves proliferation and differentiation capabilities. *Stem Cells Transl Med, 1*(12), 886-897. doi:10.5966/sctm.2012-0086

McCandlish IA, T. H., Cornwell HJ, Wright NG. (1978). A study of dogs with kennel cough. *Vet Rec, 102*, 293-301. doi:http://dx.doi.org/10.1136/vr.102.14.293

McKay, W. F., Peckham, S. M., & Badura, J. M. (2007). A comprehensive clinical review of recombinant human bone morphogenetic protein-2 (INFUSE(®) Bone Graft). *International Orthopaedics, 31*(6), 729-734. doi:10.1007/s00264-007-0418-6

Milone, M. C., & O'Doherty, U. (2018). Clinical use of lentiviral vectors. *Leukemia*. doi:10.1038/s41375-018-0106-0

Mumaw, J., Jordan, E. T., Sonnet, C., Olabisi, R. M., Olmsted-Davis, E. A., Davis, A. R., . . . Stice, S. L. (2012). Rapid Heterotrophic Ossification with Cryopreserved Poly(ethylene glycol-) Microencapsulated BMP2-Expressing MSCs. *Int J Biomater, 2012*, 861794. doi:10.1155/2012/861794

Obremskey, W. T., Marotta, J. S., Yaszemski, M. J., Churchill, L. R., Boden, S. D., & Dirschl, D. R. (2007). Symposium. The introduction of biologics in orthopaedics: issues of cost, commercialism, and ethics. *J Bone Joint Surg Am, 89*(7), 1641-1649. doi:10.2106/jbjs.f.01185

Peister, A., Mellad, J. A., Wang, M., Tucker, H. A., & Prockop, D. J. (2004). Stable transfection of MSCs by electroporation. *Gene Ther, 11*(2), 224-228. doi:10.1038/sj.gt.3302163

Shayakhmetov, D. M. (2010). Virus infection recognition and early innate responses to non-enveloped viral vectors. *Viruses, 2*(1), 244-261. doi:10.3390/v2010244

Sonnet, C., Simpson, C. L., Olabisi, R. M., Sullivan, K., Lazard, Z., Gugala, Z., . . . Olmsted-Davis, E. A. (2013). Rapid healing of femoral defects in rats with low dose sustained BMP2 expression from PEGDA hydrogel microspheres. *J Orthop Res, 31*(10), 1597-1604. doi:10.1002/jor.22407

Sweeney, N. P., Regan, C., Liu, J., Galleu, A., Dazzi, F., Lindemann, D., . . . McClure, M. O. (2016). Rapid and Efficient Stable Gene Transfer to Mesenchymal Stromal Cells Using a Modified Foamy Virus Vector. *Mol Ther, 24*(7), 1227-1236. doi:10.1038/mt.2016.91

Tannoury, C. A., & An, H. S. (2014). Complications with the use of bone morphogenetic protein 2 (BMP-2) in spine surgery. *Spine J, 14*(3), 552-559. doi:10.1016/j.spinee.2013.08.060

Valdes, M. A., Thakur, N. A., Namdari, S., Ciombor, D. M., & Palumbo, M. (2009). Recombinant bone morphogenic protein-2 in orthopaedic surgery: a review. *Arch Orthop Trauma Surg, 129*(12), 1651-1657. doi:10.1007/s00402-009-0850-8

Waehler, R., Russell, S. J., & Curiel, D. T. (2007). Engineering targeted viral vectors for gene therapy. *Nat Rev Genet, 8*(8), 573-587. doi:10.1038/nrg2141

Waning, D. L., Schmitt, A. P., Leser, G. P., & Lamb, R. A. (2002). Roles for the cytoplasmic tails of the fusion and hemagglutinin-neuraminidase proteins in budding of the paramyxovirus simian virus 5. *J Virol, 76*(18), 9284-9297.

Wei, H., Chen, Z., Elson, A., Li, Z., Abraham, M., Phan, S., . . . He, B. (2017). Developing a platform system for gene delivery: amplifying virus-like particles (AVLP) as an influenza vaccine. *NPJ Vaccines, 2*, 32. doi:10.1038/s41541-017-0031-7

Williams, D. A., & Thrasher, A. J. (2014). Concise Review: Lessons Learned From Clinical Trials of Gene Therapy in Monogenic Immunodeficiency Diseases. *Stem Cells Translational Medicine, 3*(5), 636-642. doi:10.5966/sctm.2013-0206

Xu, X. L., Tang, T., Dai, K., Zhu, Z., Guo, X. E., Yu, C., & Lou, J. (2005). Immune response and effect of adenovirus-mediated human BMP-2 gene transfer on the repair of segmental tibial bone defects in goats. *Acta Orthop, 76*(5), 637-646. doi:10.1080/17453670510041709

Yang, Y., Zengel, J., Sun, M., Sleeman, K., Timani, K. A., Aligo, J., . . . He, B. (2015). Regulation of Viral RNA Synthesis by the V Protein of Parainfluenza Virus 5. *J Virol, 89*(23), 11845-11857. doi:10.1128/JVI.01832-15

Zara, J. N., Siu, R. K., Zhang, X., Shen, J., Ngo, R., Lee, M., . . . Soo, C. (2011). High doses of bone morphogenetic protein 2 induce structurally abnormal bone and inflammation in vivo. *Tissue Eng Part A, 17*(9-10), 1389-1399. doi:10.1089/ten.TEA.2010.0555

Zhao B, K. T., Toyoda H, Takada T, Yanai T, Fukuda T, Chung UI, Koike T, Takaoka K, Kamijo R. (2006). Heparin potentiates the in vivo ectopic bone formation induced by bone morphogenetic protein-2. *J Biol Chem, 281*(32), 23246-23253.

Balmayor, E. R., & van Griensven, M. (2015). Gene therapy for bone engineering. *Front Bioeng Biotechnol, 3*, 9. doi:10.3389/fbioe.2015.00009

BC, T. (2006). Current concepts review: Orthobiologics. *Foot and Ankle International, 27*, 561-566.

Campana, V., Milano, G., Pagano, E., Barba, M., Cicione, C., Salonna, G., . . . Logroscino, G. (2014). Bone substitutes in orthopaedic surgery: from basic science to clinical practice. *J Mater Sci Mater Med, 25*(10), 2445-2461. doi:10.1007/s10856-014-5240-2

Chen, Z., Gupta, T., Xu, P., Phan, S., Pickar, A., Yau, W., . . . He, B. (2015). Efficacy of parainfluenza virus 5 (PIV5)-based tuberculosis vaccines in mice. *Vaccine, 33*(51), 7217-7224. doi:10.1016/j.vaccine.2015.10.124

D. Gothard, E. L. S., J.M. Kanczler, H. Rashidi, O. Qutachi, J. Henstock, M. Rotherham, A. El Haj, K.M. Shakesheff, R.O.C. Oreffo. (2014). Tissue engineered bone using select growth factors: A comprehensive review of animal studies and clinical translation studies in man. *European Cells and Materials, 28*, 166-208.

De Long WG, E. T., Koval K. (2007). Current concepts review: Bone grafts and bone graft substitutes in orthopaedic trauma surgery. *Journal of Bone and Joint Surgery American Edition, 89*, 649-658.

Ellis, E. L., & Delbruck, M. (1939). THE GROWTH OF BACTERIOPHAGE. *J Gen Physiol, 22*(3), 365-384.

Giannoudis, P. V., Dinopoulos, H., & Tsiridis, E. (2005). Bone substitutes: An update. *Injury-International Journal of the Care of the Injured, 36*, 20-27. doi:10.1016/j.injury.2005.07.029

Gomez-Barrena, E., Rosset, P., Lozano, D., Stanovici, J., Ermthaller, C., & Gerbhard, F. (2015). Bone fracture healing: cell therapy in delayed unions and nonunions. *Bone, 70*, 93-101. doi:10.1016/j.bone.2014.07.033

Govender S, C. C., Genant HK, Valentin-Opran A, Amit Y, Arbel R, Aro H, Atar D, Bishay M, Borner MG, Chiron P, Choong P, Cinats J, Courtenay B, Feibel R, Geulette B, Gravel C, Haas N, Raschke M, Hammacher E, van der Velde D, Hardy P, Holt M, Josten C, Ketterl RL, Lindeque B, Lob G, Mathevon H, McCoy G, Marsh D, Miller R, Munting E, Oevre S, Nordsletten L, Patel A, Pohl A, Rennie W, Reynders P, Rommens PM, Rondia J,

Rossouw WC, Daneel PJ, Ruff S, Ruter A, Santavirta S, Schildhauer TA, Gekle C, Schnettler R, Segal D, Seiler H, Snowdowne RB, Stapert J, Taglang G, Verdonk R, Vogels L, Weckbach A, Wentzensen A, Wisniewski T. (2002). Recombinant human bone morphogenetic protein-2 for treatment of open tibial fractures: a prospective, controlled, randomized study of four hundred and fifty patients. *Journal of Bone and Joint Surgery American Edition, 84*, 2123-2134.

Hacein-Bey-Abina, S., Von Kalle, C., Schmidt, M., McCormack, M. P., Wulffraat, N., Leboulch, P., . . . Cavazzana-Calvo, M. (2003). LMO2-associated clonal T cell proliferation in two patients after gene therapy for SCID-X1. *Science, 302*(5644), 415-419. doi:10.1126/science.1088547

Hsiung, G. (1972). Parainfluenza-5 virus. Infection of man and animal. *Prog Med Virol, 14*, 241-274.

Huang, Y., Chen, Z., Huang, J., Fu, Z., & He, B. (2015). Parainfluenza virus 5 expressing the G protein of rabies virus protects mice after rabies virus infection. *J Virol, 89*(6), 3427-3429. doi:10.1128/JVI.03656-14

Jay Lieberman, A. D., Sharon Stevenson, Lily Wu, Paula McAllister, Yu Po Lee, Michael Kabo, Gerald Finerman, Arnold Berk, Owen Wite. (1999). The effect of regional gene therapy with bone morphogenetic protein-2-producing bone-marrow cells on the repair of segmental femoral defects in rats. *Journal of Bone and Joint Surgery, 81-A*(7).

Jones AL, B. R., Bosse MJ, Mirza SK, Lyon TR, Webb LX, Pollak AN, Golden JD, Valentin-Opran A. (2006). Recombinant human BMP-2 and allograft compared with autogenous bone graft for reconstruction of diaphyseal tibial fractures with cortical defects. *Journal of Bone and Joint Surgery American Edition, 88*, 1431-1441.

Kohn, D. B., & Candotti, F. (2009). Gene therapy fulfilling its promise. *N Engl J Med, 360*(5), 518-521. doi:10.1056/NEJMe0809614

Kruse, P. F., & Patterson, M. K. (1973). *Tissue culture: methods and applications*: New York, Academic Press, 1973.

Lanza, A. M., Kim, D. S., & Alper, H. S. (2013). Evaluating the influence of selection markers on obtaining selected pools and stable cell lines in human cells. *Biotechnol J, 8*(7), 811-821. doi:10.1002/biot.201200364

Laurencin, C., Khan, Y., & El-Amin, S. F. (2006). Bone graft substitutes. *Expert Review of Medical Devices, 3*(1), 49-57. doi:10.1586/17434440.3.1.49

Li, Z., Mooney, A. J., Gabbard, J. D., Gao, X., Xu, P., Place, R. J., . . . He, B. (2013). Recombinant parainfluenza virus 5 expressing hemagglutinin of influenza A virus H5N1 protected mice against lethal highly pathogenic avian influenza virus H5N1 challenge. *J Virol, 87*(1), 354-362. doi:10.1128/JVI.02321-12

Lin, P., Correa, D., Lin, Y., & Caplan, A. I. (2011). Polybrene Inhibits Human Mesenchymal Stem Cell Proliferation during Lentiviral Transduction. *PLoS One, 6*(8), e23891. doi:10.1371/journal.pone.0023891

Lin, P., Lin, Y., Lennon, D. P., Correa, D., Schluchter, M., & Caplan, A. I. (2012). Efficient lentiviral transduction of human mesenchymal stem cells that preserves proliferation and differentiation capabilities. *Stem Cells Transl Med, 1*(12), 886-897. doi:10.5966/sctm.2012-0086

McCandlish IA, T. H., Cornwell HJ, Wright NG. (1978). A study of dogs with kennel cough. *Vet Rec, 102*, 293-301. doi:http://dx.doi.org/10.1136/vr.102.14.293

McKay, W. F., Peckham, S. M., & Badura, J. M. (2007). A comprehensive clinical review of recombinant human bone morphogenetic protein-2 (INFUSE(®) Bone Graft). *International Orthopaedics, 31*(6), 729-734. doi:10.1007/s00264-007-0418-6

Milone, M. C., & O'Doherty, U. (2018). Clinical use of lentiviral vectors. *Leukemia*. doi:10.1038/s41375-018-0106-0

Mumaw, J., Jordan, E. T., Sonnet, C., Olabisi, R. M., Olmsted-Davis, E. A., Davis, A. R., . . . Stice, S. L. (2012). Rapid Heterotrophic Ossification with Cryopreserved Poly(ethylene glycol-) Microencapsulated BMP2-Expressing MSCs. *Int J Biomater, 2012*, 861794. doi:10.1155/2012/861794

Obremskey, W. T., Marotta, J. S., Yaszemski, M. J., Churchill, L. R., Boden, S. D., & Dirschl, D. R. (2007). Symposium. The introduction of biologics in orthopaedics: issues of cost, commercialism, and ethics. *J Bone Joint Surg Am, 89*(7), 1641-1649. doi:10.2106/jbjs.f.01185

Peister, A., Mellad, J. A., Wang, M., Tucker, H. A., & Prockop, D. J. (2004). Stable transfection of MSCs by electroporation. *Gene Ther, 11*(2), 224-228. doi:10.1038/sj.gt.3302163

Shayakhmetov, D. M. (2010). Virus infection recognition and early innate responses to non-enveloped viral vectors. *Viruses, 2*(1), 244-261. doi:10.3390/v2010244

Sonnet, C., Simpson, C. L., Olabisi, R. M., Sullivan, K., Lazard, Z., Gugala, Z., . . . Olmsted-Davis, E. A. (2013). Rapid healing of femoral defects in rats with low dose sustained BMP2 expression from PEGDA hydrogel microspheres. *J Orthop Res, 31*(10), 1597-1604. doi:10.1002/jor.22407

Sweeney, N. P., Regan, C., Liu, J., Galleu, A., Dazzi, F., Lindemann, D., . . . McClure, M. O. (2016). Rapid and Efficient Stable Gene Transfer to Mesenchymal Stromal Cells Using a Modified Foamy Virus Vector. *Mol Ther, 24*(7), 1227-1236. doi:10.1038/mt.2016.91

Tannoury, C. A., & An, H. S. (2014). Complications with the use of bone morphogenetic protein 2 (BMP-2) in spine surgery. *Spine J, 14*(3), 552-559. doi:10.1016/j.spinee.2013.08.060

Valdes, M. A., Thakur, N. A., Namdari, S., Ciombor, D. M., & Palumbo, M. (2009). Recombinant bone morphogenic protein-2 in orthopaedic surgery: a review. *Arch Orthop Trauma Surg, 129*(12), 1651-1657. doi:10.1007/s00402-009-0850-8

van Griensven, M. (2015). Preclinical testing of drug delivery systems to bone. *Adv Drug Deliv Rev, 94*, 151-164. doi:10.1016/j.addr.2015.07.006

Waehler, R., Russell, S. J., & Curiel, D. T. (2007). Engineering targeted viral vectors for gene therapy. *Nat Rev Genet, 8*(8), 573-587. doi:10.1038/nrg2141

Waning, D. L., Schmitt, A. P., Leser, G. P., & Lamb, R. A. (2002). Roles for the cytoplasmic tails of the fusion and hemagglutinin-neuraminidase proteins in budding of the paramyxovirus simian virus 5. *J Virol, 76*(18), 9284-9297.

Wei, H., Chen, Z., Elson, A., Li, Z., Abraham, M., Phan, S., . . . He, B. (2017). Developing a platform system for gene delivery: amplifying virus-like particles (AVLP) as an influenza vaccine. *NPJ Vaccines, 2*, 32. doi:10.1038/s41541-017-0031-7

Williams, D. A., & Thrasher, A. J. (2014). Concise Review: Lessons Learned From Clinical Trials of Gene Therapy in Monogenic Immunodeficiency Diseases. *Stem Cells Translational Medicine, 3*(5), 636-642. doi:10.5966/sctm.2013-0206

Yang, Y., Zengel, J., Sun, M., Sleeman, K., Timani, K. A., Aligo, J., . . . He, B. (2015). Regulation of Viral RNA Synthesis by the V Protein of Parainfluenza Virus 5. *J Virol, 89*(23), 11845-11857. doi:10.1128/JVI.01832-15

Zara, J. N., Siu, R. K., Zhang, X., Shen, J., Ngo, R., Lee, M., . . . Soo, C. (2011). High doses of bone morphogenetic protein 2 induce structurally abnormal bone and inflammation in vivo. *Tissue Eng Part A, 17*(9-10), 1389-1399. doi:10.1089/ten.TEA.2010.0555

Zhao B, K. T., Toyoda H, Takada T, Yanai T, Fukuda T, Chung UI, Koike T, Takaoka K, Kamijo R. (2006). Heparin potentiates the in vivo ectopic bone formation induced by bone morphogenetic protein-2. *J Biol Chem, 281*(32), 23246-23253.

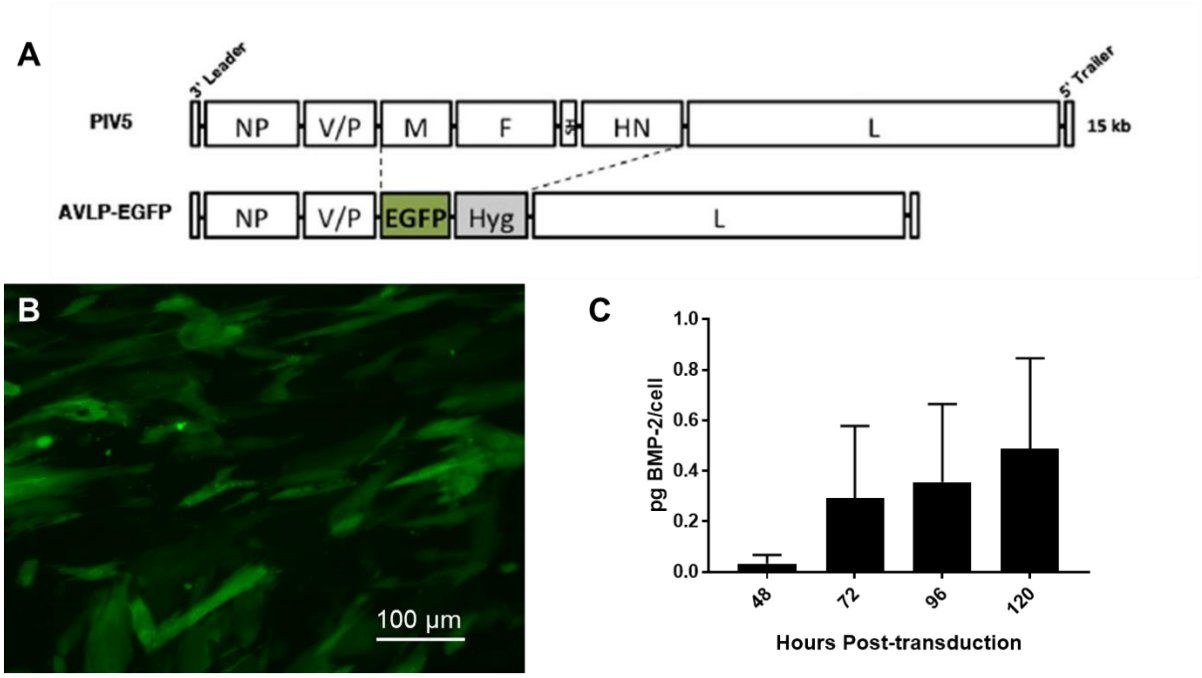

Figure 3.1: AVLP construct and transduction of MSCs. (A)The AVLP construct contains the nucleoprotein (NP), phosphoprotein (P), V protein (V), and L RNA-dependent RNA polymerase (L) from PIV-5, as well as the hygromycin-B resistance gene and either BMP-2 or eGFP. (B) Human umbilical MSCs were successfully transduced with AVLP-eGFP at a high efficiency as shown 48 hours post-transduction. (C) Human umbilical mesenchymal stem cells (huMSC) were transduced with AVLP-BMP and incubated for up to 120 hours. Both cell types secreted highly variable amounts of BMP-2. n=3, mean +/- SEM.

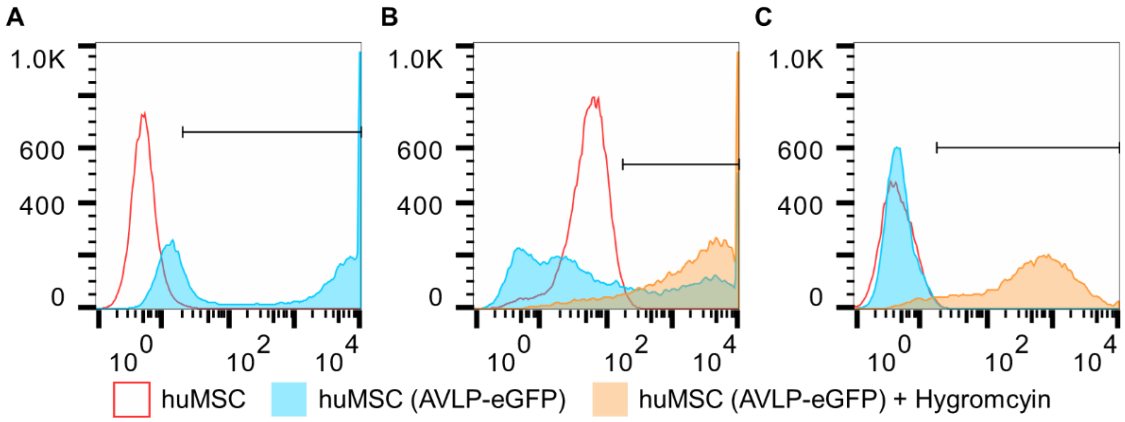

Figure 3.2: Flow cytometry of huMSC (AVLP-eGFP). Flow cytometry plot of human umbilical mesenchymal stem cells (huMSCs) 48 hours post-transduction with AVLP-eGFP (A), 7 days after selection with hygromycin B (B), and after sequential expansion for 5 passages (C).

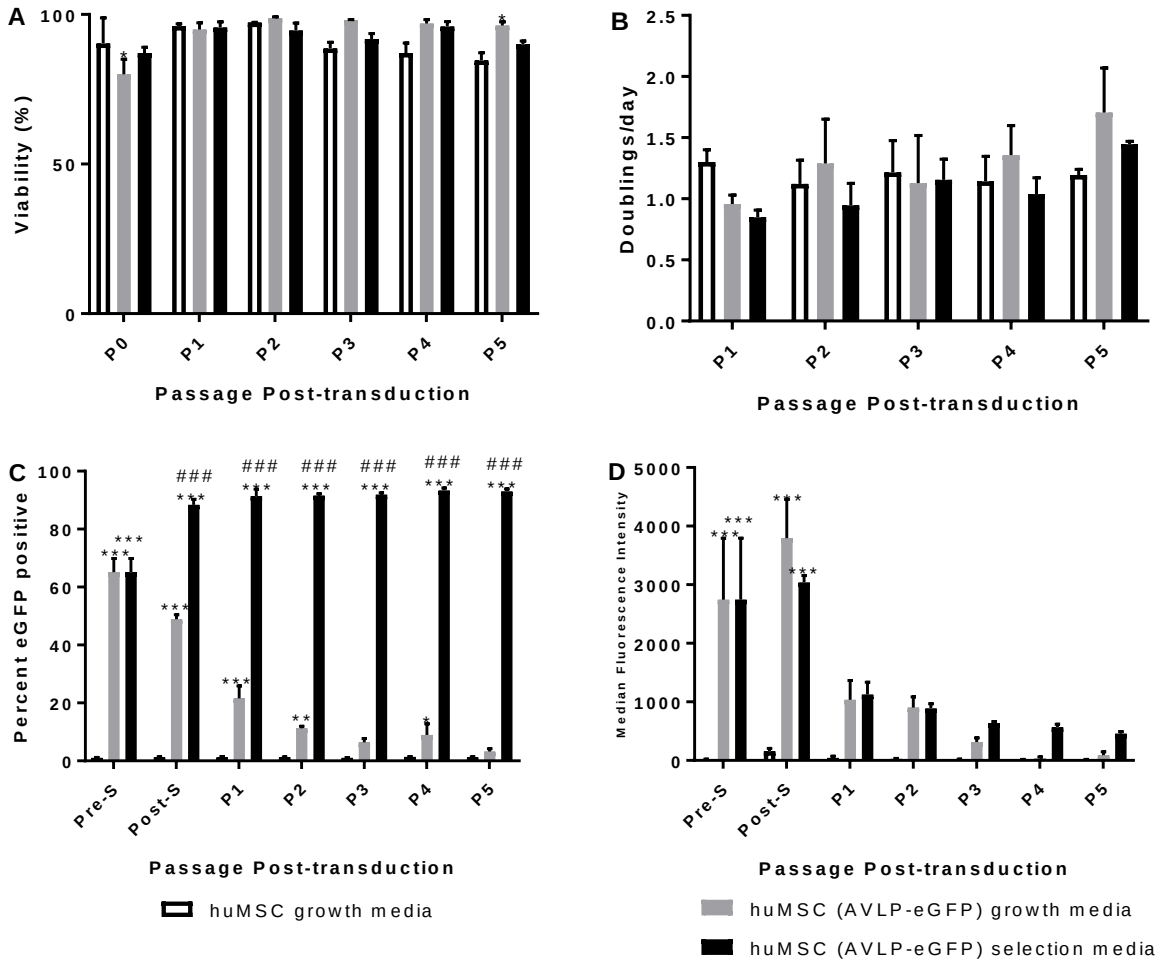

Figure 3.3: AVLP-eGFP selection in huMSCs. Human umbilical mesenchymal stem cells (huMSCs) were transduced with AVLP-eGFP and selected for with hygromycin B while being sequentially expanded. The group undergoing selection retained similar viability (A) and proliferation (B) compared to transduced cells in growth medium and nontransduced cells. Furthermore, they maintained high expression of eGFP (C), while the median fluorescence intensity of eGFP in both transduced groups decreased greatly during culture (D). N=3, mean +/- SEM. Significant difference from “huMSC” is indicated by “*”, from “huMSC (AVLP-eGFP) growth medium” by “#”. Two-way ANOVA with Bonferroni’s test.

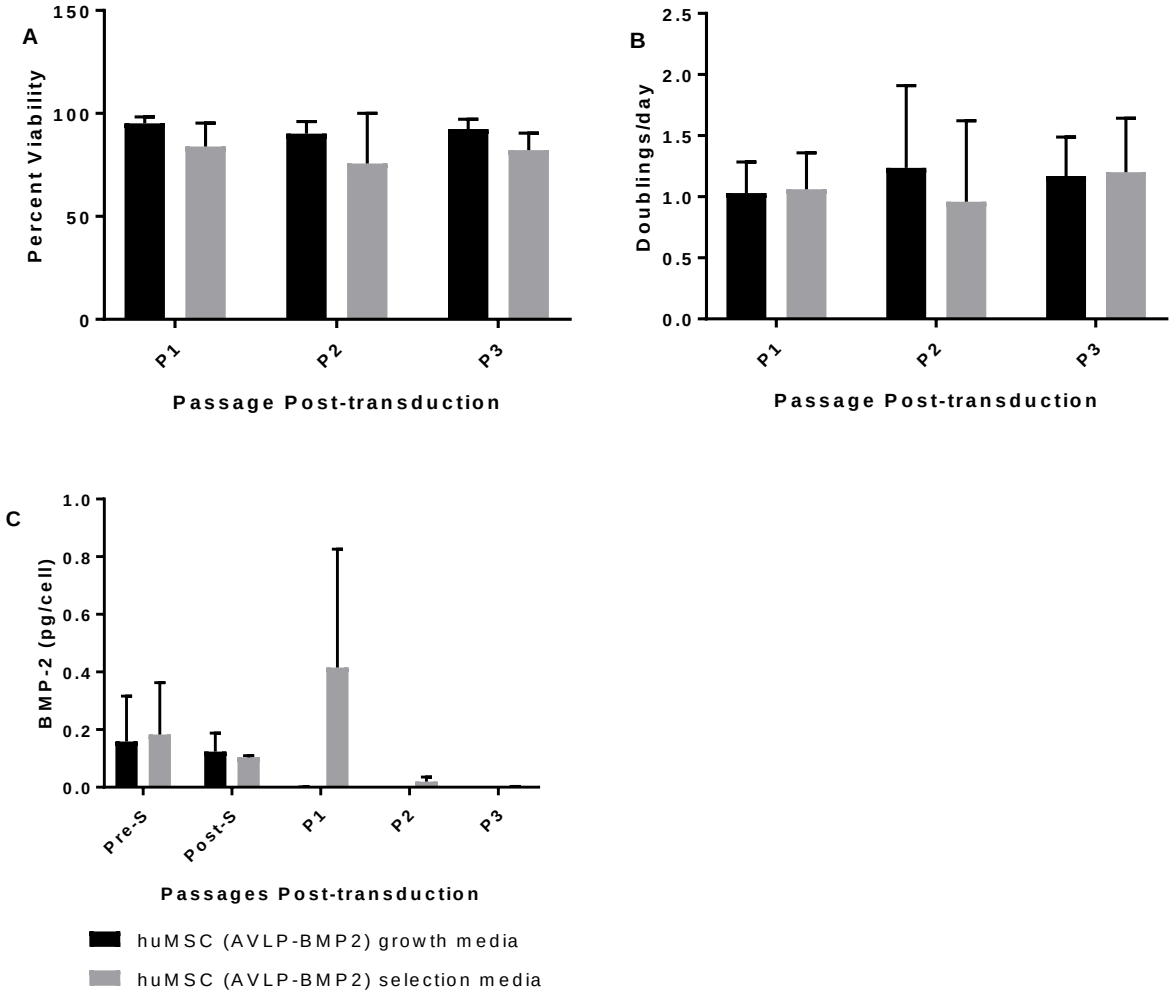

Figure 3.4: AVLP-BMP selection in huMSCs. Human umbilical mesenchymal stem cells (huMSCs) were transduced with AVLP-BMP and selected for with hygromycin B while being sequentially expanded. The group undergoing selection retained similar proliferation (A) and viability (B) but displayed high variability in expression of BMP-2 (C), while compared to transduced cells in growth medium. Non-transduced cells did not secrete detectable quantities of BMP-2 and are not shown. n=2, mean +/- SEM. Two-way ANOVA with Bonferroni's test.

$$PDL = X + 3.322(\log Y - logI)$$

Equation 3.1: Population Doubling Level. Where PDL is the population doubling level, X is the initial population doubling level, I is the initial cell number plated in the culture vessel, and Y is the final cell number at the end of the growth period. In this study, the end of the growth period corresponded with 80% confluence unless otherwise noted.

CHAPTER 4

LITERATURE REVIEW

4.1 INTRODUCTION

Each year, millions of people sustain fractures that without bone grafts, would severely impact their quality of life (Campana et al., 2014). Despite the efficacy of autologous grafts, their associated donor-site morbidity and limited availability have inspired the development of many alternatives (Khan et al., 2005). Xenografts and allografts require extensive treatment to minimize rejection and disease transmission, losing many of their benefits in the process (Flynn, 2011). Growth factors such as bone morphogenetic proteins can be effective in inducing bone formation, but thus far have been difficult to deliver at low cost with minimal complications (Zara et al., 2011). Cell-based therapies such as mesenchymal stem cells (MSCs) have shown promise in bone regeneration, although the large-scale production of efficacious clinical-grade cells remains difficult (Ami R. Amini, 2012). Recently, interest has begun to shift toward the MSC secretome, including their extracellular vesicles (EVs).

EVs are currently of great interest to biomedical research, both as a therapeutic and a diagnostic. They are comprised of exosomes and microparticles. Exosomes are recognized as being spherical vesicles between 50 and 150nm in diameter that express the tetraspanins CD9, CD63, and CD81, while microparticles are up to 1 μm in diameter (Colombo, Raposo, & Thery, 2014). Exosomes are released through fusion of an endosomal membrane compartment with the plasma membrane (Heijnen, Schiel,

Fijnheer, Geuze, & Sixma, 1999; Rozmyslowicz et al., 2003). Microparticles, on the other hand, bud directly from the plasma membrane (Colombo et al., 2014). Prokaryotic as well as eukaryotic cells secrete EVs (Raposo & Stoorvogel, 2013). Following release, they ferry their cargo consisting of proteins, lipids, and RNAs to other cells (Camussi, Deregibus, & Cantaluppi, 2013). This mediation of cell signaling has recently attracted interest for its many potential therapeutic applications.

EVs have several advantages over their parent cells. Of particular interest is the innate ability of exosomes to be taken up by certain cell types. MSC EVs, for example, preferentially accumulate in injured tissue (Grange et al., 2014). They are also well-tolerated by the body, being found in all bodily fluids (Simpson, Jensen, & Lim, 2008). Furthermore, their acellular nature may give them an easier path to clinical use than their parent cells, while being easier to store and prepare for use (Vishnubhatla, Corteling, Stevanato, Hicks, & Sinden, 2014). Prompted by these widely applicable traits, researchers have begun to investigate the effects of MSC derived EVs on bone defect healing. However, much remains to be understood about their mechanisms of action. Here, we discuss the most recent descriptions of MSC EV induced osteogenesis, and postulate that their effects are due not only to up-regulation of bone-specific pathways, but also due to their modulation of the inflammatory response to injury.

4.2 OSTEOGENIC MSC EVS

MSC EVs have already been used to successfully induce bone formation in bone defects and long bone fractures in rodent models. Calvarial defect models have been employed most often, and there are no studies involving large animal models. Without

exception, the EVs are delivered locally at the defect site, either via injection or in combination with a scaffold. These initial assessments of EV osteogenesis potential focus on bone volume and mineralization, and their upregulation of bone and mineralization associated mRNA and protein in MSCs and osteoblasts. While these studies often demonstrate osteogenesis, the mechanisms behind these effects have not been fully explored.

There is evidence that MSC derived EVs play a crucial role in natural bone fracture repair. This has been studied using a transverse femoral fracture comparing wild-type and CD9 -/- mice, which have reduced exosome production (Furuta et al., 2016). There were no differences in body weight, bone growth, or bone density between the groups prior to fracture creation (Furuta et al., 2016). However, without treatment the CD9-/- mice had a much lower bone union rate, increased period for union, and delayed endochondral ossification compared to their wild type counterparts (Furuta et al., 2016). The injection of either MSC conditioned media or MSC exosomes derived from that media into the fracture site rescued these effects, while exosome-depleted media did not (Furuta et al., 2016). Additionally, this effect was unique to MSC exosomes, as those derived from osteosarcoma did not rescue the phenotype (Furuta et al., 2016).

MSC EVs have a potent effect on osteoblast activity and differentiation and on bone regeneration (Qin, Wang, Gao, Chen, & Zhang, 2016). In vitro, EVs had comparable effects to osteogenic media and bone marrow MSC conditioned media on osteoblast mineralization (Qin et al., 2016). Additionally, EVs induced increased expression of ALP, OCN, OPN, and RUNX2 compared to normal media (Qin et al.,

2016). RNA sequencing revealed enrichment of miR-196a, -27a, -206 in EV treated BMCSCs compared to untreated controls, an effect which was removed by inhibiting those RNAs. Finally, rat calvarial bone defects were treated with a combination of EVs and a composite hydrogel (Qin et al., 2016). The EV treated group had increased bone volume compared to hydrogel only, although the defects did not bridge and there was similar bone density between groups (Qin et al., 2016). Exosomes isolated from iPSC MSCs were applied to tricalcium phosphate scaffolds, which were used to treat calvarial defects in rats (J. Zhang et al., 2016). After 8 weeks, there was an exosome dose-dependent increase in the bone volume to tissue volume fraction and tissue mineralization as measured by ALP (J. Zhang et al., 2016).

MSC EVs are not only effective at inducing bone formation in otherwise healthy animals, but also in a model of osteoporosis. Exosomes were isolated from iPSC-derived MSCs and applied to bone marrow MSCs derived from ovarectomized rats (Qi et al., 2016). Exosome-treated groups exhibited a dose-dependent increase in proliferation, alkaline phosphatase activity, and alizarin red staining (Qi et al., 2016). Additionally, exosome treated cells had increased gene expression of ALP, RUNX-2 and COL1-A1, as well as increased protein expression of RUNX2 AND COL1 (Qi et al., 2016). When used to coat B-TCP scaffolds and implanted in calvarial defects created in ovarectomized rats, exosomes exhibited a dose-dependent increase in bone mineral density, fraction of bone volume per tissue volume, and creation of new bone (Qi et al., 2016). There was also an exosome dose-dependent increase in blood vessel area and number (Qi et al., 2016). Finally, osteocalcin, osteopontin, and CD31 were shown to have exosome dose-dependent increases within the defect area (Qi et al., 2016).

EVs derived from MSCs undergoing osteogenic differentiation can be more potent than those from their naïve counterparts. MSCs were osteogenically differentiated via traditional osteogenic medium or RUNX-2 transformation, and exosomes were collected from these cells and applied to naïve MSCs (Martins, Ribeiro, Martins, Reis, & Neves, 2016). Remarkably, the EV groups outperformed their original stimuli in inducing osteogenesis, as measured by BMP2, SP7, SPP1, BGLAP/IBSP, and alkaline phosphatase expression (Martins et al., 2016). Exosomes from adipose MSCs cultured in osteogenic media for at least two days had a synergistic effect with osteogenic media on ALP production, Alizarin Red staining, and gene expression of RUNX2, ALP and COL1A1 (Li et al., 2018). Exosomes derived from two day differentiated cells were immobilized to PLGA/pDA scaffolds and used them to treat mouse calvarial defects (Li et al., 2018). Compared to empty scaffolds, the immobilized exosome treatment had higher bone volume at six weeks (Li et al., 2018). Additionally, the bone present was more mature than other groups, as shown with histochemistry (Li et al., 2018).

The effect of osteogenic differentiation is also time dependent, as demonstrated by a comparison between EVs from 2 and 4 week differentiated MSCs. EVs from the 4 week culture induced higher mRNA expression of BMP2, GDF10, BMP9, BMP6, and OSX, and higher protein expression of BMP2 and TGFB in naïve MSCs (Narayanan, Huang, & Ravindran, 2016). This effect was further corroborated by a study of EVs from 3 and 21 day differentiated MSCs, which reproduced the differences in osteogenic effects while also demonstrating considerable differences in the miRNA content of the two groups (Wang, Omar, Vazirisani, Thomsen, & Ekstrom, 2018).

In addition to osteogenic stimuli, EVs may also be influenced by culturing their parent cells in inflammatory conditions. When bone marrow MSCs were stimulated with TNF-α, their exosomes significantly increased osteoblast proliferation, bone sialoprotein expression, and mineralization as measured by alizarin red staining over exosomes from unstimulated cells (Lu, Chen, Dunstan, Roohani-Esfahani, & Zreiqat, 2017). This was suspected to be explained through increased wnt-3a expression in the conditioned exosomes (Lu et al., 2017). Inhibiting Wnt signaling abolished the effects of TNF-α preconditioning, confirming its responsibility for those effects (Lu et al., 2017).

Apart from their osteogenic effects, MSC EVs have also been shown to be chemotactic for endogenous MSCs. MSC-derived EVs increased bone marrow MSC cell proliferation and migration (J. Zhang et al., 2016). Additionally, the EV-treated cells exhibited upregulated expression of genes involving ECM interaction, focal adhesion, and PI3K-Akt signaling, which is associated with MSC proliferation, migration, and osteogenic differentiation (J. Zhang et al., 2016). Inhibiting PI3K-Akt signaling in bone MSCs prevented exosome-mediated osteogenesis (J. Zhang et al., 2016). Increased migration of MSCs across a transwell system was observed in the presence of exosomes from adipose stem cells treated with osteogenic media (Li et al., 2018). When implanted with a PLGA scaffold into a mouse calvarial defect, increased migration of MSCs into the defect space was evident in the exosome-treated group (Li et al., 2018).

These studies establish the potential for EVs as cell-free therapeutics for bone defects and provide insight on the possible mechanisms of action for osteogenic EVs. They upregulate gene and protein expression in osteogenic pathways of stem cells and

osteoblast precursors, inducing stem cell migration and osteoblast mineralization. However, it is important to note that the skeletal system does not exist in a vacuum, and multiple other systems can have significant effects on bone healing, including the immune system.

4.3 ORTHOIMMUNOLOGY

There is an important interplay between bone repair and the immune system. Soon after the injury occurs, a hematoma forms and is infiltrated by immune cells (Ono & Takayanagi, 2017). The resulting inflammation is an important first step in the repair process (Ono & Takayanagi, 2017). However, continued inflammation negatively impacts the succeeding steps in the process (Ono & Takayanagi, 2017). As in any biological repair process, different immune actors can contribute positively or negatively.

Lymphocytes, especially T-cells, can impair fracture healing. In a mouse model of mature lymphocyte absence, femoral fractures healed 25% faster than in their wild-type counterparts (Toben et al., 2011). The authors hypothesized this was due to an increase in both early bone resorption and later bone formation (Toben et al., 2011). This was accompanied by lower RNA expression of inflammatory cytokines such as TNF-a, LT-B, and IFN-y contrasted with higher expression of anti-inflammatory IL-10 in the immune compromised mice compared to wild-types (Toben et al., 2011). However, T and B cells can have beneficial effects towards bone repair. In a mouse fracture model, increased T-cells were observed in the bone marrow, and lymphocytes in general infiltrated the callus in two separate waves (Konnecke et al., 2014). Additionally, these lymphocytes, once in the bone, made direct cell-cell contact with activated osteoblasts, osteoblast precursors, and osteoclasts (Konnecke et al., 2014). Both T and

B cells expressed high amounts of osteoprotegrin, which binds RANKL to inhibit osteoclastogenesis (Konnecke et al., 2014). Another study examined the peripheral blood of human patients who were identified to have normal or delayed fracture healing (Reinke et al., 2013). While the levels of IL-6, IL-B, and TNF-a did not differ between groups, there was a correlation between the frequency and number of CD8+CD11+ T memory cells, and delayed fracture healing (Reinke et al., 2013). Additionally, these cells were found to be enriched in the hematomas of both groups, and to produce high amounts of IFN-y (Reinke et al., 2013). Furthermore, depleting CD8+ cells via antibody therapy in a mouse fracture model led to an increased bone volume to total volume ratio 21 days after surgery (Reinke et al., 2013).

T regulatory cells (T-regs) may have significant healing effects on bone. They have recently become a focus of research as they participate in a host of repair and regenerative processes in many tissues, through mechanisms which are not yet entirely clear (C. Zhang et al., 2017). In bone repair, T-reg frequency has been found to be lower in patients with delayed fracture healing, and that the T-regs they did have secreted less of the anti-inflammatory cytokine TGF-B and inhibitory markers CTLA-4 and Lag-3 (Jiang et al., 2018). T-regs from the delayed healing patients were also less suppressive of helper T-cell proliferation and they themselves proliferated less in the presence of IL-2 (Jiang et al., 2018). Additionally, T-regs have been shown to inhibit osteoclast differentiation in vitro in a paracrine-dependent manner (Kim et al., 2007).

The effect of neutrophils on the bone repair process has not yet been fully explored. However, it is known that their migration to the fracture hematoma is associated with impaired healing (Recknagel et al., 2013). In an in vitro model of

neutrophil migration toward hematoma, this behavior could be abolished by blocking C5aR and FPR, and that those receptors are likely responsible for this migration (Bastian, Mrozek, et al., 2018). C5aR1 and C5aR2 have been shown to have different effects on inflammation, but both have a positive effect on fracture healing (Kovtun et al., 2017). Additionally, when co-cultured in vitro, neutrophils significantly decreased bone marrow MSC number and ALP production compared to bone marrow MSCs alone (Bastian, Croes, et al., 2018).

Inflammatory cytokines also have a profound impact on fracture healing. Serum levels of IL-6 and TNF-a were elevated in human fracture patients (Huang et al., 2017). IL-6 was also elevated in mice post-fracture and was abrogated in a dose-dependent manner by treatment with IL-6 receptor antibody (MR16-1) (Huang et al., 2017)`. Treating mice post-fracture with MR16-1 also resulted in decreased serum levels of TNF-a. This treatment also led to increases in flexural rigidity in the injured limb at 21 days post-surgery over the IgG control (Huang et al., 2017). Additionally, the authors also showed that mRNA expression for osteoblast-specific genes type II and X procollagen at the fracture site increased in a dose dependent manner with MR16-1 (Huang et al., 2017).

4.4 EV IMMUNOMODULATION

EVs have already been demonstrated to affect the immune system. They can have either inflammatory or anti-inflammatory effects, depending on their source. For example, some immune cells produce EVs that can have inflammatory effects (Wen 2017). In terms of immunosuppression by EVs, there is great interest in those derived

from MSCs, owing to the well-described immunomodulatory properties of the cells themselves (Yu, Zhang, & Li, 2014).

Several studies have demonstrated MSC-EV suppression of immune cell proliferation. MSC-derived exosomes impaired T-cell proliferation in vitro, and when injected into rat myocardial infarcts reduced the incidence of T-cells in the injured area (Teng et al., 2015). Activated PBMCs treated with MSC-EVs decreased T-cell proliferation and increased expression of the anti-inflammatory cytokine IL-10 (Del Fattore et al., 2015). MSC derived EVs also inhibited mitogen-induced T-cell proliferation (Pachler et al., 2017). The EVs were able to inhibit mitogen-induced proliferation in a dose dependent manner, but the authors did not observe an effect on proliferation induced by the mixed lymphocyte reaction (Pachler et al., 2017). MSC exosomes also suppress the proliferation of both B and Natural Killer cells (Di Trapani et al., 2016). MSC derived EVs were added to PBMCs and sorted T, B, and Natural Killer cells (Di Trapani et al., 2016). In a mixed culture, exosomes are mostly taken up by monocytes, although more EVs were taken up by T, B, or NK cells if applied to a pure culture of said cells (Di Trapani et al., 2016). Additionally, EVs from both resting and IFN-y primed MSCs decreased the proliferation of B and NK cells, although those from IFN-y primed MSCs were more efficacious (Di Trapani et al., 2016).

MSC-derived exosomes have also been shown to encourage the development of regulatory T-cells. When they were applied to THP-1 cells, the THP-1 cells were shifted towards production of anti-inflammatory cytokines and polarized CD4+ T-cells to regulatory T-cells. The increase in T-regs was also consistent when the exosomes were used to treat a mouse allogeneic skin graft (B. Zhang et al., 2014). In another study,

when MSCs were stimulated with IFNy and TGF-B, their exosomes increased the incidence of T-regs in PBMCs. They found that this effect on T-regs was accompanied by an increase in IDO in the exosomes (Q. Zhang et al., 2018). IDO has previously been suggested as a means for MSC immunosuppression (Chinnadurai, Copland, Patel, & Galipeau, 2014). Interestingly, MSC-EVs are more effective at inducing T-reg formation than their parent cells (Cosenza, Ruiz, Maumus, Jorgensen, & Noel, 2017; Del Fattore et al., 2015).

MSC exosomes whose parent cells are treated with LPS have been shown to modify macrophage polarization (Ti et al., 2015). THP-1 cells increased their production of anti-inflammatory cytokines such as IL-10 and TGF-B, and decreased production of the inflammatory cytokines IL-1, IL-6, and TNFa 48 hours after treatments with the exosomes (Ti et al., 2015). Additionally, their expression of CD163 was higher, further indicating an anti-inflammatory M2 macrophage polarization (Ti et al., 2015). This was found to be at least partially regulated by the miRNA let-7b through the transcription factor STAT3 (Ti et al., 2015). The effect on M2 macrophage polarization was demonstrated in vivo in chronic wounds of diabetic rats (Ti et al., 2015). Wounds treated with exosomes had less inflammatory cell infiltration and more M2 macrophages at 3 days post-treatment, and a smaller wound diameter at 14 days post-treatment compared to untreated controls (Ti et al., 2015).

As shown above, MSC derived EVs have a variety of anti-inflammatory effects. They inhibit the proliferation of inflammatory cytokines and T, B, and Natural Killer cells by encouraging anti-inflammatory M2 macrophage polarization. Additionally, they are more effective than their parent cells at inducing anti-inflammatory T-reg formation. As

shown in the previous section, many of these effects are beneficial for fracture healing. It logical that MSC EVs may also have these effects when they are introduced to the bone fracture environment.

4.5 CONCLUSIONS

The challenges of whole MSC transplantation have prompted interest in the elements of their secretome, of which EVs have been found to play a significant functional role. EVs may bypass many of the challenges associated with MSCs, as they avoid many of the safety and manufacturing concerns live cell transplantation poses, while replicating many of their effects. They can induce osteogenic differentiation of MSCs and osteoblasts and have been used to repair critical-sized defects in rodent models. They are also potent regulators of immune activity and are more effective than their parent cells at inducing T-reg formation.

While extracellular vesicles show promise for bone regeneration, there is much that remains to be understood about their mechanisms of action. It is important that we recognize they can have far-reaching effects on many bodily systems. This includes the immune system, which is inextricably intertwined with the regeneration of bone and other tissue and has already been shown to be greatly impacted by EVs. Considering the effect of a potential EV therapy on T-cell proliferation, T-reg frequency, and cytokine production could be an important differential between positive results in vitro and negative results in vivo. As the study of EV-mediated fracture healing progresses, investigators would do well to include endpoints assessing immune cell response in addition to more traditional measures of bone repair.

REFERENCES

Ami R. Amini, C. T. L., Syam P. Nukavarapu. (2012). Bone Tissue Engineering: Recent Advances and Challenges. *Crit Rev Biomed Eng., 40*(5), 363-408.

Bastian, O. W., Croes, M., Alblas, J., Koenderman, L., Leenen, L. P. H., & Blokhuis, T. J. (2018). Neutrophils Inhibit Synthesis of Mineralized Extracellular Matrix by Human Bone Marrow-Derived Stromal Cells In Vitro. *Front Immunol, 9*, 945. doi:10.3389/fimmu.2018.00945

Bastian, O. W., Mrozek, M. H., Raaben, M., Leenen, L. P. H., Koenderman, L., & Blokhuis, T. J. (2018). Serum from the Human Fracture Hematoma Contains a Potent Inducer of Neutrophil Chemotaxis. *Inflammation, 41*(3), 1084-1092. doi:10.1007/s10753-018-0760-4

Campana, V., Milano, G., Pagano, E., Barba, M., Cicione, C., Salonna, G., . . . Logroscino, G. (2014). Bone substitutes in orthopaedic surgery: from basic science to clinical practice. *J Mater Sci Mater Med, 25*(10), 2445-2461. doi:10.1007/s10856-014-5240-2

Camussi, G., Deregibus, M. C., & Cantaluppi, V. (2013). Role of stem-cell-derived microvesicles in the paracrine action of stem cells. *Biochem Soc Trans, 41*(1), 283-287. doi:10.1042/bst20120192

Chinnadurai, R., Copland, I. B., Patel, S. R., & Galipeau, J. (2014). IDO-Independent Suppression of T Cell Effector Function by IFN-γ–Licensed Human Mesenchymal Stromal Cells. *The Journal of Immunology, 192*(4), 1491-1501. doi:10.4049/jimmunol.1301828

Colombo, M., Raposo, G., & Thery, C. (2014). Biogenesis, secretion, and intercellular interactions of exosomes and other extracellular vesicles. *Annu Rev Cell Dev Biol, 30*, 255-289. doi:10.1146/annurev-cellbio-101512-122326

Cosenza, S., Ruiz, M., Maumus, M., Jorgensen, C., & Noel, D. (2017). Pathogenic or Therapeutic Extracellular Vesicles in Rheumatic Diseases: Role of Mesenchymal Stem Cell-Derived Vesicles. *Int J Mol Sci, 18*(4). doi:10.3390/ijms18040889

Del Fattore, A., Luciano, R., Pascucci, L., Goffredo, B. M., Giorda, E., Scapaticci, M., . . . Muraca, M. (2015). Immunoregulatory Effects of Mesenchymal Stem Cell-Derived Extracellular Vesicles on T Lymphocytes. *Cell Transplant, 24*(12), 2615-2627. doi:10.3727/096368915x687543

Di Trapani, M., Bassi, G., Midolo, M., Gatti, A., Kamga, P. T., Cassaro, A., . . . Krampera, M. (2016). Differential and transferable modulatory effects of mesenchymal stromal cell-derived extracellular vesicles on T, B and NK cell functions. *Sci Rep, 6*, 24120. doi:10.1038/srep24120

Flynn, J. (2011). Fracture Repair and Bone Grafting. In *OKU 10: Orthopaedic Knowledge Update* (Vol. 11-21). Rosemount, IL: American Academy of Orthopaedic Surgeons.

Furuta, T., Miyaki, S., Ishitobi, H., Ogura, T., Kato, Y., Kamei, N., . . . Ochi, M. (2016). Mesenchymal Stem Cell-Derived Exosomes Promote Fracture Healing in a Mouse Model. *Stem Cells Transl Med, 5*(12), 1620-1630. doi:10.5966/sctm.2015-0285

Grange, C., Tapparo, M., Bruno, S., Chatterjee, D., Quesenberry, P. J., Tetta, C., & Camussi, G. (2014). Biodistribution of mesenchymal stem cell-derived extracellular vesicles in a model of acute kidney injury monitored by optical imaging. *International journal of molecular medicine, 33*(5), 1055-1063. doi:10.3892/ijmm.2014.1663

Heijnen, H. F., Schiel, A. E., Fijnheer, R., Geuze, H. J., & Sixma, J. J. (1999). Activated platelets release two types of membrane vesicles: microvesicles by surface shedding and exosomes derived from exocytosis of multivesicular bodies and alpha-granules. *Blood, 94*(11), 3791-3799.

Huang, L., Liu, S., Song, T., Zhang, W., Fan, J., & Liu, Y. (2017). Blockade of Interleukin 6 by Rat Anti-mouse Interleukin 6 Receptor Antibody Promotes Fracture Healing. *Biochemistry (Mosc), 82*(10), 1193-1199. doi:10.1134/s0006297917100121

Jiang, H., Ti, Y., Wang, Y., Wang, J., Chang, M., Zhao, J., & Sun, G. (2018). Downregulation of regulatory T cell function in patients with delayed fracture healing. *Clin Exp Pharmacol Physiol, 45*(5), 430-436. doi:10.1111/1440-1681.12902

Khan, S. N., Cammisa, F. P., Jr., Sandhu, H. S., Diwan, A. D., Girardi, F. P., & Lane, J. M. (2005). The biology of bone grafting. *J Am Acad Orthop Surg, 13*(1), 77-86.

Kim, Y. G., Lee, C. K., Nah, S. S., Mun, S. H., Yoo, B., & Moon, H. B. (2007). Human CD4+CD25+ regulatory T cells inhibit the differentiation of osteoclasts from peripheral blood mononuclear cells. *Biochem Biophys Res Commun, 357*(4), 1046-1052. doi:10.1016/j.bbrc.2007.04.042

Konnecke, I., Serra, A., El Khassawna, T., Schlundt, C., Schell, H., Hauser, A., . . . Schmidt-Bleek, K. (2014). T and B cells participate in bone repair by infiltrating the fracture callus in a two-wave fashion. *Bone, 64*, 155-165. doi:10.1016/j.bone.2014.03.052

Kovtun, A., Bergdolt, S., Hagele, Y., Matthes, R., Lambris, J. D., Huber-Lang, M., & Ignatius, A. (2017). Complement receptors C5aR1 and C5aR2 act differentially during the early immune response after bone fracture but are similarly involved in bone repair. *Sci Rep, 7*(1), 14061. doi:10.1038/s41598-017-14444-3

Li, W., Liu, Y., Zhang, P., Tang, Y., Zhou, M., Jiang, W., . . . Zhou, Y. (2018). Tissue-Engineered Bone Immobilized with Human Adipose Stem Cells-Derived Exosomes Promotes Bone Regeneration. *ACS Appl Mater Interfaces, 10*(6), 5240-5254. doi:10.1021/acsami.7b17620

Lu, Z., Chen, Y., Dunstan, C., Roohani-Esfahani, S., & Zreiqat, H. (2017). Priming Adipose Stem Cells with Tumor Necrosis Factor-Alpha Preconditioning Potentiates Their

Exosome Efficacy for Bone Regeneration. *Tissue Eng Part A, 23*(21-22), 1212-1220. doi:10.1089/ten.tea.2016.0548

Martins, M., Ribeiro, D., Martins, A., Reis, R. L., & Neves, N. M. (2016). Extracellular Vesicles Derived from Osteogenically Induced Human Bone Marrow Mesenchymal Stem Cells Can Modulate Lineage Commitment. *Stem Cell Reports, 6*(3), 284-291. doi:10.1016/j.stemcr.2016.01.001

Narayanan, R., Huang, C. C., & Ravindran, S. (2016). Hijacking the Cellular Mail: Exosome Mediated Differentiation of Mesenchymal Stem Cells. *Stem Cells Int, 2016*, 3808674. doi:10.1155/2016/3808674

Ono, T., & Takayanagi, H. (2017). Osteoimmunology in Bone Fracture Healing. *Curr Osteoporos Rep, 15*(4), 367-375. doi:10.1007/s11914-017-0381-0

Pachler, K., Ketterl, N., Desgeorges, A., Dunai, Z. A., Laner-Plamberger, S., Streif, D., . . . Gimona, M. (2017). An In Vitro Potency Assay for Monitoring the Immunomodulatory Potential of Stromal Cell-Derived Extracellular Vesicles. *Int J Mol Sci, 18*(7). doi:10.3390/ijms18071413

Qi, X., Zhang, J., Yuan, H., Xu, Z., Li, Q., Niu, X., . . . Li, X. (2016). Exosomes Secreted by Human-Induced Pluripotent Stem Cell-Derived Mesenchymal Stem Cells Repair Critical-Sized Bone Defects through Enhanced Angiogenesis and Osteogenesis in Osteoporotic Rats. *Int J Biol Sci, 12*(7), 836-849. doi:10.7150/ijbs.14809

Qin, Y., Wang, L., Gao, Z., Chen, G., & Zhang, C. (2016). Bone marrow stromal/stem cell-derived extracellular vesicles regulate osteoblast activity and differentiation in vitro and promote bone regeneration in vivo. *Scientific Reports, 6*, 21961. doi:10.1038/srep21961

Raposo, G., & Stoorvogel, W. (2013). Extracellular vesicles: exosomes, microvesicles, and friends. *J Cell Biol, 200*(4), 373-383. doi:10.1083/jcb.201211138

Recknagel, S., Bindl, R., Brochhausen, C., Gockelmann, M., Wehner, T., Schoengraf, P., . . . Ignatius, A. (2013). Systemic inflammation induced by a thoracic trauma alters the

cellular composition of the early fracture callus. *J Trauma Acute Care Surg, 74*(2), 531-537. doi:10.1097/TA.0b013e318278956d

Reinke, S., Geissler, S., Taylor, W. R., Schmidt-Bleek, K., Juelke, K., Schwachmeyer, V., . . . Duda, G. N. (2013). Terminally differentiated CD8(+) T cells negatively affect bone regeneration in humans. *Sci Transl Med, 5*(177), 177ra136. doi:10.1126/scitranslmed.3004754

Rozmyslowicz, T., Majka, M., Kijowski, J., Murphy, S. L., Conover, D. O., Poncz, M., . . . Ratajczak, M. Z. (2003). Platelet- and megakaryocyte-derived microparticles transfer CXCR4 receptor to CXCR4-null cells and make them susceptible to infection by X4-HIV. *Aids, 17*(1), 33-42. doi:10.1097/01.aids.0000042948.95433.3d

Simpson, R. J., Jensen, S. S., & Lim, J. W. (2008). Proteomic profiling of exosomes: current perspectives. *Proteomics, 8*(19), 4083-4099. doi:10.1002/pmic.200800109

Teng, X., Chen, L., Chen, W., Yang, J., Yang, Z., & Shen, Z. (2015). Mesenchymal Stem Cell-Derived Exosomes Improve the Microenvironment of Infarcted Myocardium Contributing to Angiogenesis and Anti-Inflammation. *Cell Physiol Biochem, 37*(6), 2415-2424. doi:10.1159/000438594

Ti, D., Hao, H., Tong, C., Liu, J., Dong, L., Zheng, J., . . . Han, W. (2015). LPS-preconditioned mesenchymal stromal cells modify macrophage polarization for resolution of chronic inflammation via exosome-shuttled let-7b. *J Transl Med, 13*, 308. doi:10.1186/s12967-015-0642-6

Toben, D., Schroeder, I., El Khassawna, T., Mehta, M., Hoffmann, J. E., Frisch, J. T., . . . Duda, G. N. (2011). Fracture healing is accelerated in the absence of the adaptive immune system. *J Bone Miner Res, 26*(1), 113-124. doi:10.1002/jbmr.185

Vishnubhatla, I., Corteling, R., Stevanato, L., Hicks, C., & Sinden, J. (2014). The Development of Stem Cell-derived Exosomes as a Cell-free Regenerative Medicine. *Journal of Circulating Biomarkers*, 1. doi:10.5772/58597

Wang, X., Omar, O., Vazirisani, F., Thomsen, P., & Ekstrom, K. (2018). Mesenchymal stem cell-derived exosomes have altered microRNA profiles and induce osteogenic differentiation depending on the stage of differentiation. *PLoS One, 13*(2), e0193059. doi:10.1371/journal.pone.0193059

Yu, B., Zhang, X., & Li, X. (2014). Exosomes derived from mesenchymal stem cells. *Int J Mol Sci, 15*(3), 4142-4157. doi:10.3390/ijms15034142

Zara, J. N., Siu, R. K., Zhang, X., Shen, J., Ngo, R., Lee, M., . . . Soo, C. (2011). High doses of bone morphogenetic protein 2 induce structurally abnormal bone and inflammation in vivo. *Tissue Eng Part A, 17*(9-10), 1389-1399. doi:10.1089/ten.TEA.2010.0555

Zhang, B., Yin, Y., Lai, R. C., Tan, S. S., Choo, A. B., & Lim, S. K. (2014). Mesenchymal stem cells secrete immunologically active exosomes. *Stem Cells Dev, 23*(11), 1233-1244. doi:10.1089/scd.2013.0479

Zhang, C., Li, L., Feng, K., Fan, D., Xue, W., & Lu, J. (2017). 'Repair' Treg Cells in Tissue Injury. *Cell Physiol Biochem, 43*(6), 2155-2169. doi:10.1159/000484295

Zhang, J., Liu, X., Li, H., Chen, C., Hu, B., Niu, X., . . . Wang, Y. (2016). Exosomes/tricalcium phosphate combination scaffolds can enhance bone regeneration by activating the PI3K/Akt signaling pathway. *Stem Cell Res Ther, 7*(1), 136. doi:10.1186/s13287-016-0391-3

Zhang, Q., Fu, L., Liang, Y., Guo, Z., Wang, L., Ma, C., & Wang, H. (2018). Exosomes originating from MSCs stimulated with TGF-beta and IFN-gamma promote Treg differentiation. *J Cell Physiol, 233*(9), 6832-6840. doi:10.1002/jcp.26436

CHAPTER 5

ACIDIC PRECONDITIONED MSCS PRODUCE EXTRACELLULAR VESICLES THAT INCREASE REGULATORY T-CELL FREQUENCY IN VITRO[3]

[3] Seth Andrews, Timothy Maughon, Steven Stice. To be submitted to the Journal of Immunology and Regenerative Medicine.

5.1 ABSTRACT

Despite several decades of research concerning mesenchymal stem cells, they have been difficult to translate to clinical use. Extracellular vesicles are thought be responsible for a large portion of MSCs' beneficial effects, including immunosuppression. MSCs and their EVs have been shown to respond to different culture environments. We cultured MSCs in different aspects of the injury microenvironment and compared the characteristics of their EVs as well as their uptake by and suppression of different T-cell subsets. We found that MSCs and their EVs interact very differently with T-cells and showed for the first time that EVs from acidic preconditioned MSCs increase regulatory T-cell frequency in vitro. We conclude that this provides an interesting avenue for future therapeutics, although further research will be required to determine its mechanisms.

5.2 INTRODUCTION

Mesenchymal stem cells (mesenchymal stromal cells, MSCs) have been the focus of a great deal of the tissue engineering and regenerative medicine research over the past two decades. Initially of interest for differentiation and transplantation, they have recently been valued for the pro-regenerative and ani-inflammatory properties of their secretome (Yeo et al., 2013). MSC conditioned media has improved healing of myriad conditions, including bone defects, myocardial infarction, osteoarthritis, and colitis (Vizoso, Eiro, Cid, Schneider, & Perez-Fernandez, 2017). Despite this, there have been numerous challenges in translating their potential to clinical success, including storage and safety issues. Recently thawed MSCs have found to have diminished efficacy and increased need for a recovery when compared to non-thawed MSCs. Additionally,

transplantation of any live dividing cells raises concerns about tumorgenicity (Galipeau, 2013; Volarevic et al., 2018). Extracellular vesicles (EVs) derived from the MSC secretome, found in the accompanying conditioned media of MSCs, have emerged as a potential answer to some of these challenges.

Extracellular vesicles are nanoscale vesicles secreted by cells for intercellular signaling via the transfer of bioactive molecules including RNA, proteins, and lipids (Camussi, Deregibus, Bruno, Cantaluppi, & Biancone, 2010). They include exosomes, which are released through fusion of intracellular multivesicular bodies with the plasma membrane, and microparticles, which bud directly from the plasma membrane (Colombo, Raposo, & Thery, 2014). EVs are produced by all cells, but those derived from MSCs have shown regenerative effects in a wide range of applications. MSC-derived EVs have improved recovery from myocardial ischemia and reperfusion injury (Lai et al., 2010), stroke (Xin et al., 2013), gentamicin induced acute kidney injury (Reis et al., 2012), and allogeneic skin grafts (B. Zhang et al., 2014) in vivo. Being acellular, EVs are not subject to many of the safety concerns MSCS are, and they are easier to characterize and standardize for therapeutic use (Vishnubhatla, Corteling, Stevanato, Hicks, & Sinden, 2014). There is also substantial evidence that the cargo and function of EVs can be influenced by the extracellular environment of their parent cells, potentially increasing their therapeutic potency (de Jong et al., 2012; Kucharzewska & Belting, 2013).

MSCs respond to inflammatory environments by upregulating their regenerative and anti-inflammatory properties. This response encompasses a wide range of factors, including upregulation of VEGF, IDO, TGF-B, and PGE2 (Madrigal, Rao, & Riordan, 2014). The injury microenvironment is often characterized by local hypoxia and acidosis,

as well as the presence of inflammatory cytokines such as TNF-α and IFN-γ. Inflammatory and hypoxic preconditioning has also been shown to increase the potency of EV immunomodulation (Di Trapani et al., 2016; Lo Sicco et al., 2017; Q. Zhang et al., 2018). However, acidic preconditioning has not been investigated in this manner, and different treatments have not been compared within the same study.

The objectives of this study were to compare the effects of different aspects of an inflammatory environment on MSC-EVs and compare their immunomodulation to each other as well as their parent cells. We found that preconditioning has significant effects on EV secretion, size, and surface markers. Additionally, while their parent MSCs are suppressive of effector T-cells, EVs from MSCs cultured in an acidic environment induce the formation of regulatory T-cells. These findings contribute to evidence of EV alteration by the extracellular environment and provide new avenues for both therapeutic applications and understanding of EV biogenesis.

5.3 METHODS

Cell culture and preconditioning

Human umbilical MSCs (Lifeline Cell Technologies) were plated at 5000 cells/cm^2 on tissue culture flasks in complete medium (Alpha-Minimum Essential Medium (Gibco), 10% defined fetal bovine serum (Hyclone), 2 mM L-glutamine, 50 U/mL penicillin, 50 µg/mL streptomycin (all from Gibco/Invitrogen)) and allowed to grow to 80% confluence (20,000–25,000 cells/cm^2). They were harvested using 0.05% trypsin (Gibco) and replated. All proliferation cultures were maintained at 37°C and at 5% CO_2.

Several environments were used to precondition the MSCs when they reached 80% confluence (S1). Metabolic acidosis was induced through the addition of HCl to

complete media to bring the pH to ~7.1. These MSCs were termed LPH-MSCs, with their EVs being LPH-EV. A hypoxic environment was created by placing the cell culture vessels in a hypoxia incubator chamber (STEMCELL Technologies, Cambridge MA), which was then filled with a gas mixture containing 2% O_2, 5% CO_2, and 93% N_2 (Airgas). The MSCs undergoing this preconditioning were LO2-MSCs, and their EVs were LO2-EV. An inflammatory environment was created by adding the cytokines TNF-a and IFN-y (Sigma) to the media at 15 and 20 ng/mL, respectively. These MSCs were named INF-MSCs, with their EVs being INF-EV. These environments were used separately to precondition MSCs for 48 hours at 37°C prior to receiving exosome isolation media or being place in co-culture with PBMCs. Control MSCs remained in normal culture as described above for 48 hours. They and their EVs were NC-MSC and NC-EV, respectively.

Peripheral blood mononuclear cells (PBMCs, STEMCELL Technologies, Cambridge MA) were thawed into RPMI media (RPMI 1640, 10% FBS, 50 U/mL penicillin, 50 µg/mL streptomycin) and rested overnight at 37°C and at 5% CO_2 prior to use in experiments.

Exosome isolation and characterization

After preconditioning, MSCs were rinsed twice with PBS before adding fresh serum free medium (Alpha-Minimum Essential Medium (Gibco), 2 mM L-glutamine, 50 U/mL penicillin, 50 µg/mL streptomycin (all from Gibco/Invitrogen)) and incubating for 24 hours. The resulting conditioned media were collected and passed through 0.22 µm filters to remove cells and large debris. The media were then subjected to ultrafiltration with a 100kDa MWCO (Amicon, Millipore-Sigma) at 4000g for 10 minutes. The EVs remained

on top of the filter and were then washed twice with PBS +/+ (Thermo Fisher Scientific, Waltham, MA) at 2000g for 10 minutes. The EVs in PBS+/+ were then collected, aliquoted, and frozen at -20^{o}C.

For each exosome isolation, nanoparticle tracking analysis (NTA) was performed using a Nanosight NS3200 (Nanosight, Salisbury UK) according to the manufacturer's recommendations. A minimum of three samples and five one-minute analysis runs were performed for each exosome isolation.

Surface marker characterization was performed using the MACSPLEX Exosome Kit (Miltenyi Biotec, Bergisch Gladbach, Germany) according to the manufacturer's directions. An equal number of exosomes as determined by NTA were loaded from each isolation in triplicate.

Immunomodulation assay

For MSC co-culture wells, MSCs were plated at 20,000 cells/cm^2 in complete medium and allowed to adhere overnight. They were then subjected to preconditioning as previously described, followed by two PBS -/- washes.

PBMCs were stained with Carboxyfluorescein succinimidyl ester (CFSE, Thermo Fisher Scientific, Waltham, MA) according to the manufacturer's instructions for the T-cell suppression assay, or left unstained for the EV uptake assay, and 500,000 were added to each well. Stimulating anti-CD3/CD28 Dynabeads (Thermo Fisher Scientific, Waltham, MA) were added at 500,000 each per well. 10^9 EVs were added to the appropriate wells. For the uptake assay, EVs were stained with CFSE (Thermo Fisher Scientific, Waltham, MA) following a protocol modified from Morales-Kastresana (Morales-Kastresana et al., 2017).

The assays took place in complete RPMI medium formulated as above, but with EV-depleted FBS. EVs were depleted by centrifuging FBS at 100,000g for 1 hour at 4C (Sorvall WX Ultra 80, Thermo Fisher Scientific, Waltham, MA) and using the supernatant (Li 2017).

The cultures incubated for 24 hours in the case of the uptake experiments, and for 5 days in the case of the T-cell suppression experiments. Cultures were maintained at 37C, 5%CO_2 for the duration of the experiments.

Following incubation, the PBMCs were harvested and stained for flow cytometry using one of two panels. Panel 1 was composed of Pacific Blue anti-CD4, APC anti-CD8, Brilliant Violet 711 anti-CD25, and PE anti-FOXP3. Panel 2 included Pacific Blue anti-CD4, APC anti-CD8, PE anti-IFN-γ, and Brilliant Violet 711 anti-TNF-α. PBMCs were first washed, then stained with Zombie Yellow viability dye, blocked with 2% FBS and FC receptors blocked with Trustain FcX. They were then stained for CD4, CD8, and CD25 as appropriate at room temperature in the dark for 30 minutes and fixed in 4% PFA for Panel 2 or FOXP3 TrueNuclear fix for Panel 1 before storing overnight in the dark at 4C. Panel 1 was then permeabilized with TrueNuclear permeabilization buffer and stained for FOXP3 according to the manufacturer's directions. Panel 2 was permeabilized with Permwash (BD Biosciences) and stained for IFN-γ and TNF-α. Samples were resuspended in 2% FBS at 4C in the dark for up to 2 days before flow analysis. All antibodies and reagents were from Biolegend (San Diego, CA) unless otherwise specified and were used at previously titrated optimal concentrations.

Flow Cytometry

All flow analysis was performed using a CytoFLEX S (Beckman Coulter, Hialeah, Florida), with 20,000 events collected per sample for the uptake and immunosuppression assays (S2). All data was analyzed using FlowJo software (Treestar, Inc., Ashland, Oregon). Cellular debris, activating beads, and doublets were gated out via scatter properties. Single-stain controls were used to generate compensation matrices, and Fluorescence-minus one controls were used to determine positive populations of Zombie Yellow negative cells. Example scatter plots for the gating strategy are shown in Fig. S2.

All activation parameters of T-cells including CD25, FOXP3, TNF-α, and IFN-γ expression were normalized according to Equation 5.1, so that fully activated samples have an average value of 100 and fully suppressed samples have an average value of 0 (Klinker, Marklein, Lo Surdo, Wei, & Bauer, 2017). T-cell proliferation was calculated according to Equation 5.2, where MI is the median fluorescence intensity of samples, and PS is the proliferation score (Asquith et al., 2006).

Statistics

All data is expressed as mean +/- SEM, with all experiments performed in triplicate. All statistical tests were one-way ANOVA against controls unless stated otherwise with Dunnett's post-hoc test using Prism (Graphpad, San Diego CA).

5.4 RESULTS

Exosome characterization

NTA analysis of EVs showed monomodal size distributions typical of exosomes for NC-EV, LO2-EV, and LPH-EV (Fig. 1A-C). The size distribution of INF-EV was bimodal, with a small diameter population consistent with exosomes in addition to a larger diameter population (Fig. 1D). This is reflected in the mean sizes of the EVs, in which

INF-EV had a significantly higher mean diameter than NC-EV ($p<0.0001$), while LPH-EV and LO2-EV did not differ in size from the control (Fig. 1E). DLS analysis was used to confirm the presence of a larger population in the INF-EV group and generated similar results, despite interference from the bimodal distribution (S3). NTA analysis also revealed significantly higher EV production per cell from LO2-MSC ($p<0.0001$) and LPH-EV ($p = 0.0028$) compared to NC-MSC (Fig. 1F).

Surface marker characterization via MACSPLEX analysis revealed significant changes in the expression of EV surface markers in the preconditioned groups compared to the NC-EV group (Fig. 2). CD9, CD63, and CD81 exosome markers were present all the EV groups, although to varying degrees. CD63 was elevated in LPH-EV ($p = 0.002$), LO2-EV ($p= 0.0076$), and INF-EV ($p < 0.0001$). CD9 was decreased in LO2-EV ($p = 0.0374$) and INF-EV ($p < 0.0001$), while CD81 was decreased in LO2-EV ($p = 0.0004$) and INF-EV ($p < 0.0001$). INF-EV had greatly decreased expression of CD29 (Integrin beta-1, $p < 0.0001$), CD44 ($p < 0.0001$), CD49e (Integrin alpha-5, $p < 0.0001$), CD105 (Endoglin, $p < 0.0001$), and melanoma-associated chondroitin sulfate proteoglycan (MCSP, $p < 0.0001$). On the other hand, LO2-EV were significantly elevated in their expression of MCSP ($p < 0.0001$), CD44 ($p < 0.0001$), and CD29 ($p = 0.0002$) compared to NC-EV. LPH-EV had significantly lower expression of CD29 ($p = 0.0354$).

Exosome Uptake

CFSE-labeled exosome uptake was determined by %CFSE+ cells from each population at 24 hours post-treatment. LPH-EV had the highest uptake in all groups (Fig. 3). Percent CFSE+ cells was significantly greater than the untreated control LPH-EV treated cells for helper T-cells ($p = 0.0126$, Fig. 3A), cytotoxic T-cells ($p = 0.0115$, Fig.

3B), activated helper T-cells, ($p = 0.0111$, Fig. 3C), activated cytotoxic T-cells ($p = 0.0032$, Fig. 3D), CD4+ T-regs (Fig. 3E, $p = 0.0104$), and CD8+ T-regs (Fig. 3F, $p = 0.0055$). Notably, uptake was lowest in non-T-cells (Fig. 3G).

Proliferation

All MSC groups tended to decrease T-cell proliferation (Fig. 4). This effect was significant in CD8+ cells for INF-MSC ($p = 0.0012$), LO2-MSC ($p < 0.0001$), LPH-MSC ($p < 0.0001$), and NC-MSC ($p < 0.001$).

T-cell activation at 5 days

PBMCs were subjected to flow analysis to determine T-cell activation after 5 days incubation. CD25 expression in helper T-cells was significantly reduced by INF-MSC ($p<0.0001$), LO2-MSC ($p = 0.001$), LPH-MSC ($p = 0.009$), and NC-MSC ($p = 0.001$) co-culture, while LPH-EV reduced it but was not significant (Fig. 5A). CD25 expression was similarly reduced in cytotoxic T-cells by INF-MSC ($p = 0.013$), LO2-MSC ($p = 0.040$), LPH-MSC ($p = 0.018$), and NC-MSC ($p = 0.012$) co-culture, while LPH-EV reduced it but was not significant (Fig. 5B). The incidence of T-regs was increased by LPH-EV for both CD4+ ($p = 0.061$) and CD8+ ($p = 0.030$) cells, while it tended to be decreased by MSC groups (Fig. 5C-D). Frequency of T-cell subsets was unaffected 24 hours post-treatment (S4). All MSC groups tended to decrease TNF-α and IFN-γ expression in both helper T-cells and cytotoxic T-cells, but the only significant reductions were by LPH-MSC ($p = 0.029$) and NC-MSC ($p = 0.035$) on IFN-γ in cytotoxic T-cells (Fig. 5E-H).

5.5 DISCUSSION

The interactions between EVs, their parent cells, and their target cells are just beginning to be explored. However, there is growing evidence that the MSC

microenvironment has substantial effects on the function of their secreted EVs. In this study, we investigated the effects of different aspects of the injury microenvironment on MSCs and their secreted EVs. We found that while the number, size, and surface markers of secreted EVs varied substantially with preconditioning treatments, only those from acidosis preconditioned MSCs had any immunosuppressive effects.

EV biogenesis and secretion is known to take place through several mechanisms, including ESCRT, sphingomyelinases, RAB GTPases, and SNARE proteins (Colombo et al., 2014). Sphingomyelinases have been shown to contribute to the biogenesis and release of MSC-EVs, and their activity is known to be affected by pH (Menck et al., 2017; S. S. Tan et al., 2013). EV release and uptake of cancer cells increases when cultured in low pH, but a mechanism for this has not been discovered (Parolini et al., 2009). Hypoxia and TNF-α/IFN-γ treatment have both been shown to increase EV release from MSCs (Di Trapani et al., 2016; Lo Sicco et al., 2017). This is the first instance of increased EV secretion by MSCs in an acidic environment. More work is needed to determine if this is a specific therapeutic response or a simpler matter of increased enzyme activity.

Different classifications of EVs are differentiated from one another largely by their sizes. Exosomes range from 50-150nm, while microparticles, which bud from the plasma membrane, can be up to 1um in diameter (Colombo et al., 2014). This could be the source of the large-diameter population of EVs present in the INF-MSC-EVs. EVs from both IFN-γ and TNF-α/IFN-γ preconditioned MSCs have been observed with right-skewed size distributions previously (Di Trapani et al., 2016; Goncalves et al., 2017). The biogenesis of microparticles differs from that of exosomes, and their function has been shown to differ as well (Cosenza, Ruiz, Maumus, Jorgensen, & Noel, 2017). If INF-EV contain a

significant population of microparticles, this could affect the overall potency of the EV population, possibly explaining the lack of immunomodulation by that group compared to other studies.

Cellular recognition and uptake of EVs is regulated at least in part by their surface markers, which can vary based on the environment of their parent cells. CD54 (ICAM-1), CD106 (VCAM-1), and CD274 (PDL-1) were upregulated in TNF-α/IFN-γ primed MSC-EVs (Di Trapani et al., 2016). All three are important to cell-contact mediated immunomodulation by MSCs (English, Barry, Field-Corbett, & Mahon, 2007; X. Fu et al., 2009; Ren et al., 2010). In another study, EVs from hypoxia-conditioned MSCs had increased CD63 expression, while CD105 expression was unchanged (Lo Sicco et al., 2017). On the other hand, IFN-γ + TGF-β stimulation of MSCs did not change the expression of their surface markers (Q. Zhang et al., 2018). We observed decreases in adhesion-related markers in INF-EV, while the same markers were upregulated in LO2-EV. Many of these markers are commonly expressed on MSCs, and these changes in expression by their EVs may reflect a similar change in the parent cells, as EV membrane composition is partially derived from them (Chaput & Thery, 2011). The changes we observed between EV groups could be partially responsible for their differential uptake by PBMCs.

MSC-EV uptake and their immunomodulation of different immune cell types is an active area of research. In one study, MSC-EVs were primarily taken up by macrophages, which were directed to the anti-inflammatory M2 type and inhibited the growth of other cells. The EVs decreased proliferation of B and NK cells, and had little effect on the proliferation of T-cells (Di Trapani et al., 2016). Additionally, MSC-EV uptake by

monocytes has been associated with apoptosis of those monocytes within 24 hours post-treatment (Goncalves et al., 2017). The results of this study run counter, with very little MSC-EV uptake by non-T-cells observed. Our results are more in agreement with another study in which MSC-EVs applied to PBMCs have also consistently associated with T-cells compared to macrophages or NK cells, decreased T-cell proliferation, increased IL-10 expression, and increased T-regs (Del Fattore et al., 2015). This increase has been reported elsewhere as well (Q. Zhang et al., 2018). While several groups have investigated MSC-EV uptake by subsets of immune cells, this study is the first to examine differential uptake by effector and regulatory T-cells. The noted differences in surface marker expression may contribute to the differential uptake by T-cell subsets of the preconditioned EV groups. It should also be noted that the immune cells in the studies referenced here were stimulated with a variety of methods, which have varying degrees of relevance and effectiveness (Roh, 2018). Further work will be required to determine the causes of differential EV uptake.

MSC preconditioning with inflammatory cytokines or hypoxia is widely used to "prime" their immunomodulatory capabilities, and this has begun to be investigated in their secreted EVs as well. TNF-α and IFN-γ primed MSCs were significantly more efficacious in their inhibition of T, B, and NK cell proliferation than their resting counterparts. EVs from primed MSCs also inhibited the proliferation of B and NK cells more so than those from resting ones (Di Trapani et al., 2016). EVs from MSCs in hypoxic preconditioning were more effective than their resting counterparts in inducing macrophage proliferation and type 2 macrophage polarization (Lo Sicco et al., 2017). When MSCs were primed with IL-1β, their EVs decreased TNF-α, and increased IL-10

expression in macrophages, compared to both stimulated control macrophages and those treated with EVs from resting MSCs (Song et al., 2017). TGF-β and IFN-γ stimulated MSCs produced EVs that were more effective in inducing T-reg formation than those from resting MSCs (Q. Zhang et al., 2018).

To our knowledge, this is the first study showing changes in MSC-EV immunomodulation through acidic preconditioning. However, the effect of environmental pH on MSCs has previously been investigated regarding their interactions with various cancers. MSCs cultured in an acidic environment enhanced *in vivo* melanoma growth, partly through their increased expression of TGF-B (Peppicelli et al., 2015). TGF-B is a potent growth factor and has been shown to induce the formation of T-regs (S. Fu et al., 2004). Acidic conditioned MSCs upregulated osteosarcoma expression of CXCL5 and CCL5 (Avnet et al., 2017). These chemokines have also been implicated the formation and recruitment of T-regs, respectively (Shi et al., 2014; M. C. B. Tan et al., 2009; Wang et al., 2016). The acidic tumor microenvironment has also been shown to increase the release of EVs from cancer cells (Ban, Lee, Im, & Kim, 2015; Parolini et al., 2009). These findings may help explain the increased incidence of T-regs when treated with acidic preconditioned MSC-EVs and provide avenues for future research.

This study was focused on differences in the secretion, uptake, and potency of EVs, and thus did not assay their nucleic acids. However, MSC derived EVs contain a wide range of micro RNAs (miRNAs), most of which are associated with angiogenesis and tissue remodeling (Ferguson et al., 2018). Certain miRNAs have been shown to have increased frequency in EVs whose parent MSCs were preconditioned with some aspect of the inflammatory environment. When MSCs were stimulated with TNF-α and IFN-γ,

miRNA-155 was increased in their EVs (Di Trapani et al., 2016). Similarly, IL-1β preconditioning of MSCs upregulated miR-146a, which has previously been shown to regulate the T-cell response through the NFκβ pathway (Meisgen et al., 2014; Song et al., 2017). MSCs cultured in hypoxia have increased miR-223, miR-146b, miR126, and miR199a (Lo Sicco et al., 2017). It is possible that the upregulation of T-regs by LPH-EVs is due to change in their miRNA content; this warrants further study.

We observed MSCs suppressing T-cell activation much more than their isolated EVs. This is in line with previous studies, which have indicated that MSCs interact with T-cells differently than their isolated EVs. As we observed, MSCs are more effective than their EVs alone at inhibiting T-cell proliferation (Cosenza et al., 2017; Del Fattore et al., 2015; Di Trapani et al., 2016; Pachler et al., 2017). However, inhibition of EV secretion impairs the T-cell proliferation suppression of MSC co-culture, so EVs likely play some role in this process (Di Trapani et al., 2016). Isolated MSC-EVs also induce T-reg formation, even when their parent cells do not (Cosenza et al., 2017; Del Fattore et al., 2015). We observed this phenomenon between the LPH-MSC and LPH-EV groups. There were few differences between the T-cell suppression of different MSC groups in this study. As activated PBMCs create an inflammatory environment of their own, it could be that any effects from the MSCs' previous culture were overridden by cytokines and signals produced by the PBMCs.

Extracellular vesicles remain an emerging field, and there is still wide variation in their isolation and storage, which may have significant effects on their potency. These competing methods of isolation can lose certain populations of EVs, subject them to different stresses, or result in final products with different purities (Li & Hua, 2017). EVs

frozen at -80C after isolation and thawed before use have been found to decrease in immunomodulatory potency (Cosenza et al., 2017). It will be important to optimize these methods to enable proper assessment of EV properties and comparison of EV studies.

The contributors to exosome secretion and function are still being explored. This study shows, for the first time, that MSC-EVs are shifted towards an anti-inflammatory role by an acidic extracellular environment, which could hold great potential to both our understanding of EVs and their eventual translation to therapeutic use. This study adds to a growing body of evidence concerning the enhancement of EV immunosuppression through cues in the extracellular environment of their parent MSCs. However, there is not yet a consensus on which cues significantly impact EV function, and what mechanisms they may work through. Comparison of the miRNA, protein, and lipid cargo of EVs from different preconditioning methods could be a future avenue to examine any possible mechanisms for their differing immunosuppression potencies, as well as comparison across multiple donors and tissue sources.

REFERENCES

Asquith, B., Debacq, C., Florins, A., Gillet, N., Sanchez-Alcaraz, T., Mosley, A., & Willems, L. (2006). Quantifying lymphocyte kinetics in vivo using carboxyfluorescein diacetate succinimidyl ester (CFSE). *Proceedings: Biological Sciences, 273*(1590), 1165-1171. doi:10.1098/rspb.2005.3432

Avnet, S., Di Pompo, G., Chano, T., Errani, C., Ibrahim-Hashim, A., Gillies, R. J., . . . Baldini, N. (2017). Cancer-associated mesenchymal stroma fosters the stemness of osteosarcoma cells in response to intratumoral acidosis via NF-kappaB activation. *International Journal of Cancer, 140*(6), 1331-1345. doi:10.1002/ijc.30540

Ban, J. J., Lee, M., Im, W., & Kim, M. (2015). Low pH increases the yield of exosome isolation. *Biochem Biophys Res Commun, 461*(1), 76-79. doi:10.1016/j.bbrc.2015.03.172

Camussi, G., Deregibus, M. C., Bruno, S., Cantaluppi, V., & Biancone, L. (2010). Exosomes/microvesicles as a mechanism of cell-to-cell communication. *Kidney International, 78*(9), 838-848. doi:10.1038/ki.2010.278

Chaput, N., & Thery, C. (2011). Exosomes: immune properties and potential clinical implementations. *Seminars in Immunopathology, 33*(5), 419-440. doi:10.1007/s00281-010-0233-9

Colombo, M., Raposo, G., & Thery, C. (2014). Biogenesis, secretion, and intercellular interactions of exosomes and other extracellular vesicles. *Annu Rev Cell Dev Biol, 30*, 255-289. doi:10.1146/annurev-cellbio-101512-122326

Cosenza, S., Ruiz, M., Maumus, M., Jorgensen, C., & Noel, D. (2017). Pathogenic or Therapeutic Extracellular Vesicles in Rheumatic Diseases: Role of Mesenchymal Stem Cell-Derived Vesicles. *Int J Mol Sci, 18*(4). doi:10.3390/ijms18040889

de Jong, O. G., Verhaar, M. C., Chen, Y., Vader, P., Gremmels, H., Posthuma, G., . . . van Balkom, B. W. (2012). Cellular stress conditions are reflected in the protein and RNA content of endothelial cell-derived exosomes. *J Extracell Vesicles, 1*. doi:10.3402/jev.v1i0.18396

Del Fattore, A., Luciano, R., Pascucci, L., Goffredo, B. M., Giorda, E., Scapaticci, M., . . . Muraca, M. (2015). Immunoregulatory Effects of Mesenchymal Stem Cell-Derived Extracellular Vesicles on T Lymphocytes. *Cell Transplantation, 24*(12), 2615-2627. doi:10.3727/096368915x687543

Di Trapani, M., Bassi, G., Midolo, M., Gatti, A., Kamga, P. T., Cassaro, A., . . . Krampera, M. (2016). Differential and transferable modulatory effects of mesenchymal stromal cell-derived extracellular vesicles on T, B and NK cell functions. *Sci Rep, 6*, 24120. doi:10.1038/srep24120

English, K., Barry, F. P., Field-Corbett, C. P., & Mahon, B. P. (2007). IFN-gamma and TNF-alpha differentially regulate immunomodulation by murine mesenchymal stem cells. *Immunology Letters, 110*(2), 91-100. doi:10.1016/j.imlet.2007.04.001

Ferguson, S. W., Wang, J., Lee, C. J., Liu, M., Neelamegham, S., Canty, J. M., & Nguyen, J. (2018). The microRNA regulatory landscape of MSC-derived exosomes: a systems view. *Sci Rep, 8*(1), 1419. doi:10.1038/s41598-018-19581-x

Fu, S., Zhang, N., Yopp, A. C., Chen, D., Mao, M., Chen, D., . . . Bromberg, J. S. (2004). TGF-beta induces Foxp3 + T-regulatory cells from CD4 + CD25 - precursors. *American Journal of Transplantation, 4*(10), 1614-1627. doi:10.1111/j.1600-6143.2004.00566.x

Fu, X., Han, B., Cai, S., Lei, Y., Sun, T., & Sheng, Z. (2009). Migration of bone marrow-derived mesenchymal stem cells induced by tumor necrosis factor-α and its possible role in wound healing. *Wound Repair and Regeneration, 17*(2), 185-191. doi:10.1111/j.1524-475X.2009.00454.x

Galipeau, J. (2013). The mesenchymal stromal cells dilemma--does a negative phase III trial of random donor mesenchymal stromal cells in steroid-resistant graft-versus-host disease represent a death knell or a bump in the road? *Cytotherapy, 15*(1), 2-8. doi:10.1016/j.jcyt.2012.10.002

Goncalves, F. D. C., Luk, F., Korevaar, S. S., Bouzid, R., Paz, A. H., Lopez-Iglesias, C., . . . Hoogduijn, M. J. (2017). Membrane particles generated from mesenchymal stromal cells modulate immune responses by selective targeting of pro-inflammatory monocytes. *Sci Rep, 7*(1), 12100. doi:10.1038/s41598-017-12121-z

Klinker, M. W., Marklein, R. A., Lo Surdo, J. L., Wei, C. H., & Bauer, S. R. (2017). Morphological features of IFN-gamma-stimulated mesenchymal stromal cells predict overall immunosuppressive capacity. *Proc Natl Acad Sci U S A, 114*(13), E2598-E2607. doi:10.1073/pnas.1617933114

Kucharzewska, P., & Belting, M. (2013). Emerging roles of extracellular vesicles in the adaptive response of tumour cells to microenvironmental stress. *J Extracell Vesicles, 2*. doi:10.3402/jev.v2i0.20304

Lai, R. C., Arslan, F., Lee, M. M., Sze, N. S., Choo, A., Chen, T. S., . . . Lim, S. K. (2010). Exosome secreted by MSC reduces myocardial ischemia/reperfusion injury. *Stem Cell Res, 4*(3), 214-222. doi:10.1016/j.scr.2009.12.003

Li, N., & Hua, J. (2017). Interactions between mesenchymal stem cells and the immune system. *Cellular and Molecular Life Sciences, 74*(13), 2345-2360. doi:10.1007/s00018-017-2473-5

Lo Sicco, C., Reverberi, D., Balbi, C., Ulivi, V., Principi, E., Pascucci, L., . . . Tasso, R. (2017). Mesenchymal Stem Cell-Derived Extracellular Vesicles as Mediators of Anti-Inflammatory Effects: Endorsement of Macrophage Polarization. *Stem Cells Transl Med, 6*(3), 1018-1028. doi:10.1002/sctm.16-0363

Madrigal, M., Rao, K. S., & Riordan, N. H. (2014). A review of therapeutic effects of mesenchymal stem cell secretions and induction of secretory modification by different culture methods. *Journal of Translational Medicine, 12*, 260. doi:10.1186/s12967-014-0260-8

Meisgen, F., Xu Landen, N., Wang, A., Rethi, B., Bouez, C., Zuccolo, M., . . . Pivarcsi, A. (2014). MiR-146a negatively regulates TLR2-induced inflammatory responses in keratinocytes. *Journal of Investigative Dermatology, 134*(7), 1931-1940. doi:10.1038/jid.2014.89

Menck, K., Sonmezer, C., Worst, T. S., Schulz, M., Dihazi, G. H., Streit, F., . . . Gross, J. C. (2017). Neutral sphingomyelinases control extracellular vesicles budding from the plasma membrane. *J Extracell Vesicles, 6*(1), 1378056. doi:10.1080/20013078.2017.1378056

Morales-Kastresana, A., Telford, B., Musich, T. A., McKinnon, K., Clayborne, C., Braig, Z., . . . Jones, J. C. (2017). Labeling Extracellular Vesicles for Nanoscale Flow Cytometry. *Scientific Reports, 7*(1), 1878. doi:10.1038/s41598-017-01731-2

Pachler, K., Ketterl, N., Desgeorges, A., Dunai, Z. A., Laner-Plamberger, S., Streif, D., . . . Gimona, M. (2017). An In Vitro Potency Assay for Monitoring the Immunomodulatory Potential of Stromal Cell-Derived Extracellular Vesicles. *Int J Mol Sci, 18*(7). doi:10.3390/ijms18071413

Parolini, I., Federici, C., Raggi, C., Lugini, L., Palleschi, S., De Milito, A., . . . Fais, S. (2009). Microenvironmental pH is a key factor for exosome traffic in tumor cells. *J Biol Chem, 284*(49), 34211-34222. doi:10.1074/jbc.M109.041152

Peppicelli, S., Bianchini, F., Toti, A., Laurenzana, A., Fibbi, G., & Calorini, L. (2015). Extracellular acidity strengthens mesenchymal stem cells to promote melanoma progression. *Cell Cycle, 14*(19), 3088-3100. doi:10.1080/15384101.2015.1078032

Reis, L. A., Borges, F. T., Simoes, M. J., Borges, A. A., Sinigaglia-Coimbra, R., & Schor, N. (2012). Bone marrow-derived mesenchymal stem cells repaired but did not prevent gentamicin-induced acute kidney injury through paracrine effects in rats. *PLoS One, 7*(9), e44092. doi:10.1371/journal.pone.0044092

Ren, G., Zhao, X., Zhang, L., Zhang, J., L'Huillier, A., Ling, W., . . . Shi, Y. (2010). Inflammatory cytokine-induced intercellular adhesion molecule-1 and vascular cell adhesion molecule-1 in mesenchymal stem cells are critical for immunosuppression. *Journal of Immunology, 184*(5), 2321-2328. doi:10.4049/jimmunol.0902023

Roh, K. H. (2018). Artificial Methods for T Cell Activation: Critical Tools in T Cell Biology and T Cell Immunotherapy. *Advances in Experimental Medicine and Biology, 1064*, 207-219. doi:10.1007/978-981-13-0445-3_13

Shi, G., Han, J., Liu, G., Hao, Y., Ma, Y., Li, T., . . . Zeng, H. (2014). Expansion of activated regulatory T cells by myeloid-specific chemokines via an alternative pathway in CSF of bacterial meningitis patients. *European Journal of Immunology, 44*(2), 420-430. doi:doi:10.1002/eji.201343572

Song, Y., Dou, H., Li, X., Zhao, X., Li, Y., Liu, D., . . . Hou, Y. (2017). Exosomal miR-146a Contributes to the Enhanced Therapeutic Efficacy of Interleukin-1beta-Primed Mesenchymal Stem Cells Against Sepsis. *Stem Cells, 35*(5), 1208-1221. doi:10.1002/stem.2564

Tan, M. C. B., Goedegebuure, P. S., Belt, B. A., Flaherty, B., Sankpal, N., Gillanders, W. E., . . . Linehan, D. C. (2009). Disruption of CCR5-dependent homing of regulatory T cells inhibits tumor growth in a murine model of pancreatic cancer. *Journal of immunology (Baltimore, Md. : 1950), 182*(3), 1746-1755.

Tan, S. S., Yin, Y., Lee, T., Lai, R. C., Yeo, R. W., Zhang, B., . . . Lim, S. K. (2013). Therapeutic MSC exosomes are derived from lipid raft microdomains in the plasma membrane. *J Extracell Vesicles, 2*. doi:10.3402/jev.v2i0.22614

Vishnubhatla, I., Corteling, R., Stevanato, L., Hicks, C., & Sinden, J. (2014). The Development of Stem Cell-derived Exosomes as a Cell-free Regenerative Medicine. *Journal of Circulating Biomarkers*, 1. doi:10.5772/58597

Vizoso, F. J., Eiro, N., Cid, S., Schneider, J., & Perez-Fernandez, R. (2017). Mesenchymal Stem Cell Secretome: Toward Cell-Free Therapeutic Strategies in Regenerative Medicine. *International Journal of Molecular Sciences, 18*(9), 1852. doi:10.3390/ijms18091852

Volarevic, V., Markovic, B. S., Gazdic, M., Volarevic, A., Jovicic, N., Arsenijevic, N., . . . Stojkovic, M. (2018). Ethical and Safety Issues of Stem Cell-Based Therapy. *International Journal of Medical Sciences, 15*(1), 36-45. doi:10.7150/ijms.21666

Wang, X., Lang, M., Zhao, T., Feng, X., Zheng, C., Huang, C., . . . Ren, H. (2016). Cancer-FOXP3 directly activated CCL5 to recruit FOXP3+Treg cells in pancreatic ductal adenocarcinoma. *Oncogene, 36*, 3048. doi:10.1038/onc.2016.458

https://www.nature.com/articles/onc2016458#supplementary-information

Xin, H., Li, Y., Cui, Y., Yang, J. J., Zhang, Z. G., & Chopp, M. (2013). Systemic administration of exosomes released from mesenchymal stromal cells promote functional recovery and

neurovascular plasticity after stroke in rats. *Journal of Cerebral Blood Flow and Metabolism, 33*(11), 1711-1715. doi:10.1038/jcbfm.2013.152

Yeo, R. W., Lai, R. C., Zhang, B., Tan, S. S., Yin, Y., Teh, B. J., & Lim, S. K. (2013). Mesenchymal stem cell: an efficient mass producer of exosomes for drug delivery. *Adv Drug Deliv Rev, 65*(3), 336-341. doi:10.1016/j.addr.2012.07.001

Zhang, B., Yin, Y., Lai, R. C., Tan, S. S., Choo, A. B., & Lim, S. K. (2014). Mesenchymal stem cells secrete immunologically active exosomes. *Stem Cells Dev, 23*(11), 1233-1244. doi:10.1089/scd.2013.0479

Zhang, Q., Fu, L., Liang, Y., Guo, Z., Wang, L., Ma, C., & Wang, H. (2018). Exosomes originating from MSCs stimulated with TGF-beta and IFN-gamma promote Treg differentiation. *J Cell Physiol, 233*(9), 6832-6840. doi:10.1002/jcp.26436

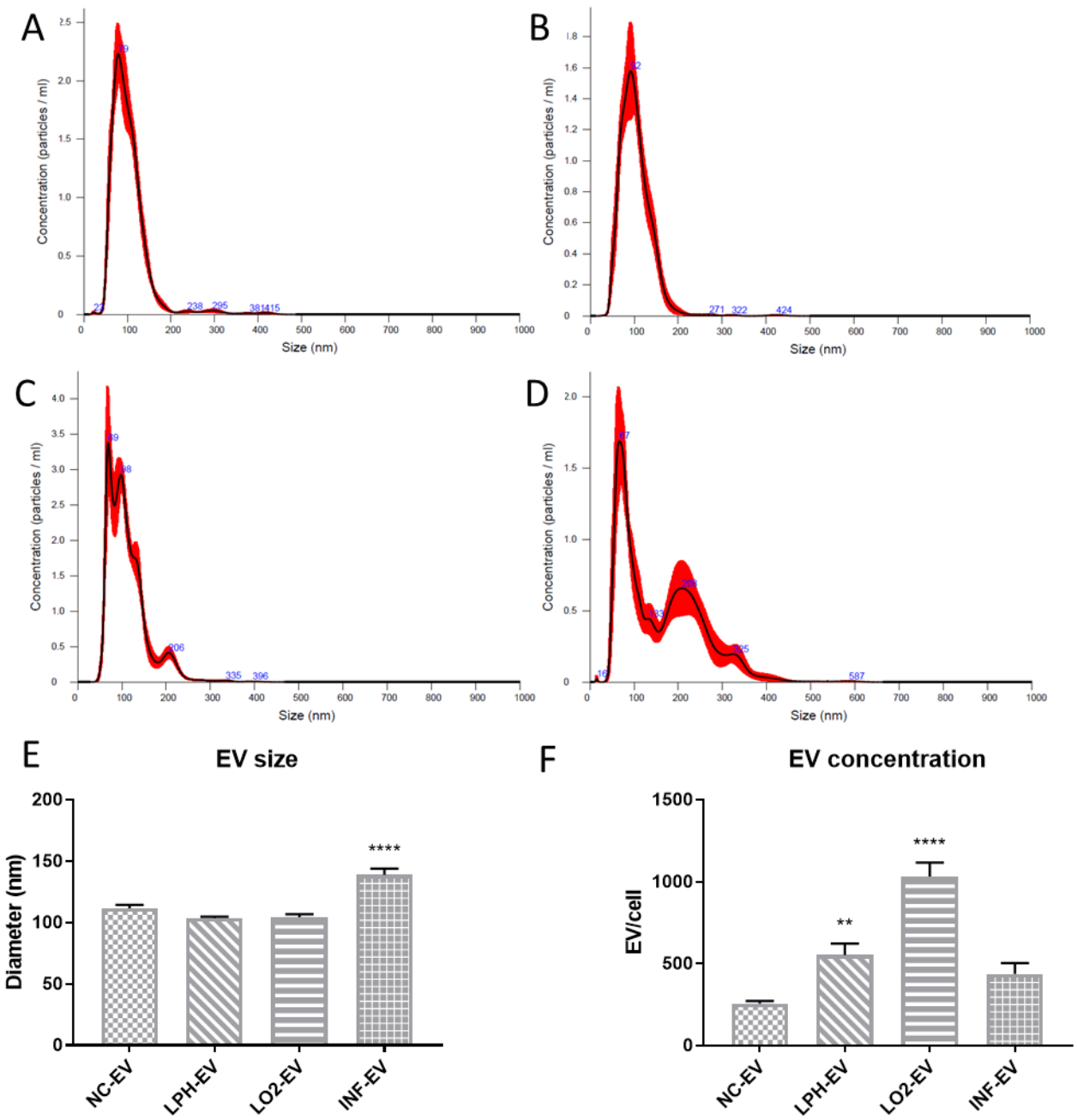

Figure 5.1: EV characterization: Representative size distributions of MSC-Evs. Inflammatory preconditioning resulted in the isolation of a large-diameter population of EVs along with exosomes. Hypoxic and acidic preconditioning increased EV release. (A) Normal Culture, (B) Low pH, (C) Low O_2, (D) IFN-γ + TNF-α

(E): EV diameter across MSC culture conditions as determined by NTA. (F): EV concentration across MSC culture conditions as determined by NTA. One-way ANOVA. Data is presented as means +/- SEM. (*,**, ***,****) indicate significant difference from Normal Culture at p < 0.05, 0.01, 0.001, 0.0001 by Dunnett's post-hoc test.

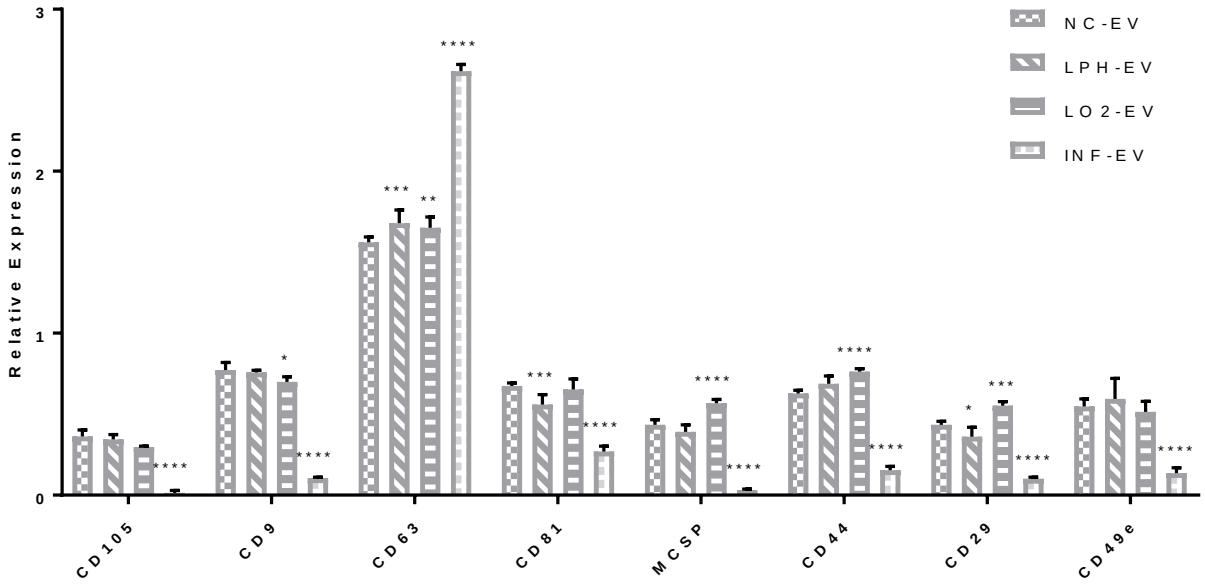

Figure 5.2: Relative expression of EV surface markers across MSC culture conditions as determined by MACSPLEX analysis. There were significant differences in the expression of exosome and cells signaling and adhesion markers across different MSC preconditioning methods. Two-way ANOVA. Data is presented as means +/- SEM. (*,**, ***,****) indicate significant difference from Normal Culture at p < 0.05, 0.01, 0.001, 0.0001 by Dunnett's post-hoc test.

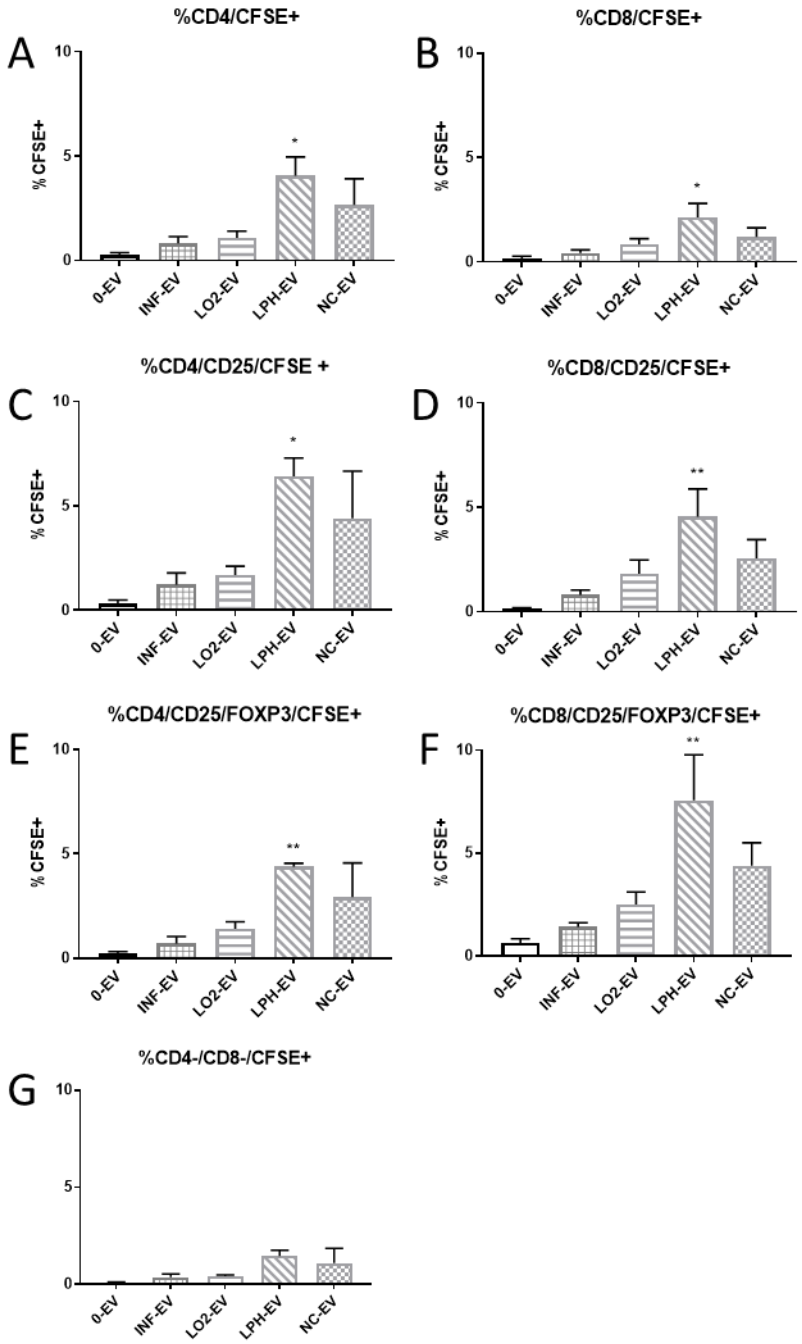

Figure 5.3: Comparative CFSE-EV uptake by T-cell subsets after 24 hours. LPH-EV treated PBMCs had significantly higher CFSE+ frequency than untreated cells, indicating uptake of EVs. (A): Frequency of CD4+ cells positive for CFSE. (B):

Frequency of CD8+ cells positive for CFSE. (C): Frequency of CD4+/CD25+ cells positive for CFSE. (D): Frequency of CD8+/CD25+ cells positive for CFSE. (E): Frequency of CD4+/CD25+/FOXP3+ cells positive for CFSE. (F): Frequency of CD8+/CD25+/FOXP3+ cells positive for CFSE. (G): Frequency of CD4-/CD8-cells positive for CFSE. Data is presented as means +/- SEM. (*,**, ***,****) indicate significant difference from Normal Culture at $p < 0.05$, 0.01, 0.001, 0.0001 by Dunnett's post-hoc test of one-way ANOVA.

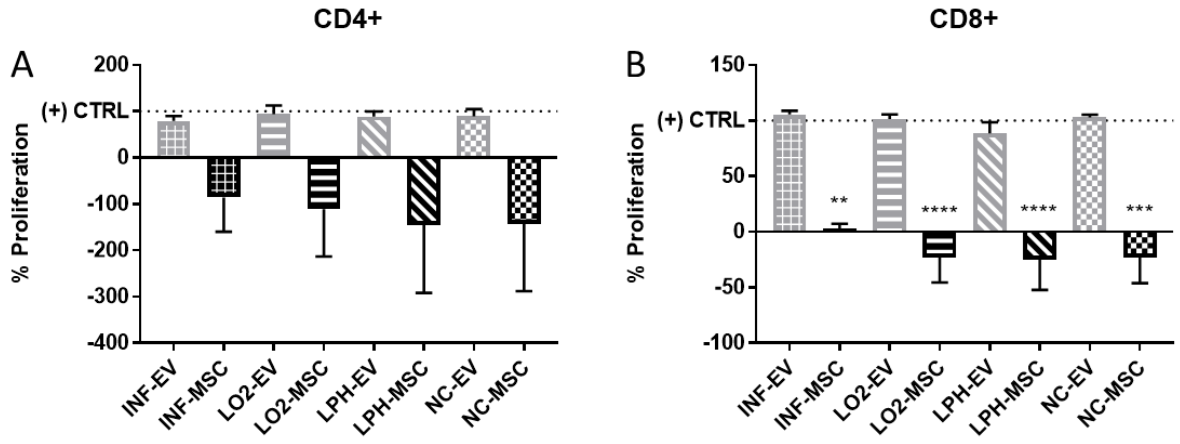

Figure 5.4: Comparative proliferation of T-cell subsets 5 days after treatment with EVs or MSCs as measured by CFSE dilution. EVs did not affect the proliferation of T-cells, while MSCs greatly decreased it. (A): CD4+ cells. (B): CD8+ cells. Data is presented as means +/- SEM. (*,**, ***,****) indicate significant difference from (+) CTRL at $p < 0.05$, 0.01, 0.001, 0.0001 by Dunnett's post-hoc test of one-way ANOVA.

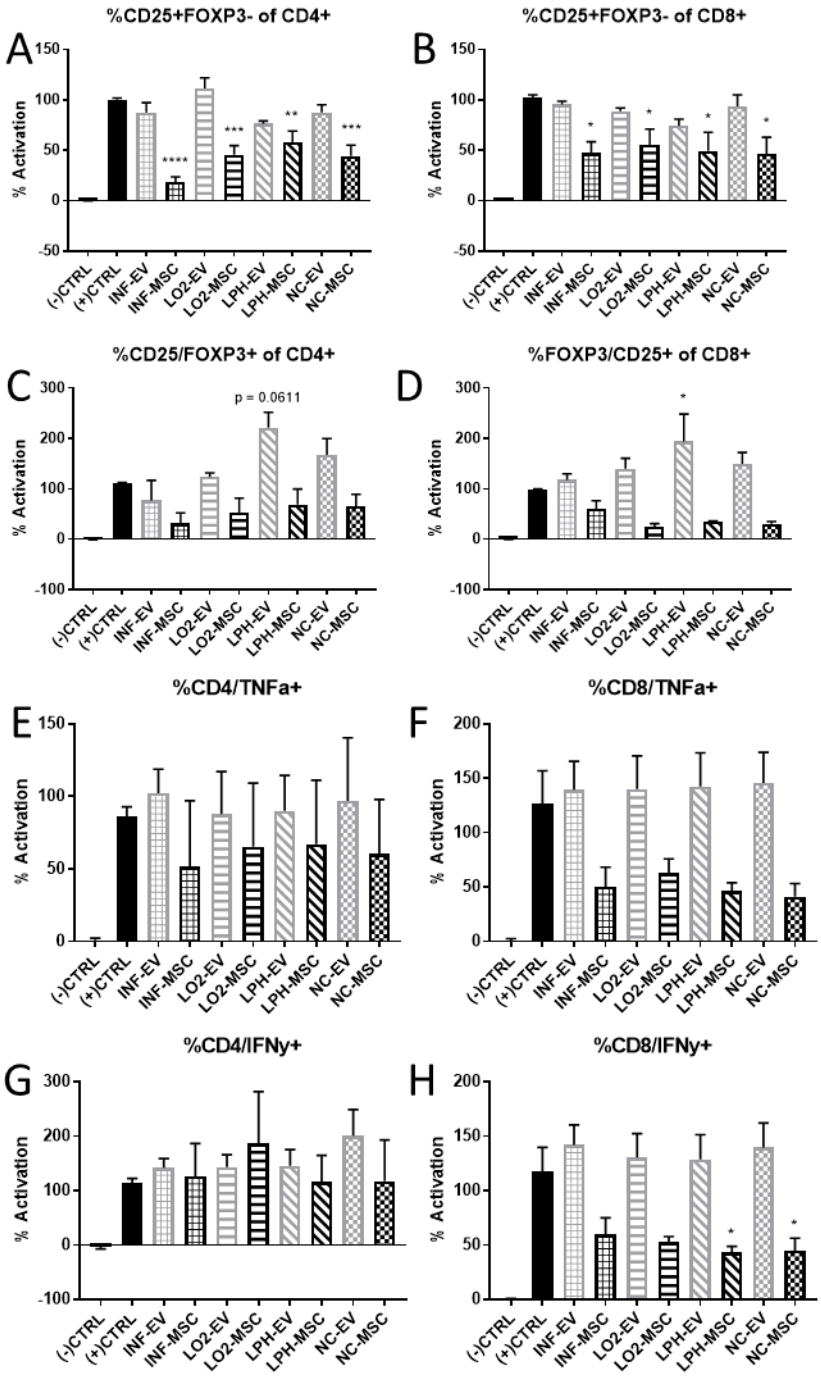

Figure 5.5: Comparative activation of T-cell subsets 5 days after treatment with EVs or MSCs. Overall, MSCs had significant effects on T-effector cells frequency, while LPH-MSC-EVs had significant effects on T-reg frequency. (A): Frequency of

CD4+/CD25+/FOXP3- cells. (B): Frequency of CD8+/CD25+/FOXP3- cells. (C): Frequency of CD4+/CD25+/FOXP3+ cells. (D): Frequency of CD8+/CD25+/FOXP3+ cells. (E): Frequency of CD4+/TNF-α+ cells. (F): Frequency of CD8+/ TNF-α+ cells. (G): Frequency of CD4+/IFN-y+ cells. (H): Frequency of CD8+/ IFN-y+ cells. Data is presented as means +/- SEM. (*,**, ***,****) indicate significant difference from (+) CTRL at $p < 0.05, 0.01, 0.001, 0.0001$ by Dunnett's post-hoc test of one-way ANOVA.

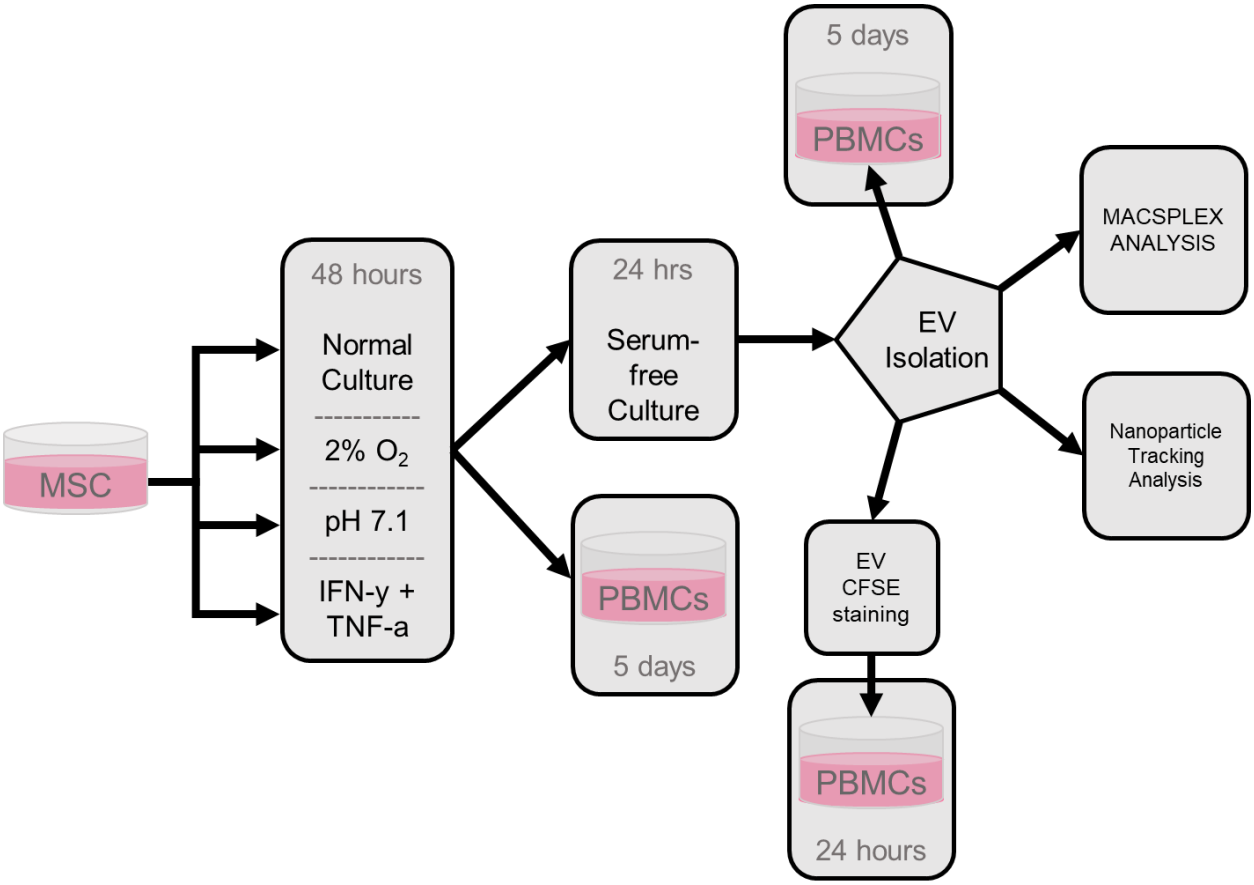

Supplementary Figure 5.1: Experimental workflow. MSCs were split into groups that each underwent different preconditioning steps. MSCs were then either co-cultured with PBMCs for 5 days or used for EV isolation. Isolated EVs were incubated for 5 days with

PBMCs, stained with CFSE and incubated for 24 hours with PBMCs, or used in MACSPLEX or NTA analysis.

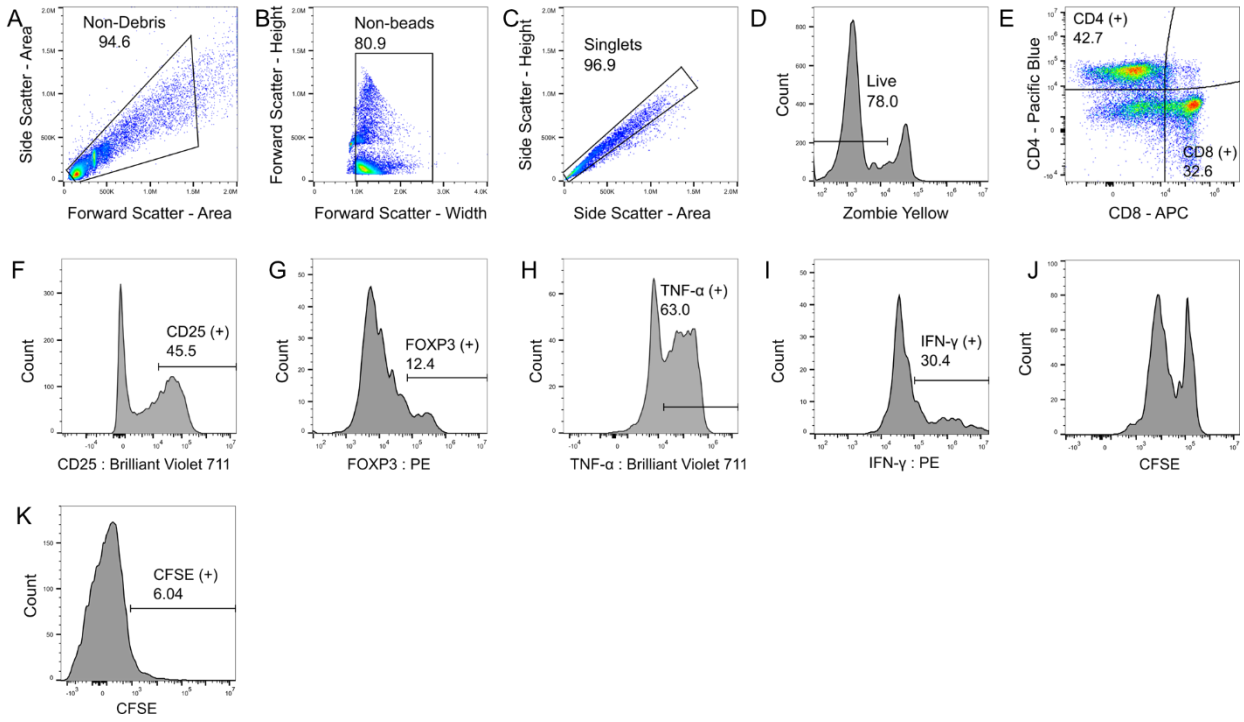

Supplementary Figure 5.2: Flow analysis diagram. After successively gating out debris (A), activating beads (B) and doublets (C), live PBMCs (D) were gated based on CD4 and CD8 expression (E). Single-positive cells were then analyzed based on the panel they were stained with. Panel 1 was first gated by CD25 expression (F), then CD25+ cells were gated by FOXP3 expression (G). Panel 2 was gated separately by TNF-α and IFN-γ. The median fluorescence intensity of CFSE (J) was calculated for all samples to be used in proliferation calculations. For EV uptake, the populations from Panel 1 were determined at 24 hours post-treatment and T-cell subpopulations were gated by CFSE intensity (K). All gates were determined by FMO controls after compensation.

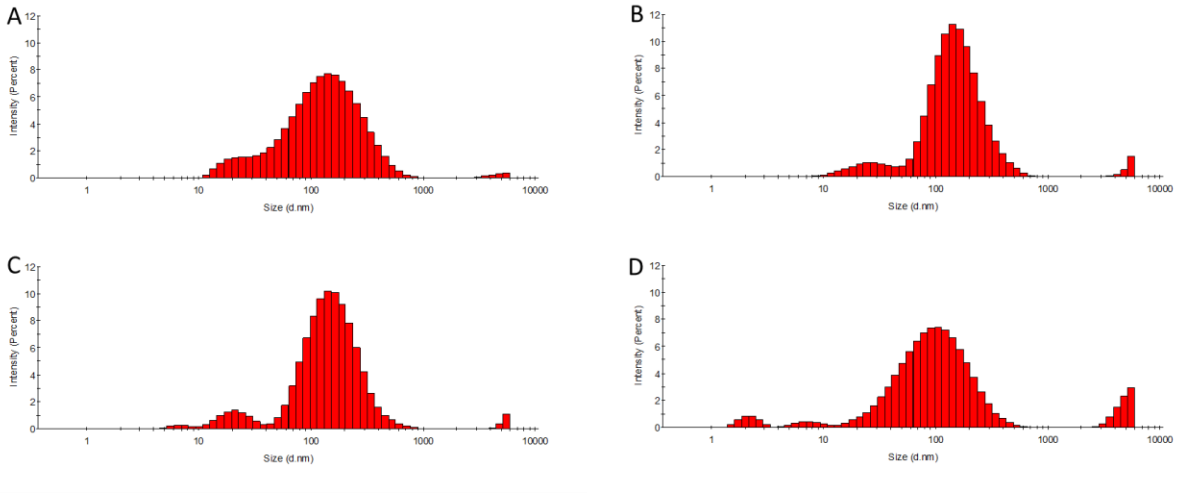

Supplementary Figure 5.3: Dynamic Light Scattering of EVs. Histograms of EV size distribution confirming the existence of a large-diameter population present in INF-MSC-EV at a high concentration (D) that is absent in NC-EV (A), LO2-EV (B), and LPH-EV (C).

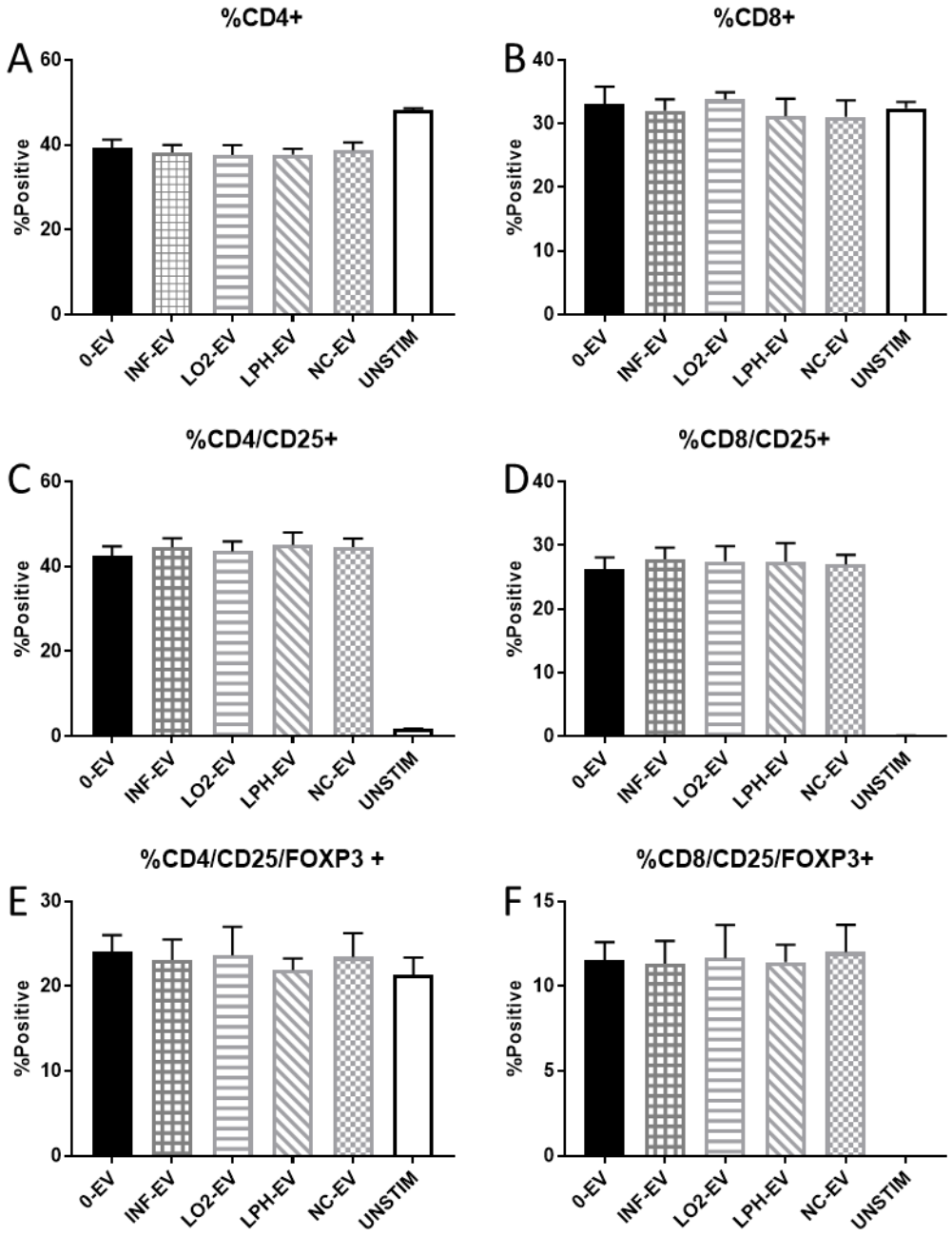

Supplementary Figure 5.4: Comparative activation of T-cell subsets 24 hours after treatment with CFSE-EVs. There were no significant differences between treatment groups. (A): Frequency of CD4+ cells. (B): Frequency of CD8+ cells. (C): Frequency of CD4+/CD25+ cells. (D): Frequency of CD8+/CD25+ cells. (E): Frequency of

CD4+/CD25+/FOXP3+ cells. (F): Frequency of CD8+/CD25+/FOXP3+ cells. Data is presented as means +/- SEM. No significant differences from 0-EV group by Dunnett's post-hoc test of one-way ANOVA.

$$\%Activation = 100\left(\frac{Y_{EXPERIMENTAL} - \overline{Y_{NEGATIVE}}}{\overline{Y_{POSITIVE}} - \overline{Y_{NEGATIVE}}}\right)$$

Equation 5.1: Normalization of T-cell activation parameters of experimental groups ($Y_{EXPERIMENTAL}$) to a percentage of the difference between negative ($Y_{NEGATIVE}$) and positive ($Y_{POSITIVE}$) controls.

$$MI_{stimulated} = \frac{MI_{nonstimulated}}{2^{PS}}$$

Equation 5.2: Calculation of proliferation score (PS) based on CFSE median fluorescence intensities of stimulated ($MI_{stimulated}$)and nonstimulated ($MI_{nonstimulated}$) PBMCs.

CHAPTER 6

CONCLUSION

The goal of this dissertation was to explore how the MSC secretome might be manipulated for therapeutic benefit. To address this aim, MSCs were either transduced with viral vectors or preconditioned in various culture conditions. This demonstrated the feasibility of lentiviral transduced MSCs combined with a CS-GAG scaffold to heal critical-sized bone defects, AVLP transduced MSCs to express transgenes, and acidic preconditioning of MSCs to alter the immunomodulation of their EVs.

Chapter One compared the rhBMP-2 release and critical defect repair by lentiviral transduced MSCs seeded in CS-GAG scaffolds with that of rhBMP-2 loaded collagen or CS-GAG scaffolds. The aim was to improve bone formation with more gradual rhBMP-2 release in the defect space. We found that both BMP-MSC and CS-GAG had more gradual release kinetics than collagen scaffolds, and that all three groups had comparable bone formation. This study involved three different lab groups at two universities, which made communication of each lab's goals, expectations and limitations challenging at times. Additionally, this was my first study involving animal work, and were I to do this study again I would prepare more thoroughly for that portion by ensuring more than enough MSCs and rhBMP-2 were available. Finally, the use of lentivirus to achieve MSC transduction was problematic, ceasing MSC proliferation and precluding the creation of stably expressing lines.

Having compared the BMP-2 release kinetics and defect healing capabilities of these different systems, other questions regarding BMP-MSCs present themselves. One of the main concerns associated with rhBMP-2 use clinically is a heightened and uncontrolled inflammatory response (Ritting, Weber, & Lee, 2012; Tannoury & An, 2014). The fracture environment is also naturally inflamed, which if left unchecked, can lead to impaired bone formation (Ono & Takayanagi, 2017). While this was not directly investigated in this study, MSC delivery may mitigate these risks, given MSCs have extensive immunomodulatory capabilities and can influence multiple immune cell types (Chiesa et al., 2011; Corcione et al., 2006; English, 2013; Maggini et al., 2010). Future work exploring how MSC therapy may improve rhBMP-2-mediated bone healing by limiting adverse effects could be impactful for clinicians.

This study is the first to show bone regeneration using CS-GAG scaffolds and presents interesting options for further study of the hydrogel in this capacity. The GAG+BMP-2 MSC system could potentially be enhanced further through incorporation of cell-adhesive ligands. In the context of bone repair, the fibronectin motif RGD (Kolambkar et al., 2011) and the collagen-mimetic peptide GFOGER (Wojtowicz et al., 2010) have been shown to be effective in promoting new bone formation. These studies have demonstrated that including cell adhesion ligands in the biomaterial scaffold can improve healing for both rhBMP-2 delivery as well as cell delivery approaches. Shekaran et al. showed that GFOGER delivered with a low dose of rhBMP-2 actually increased recruitment of CD45-/CD90+ osteoprogenitor cells to a radial defect compared to collagen sponge with rhBMP-2 (Shekaran et al., 2014). In addition, Moshaverinia et al. demonstrated that osteogenic differentiation of multiple types of MSCs was enhanced

when the cells were encapsulated in RGD alginate microspheres compared to non-functionalized alginate (Moshaverinia et al., 2014). For our study, we tested both rhBMP-2 and MSC delivery approaches with a non-functionalized GAG gel and observed comparable healing to collagen sponge with rhBMP-2. Based on these findings from other labs, it seems plausible that functionalizing our GAG gel with RGD or GFOGER in the future could potentially result in even better outcomes, such as increased migration of endogenous cells into the defect space, or longer retention of transplanted BMP2-MSCs.

Given these questions and possibilities, a new study can be envisioned that investigates them. This would aim to determine the effect of RGD functionalization on endogenous cell migration and transplanted MSC retention, the effect of BMP-MSCs on inflammation, and the combined effect of these components on critically sized bone defect healing. This could be accomplished through in vitro studies of cell migration and BMP-2 expression, and an in vivo study in a wild-type rat model of critical sized femoral defects. The latter experiment would not only examine defect bridging, bone volume and density, but also use immunohistochemistry to determine the frequency of different types of bone cells and immune cells.

Chapter 2 describes the use of an AVLP derived from PIV-5 to induce transgene expression in MSCs with the goal of replacing the lentiviral transduction in Chapter 1. To do this, we collaborated with the He lab of the University of Georgia Veterinary College, which had been successful in using the vector to induce viral protein expression for vaccines. While we were successful in attaining long-term stable expression of EGFP, the expression of rhBMP-2 proved to be much more variable. I initially planned to conduct a study similar to Chapter One using AVLP, but we eventually realized that this would not

be feasible. This was due to both the variable results in rhBMP-2 expression, and the lack of resources the He lab was able to devote to the project. The titer of AVLP required to attain high rhBMP-2 expression levels in our MSCs was prohibitively labor intensive for them. If I were starting this study today, I would first get a clearer picture of how much time our collaborators were able to devote to the project, and what their capabilities for manufacturing vector were.

AVLP-eGFP was able to induce consistent, high, and sustained expression of eGFP in MSCs. There are several options for improving the ability of AVLP to consistently induce high BMP-2 expression. It may be possible to infect cells at a high MOI without a cytopathic effect. This is associated with an increased copy number per cell which could lead to increased protein expression (Ellis & Delbruck, 1939). Additionally, transfection aids such as Polybrene or protamine sulfate can be used to increase initial transduction efficiency by reducing charge repulsion between cells and the virus (Lin et al., 2012). Different strategies for encouraging packaging, assembling, and budding of the construct may increase the efficiency and consistency of AVLP-BMP2. For example, the F protein, which mediates fusion with host cells, can be modified to increase its efficiency (Waning, Schmitt, Leser, & Lamb, 2002). Finally, a different selection marker could be used to select for higher-expressing cells. The bleomycin analogue Zeocin™ has been shown to outperform hygromycin-B in selection efficiency (Lanza, Kim, & Alper, 2013). A future study could take advantage of these methods to improve BMP-MSC generation via AVLP transduction and compare their BMP2 secretion and osteogenic potential to those generated using lentiviruses and adenoviruses. This could be done through both in vitro

experiments such as ELISA of BMP-2 secretion and in vivo experiments examining ectopic bone formation in mice.

Additionally, AVLP could be useful in several applications beyond secretion of BMP-2. As mentioned above, AVLP has been used successfully in vaccines which induce expression of specific adhesion markers (Wei et al., 2017). AVLP could be used for other cell surface modifications, including generation of CAR T-cells for cancer therapy, cell tracking, and labelling or modifying extracellular vesicles such as exosomes. Further work is needed to realize the full potential of the AVLP vector.

Chapter 3 deals with the manipulation of EVs, another aspect of the MSC secretome. We compared the ability of MSCs and their EVs to suppress T-cell activation when the MSCs were cultured in various aspects of inflammation. We found that MSCs outperformed their EVs in T-cell effector suppression regardless of the preconditioning applied, but LPH-EVs were effective in encouraging the formation of regulatory T-cells while none of the MSCs were. The absence of collaborators was a change of pace and came with its own challenges. I found that I did not identify bottlenecks to the experimental workflow for some time, such as the process of generating MSC-EVs, which caused a long lead time for experiments, especially when I was iterating on the experimental design. Additionally, my first attempts to design and optimize the multi-color flow cytometry panel could have been more purposeful and efficient. Also, we were unable to tell whether a lack of T cell suppression by spent media groups was due to our exosome isolation methods. This precluded us from determining the relative effects of MSC contact, EV, and secreted factor mediated suppression. Finally, I underestimated our lab's FBS usage, which resulted in a shortage for the experiments and limited our scope somewhat.

If I were to start this project now, I would set aside or purchase FBS, use MSC co-culture as an immunomodulation control in my preliminary experiments sooner, and scale up my EV production from the beginning. This would allow faster, more efficient iteration on preliminary work, and the possibility of using PBMCs from multiple donors.

There is substantial evidence that EVs are taken up by and affect monocytes and macrophages, switching them to the anti-inflammatory M2 type (Di Trapani et al., 2016; Lo Sicco et al., 2017). MSC-EVs have also had suppressive effects on B and NK cells (Di Trapani et al., 2016). We saw little evidence of uptake by non-T-cells, but we did not verify this directly, nor did we assay activation of these cell types. Future studies could examine the effects of these MSC and EV variants on monocytes, macrophages, B cells, and NK cells. This would be done through assaying the frequency and proliferation of the different cell types in the presence of EVs and MSCs, as well as their expression of inflammatory or anti-inflammatory markers.

Additionally, the mechanism by which LPH-EVs induce T-reg formation should be explored. Possible avenues for study include protein and miRNA content of MSC-EVs. MSCs have previously been shown to upregulate their expression of TGF-B in response to an acidic extracellular environment, which itself induces T-reg formation (Fu et al., 2004; Peppicelli et al., 2015). On the other hand, many EV effects are believed to take place through miRNA transfer, and the miRNA content of EVs from preconditioned MSCs has been implicated in their differing immunosuppressive potencies (Di Trapani et al., 2016; Lo Sicco et al., 2017; Meisgen et al., 2014). A future study could assay the MSC-EV variants discussed here for changes in their protein content, including TGF-B and IDO (Zhang et al., 2018). We could then identify any elevated proteins and block their

associated pathways in subsequent experiments to determine if any of them are responsible for the upregulation of T-regs. A similar approach could be taken with miRNAs, assaying their presence in the EVs with microarrays, performing target prediction and pathway analysis to identify likely candidates, and then transfecting PBMCs with their mimics or inhibitors. T-reg formation and function is known to be affected by miR-21, miR-146a, and miR-181, all of which have been found in MSC-EVs (Liu, Ouyang, Zeng, Luo, & Lu, 2019; Lu et al., 2010; Rouas et al., 2009; Ti, Hao, Fu, & Han, 2016).

REFERENCES

Chiesa, S., Morbelli, S., Morando, S., Massollo, M., Marini, C., Bertoni, A., . . . Uccelli, A. (2011). Mesenchymal stem cells impair in vivo T-cell priming by dendritic cells. *Proc Natl Acad Sci U S A, 108*(42), 17384-17389. doi:10.1073/pnas.1103650108

Corcione, A., Benvenuto, F., Ferretti, E., Giunti, D., Cappiello, V., Cazzanti, F., . . . Uccelli, A. (2006). Human mesenchymal stem cells modulate B-cell functions. *Blood, 107*(1), 367-372. doi:10.1182/blood-2005-07-2657

Di Trapani, M., Bassi, G., Midolo, M., Gatti, A., Kamga, P. T., Cassaro, A., . . . Krampera, M. (2016). Differential and transferable modulatory effects of mesenchymal stromal cell-derived extracellular vesicles on T, B and NK cell functions. *Sci Rep, 6*, 24120. doi:10.1038/srep24120

Ellis, E. L., & Delbruck, M. (1939). THE GROWTH OF BACTERIOPHAGE. *J Gen Physiol, 22*(3), 365-384.

English, K. (2013). Mechanisms of mesenchymal stromal cell immunomodulation. *Immunol Cell Biol, 91*(1), 19-26. doi:10.1038/icb.2012.56

Fu, S., Zhang, N., Yopp, A. C., Chen, D., Mao, M., Chen, D., . . . Bromberg, J. S. (2004). TGF-beta induces Foxp3 + T-regulatory cells from CD4 + CD25 - precursors. *American Journal of Transplantation, 4*(10), 1614-1627. doi:10.1111/j.1600-6143.2004.00566.x

Kolambkar, Y. M., Dupont, K. M., Boerckel, J. D., Huebsch, N., Mooney, D. J., Hutmacher, D. W., & Guldberg, R. E. (2011). An alginate-based hybrid system for growth factor delivery in the functional repair of large bone defects. *Biomaterials, 32*(1), 65-74. doi:10.1016/j.biomaterials.2010.08.074

Lanza, A. M., Kim, D. S., & Alper, H. S. (2013). Evaluating the influence of selection markers on obtaining selected pools and stable cell lines in human cells. *Biotechnol J, 8*(7), 811-821. doi:10.1002/biot.201200364

Lin, P., Lin, Y., Lennon, D. P., Correa, D., Schluchter, M., & Caplan, A. I. (2012). Efficient lentiviral transduction of human mesenchymal stem cells that preserves proliferation and differentiation capabilities. *Stem Cells Transl Med, 1*(12), 886-897. doi:10.5966/sctm.2012-0086

Liu, W., Ouyang, H., Zeng, Q., Luo, R., & Lu, G. (2019). Decreased Treg-derived miR-181a and miR-155 correlated with reduced number and function of Treg cells in allergic rhinitis children. *European Archives of Oto-Rhino-Laryngology, 276*(4), 1089-1094. doi:10.1007/s00405-019-05304-z

Lo Sicco, C., Reverberi, D., Balbi, C., Ulivi, V., Principi, E., Pascucci, L., . . . Tasso, R. (2017). Mesenchymal Stem Cell-Derived Extracellular Vesicles as Mediators of Anti-Inflammatory Effects: Endorsement of Macrophage Polarization. *Stem Cells Transl Med, 6*(3), 1018-1028. doi:10.1002/sctm.16-0363

Lu, L. F., Boldin, M. P., Chaudhry, A., Lin, L. L., Taganov, K. D., Hanada, T., . . . Rudensky, A. Y. (2010). Function of miR-146a in controlling Treg cell-mediated regulation of Th1 responses. *Cell, 142*(6), 914-929. doi:10.1016/j.cell.2010.08.012

Maggini, J., Mirkin, G., Bognanni, I., Holmberg, J., Piazzon, I. M., Nepomnaschy, I., . . . Geffner, J. R. (2010). Mouse bone marrow-derived mesenchymal stromal cells turn activated macrophages into a regulatory-like profile. *PLoS One, 5*(2), e9252. doi:10.1371/journal.pone.0009252

Meisgen, F., Xu Landen, N., Wang, A., Rethi, B., Bouez, C., Zuccolo, M., . . . Pivarcsi, A. (2014). MiR-146a negatively regulates TLR2-induced inflammatory responses in keratinocytes. *Journal of Investigative Dermatology, 134*(7), 1931-1940. doi:10.1038/jid.2014.89

Moshaverinia, A., Chen, C., Xu, X., Akiyama, K., Ansari, S., Zadeh, H. H., & Shi, S. (2014). Bone regeneration potential of stem cells derived from periodontal ligament or gingival tissue sources encapsulated in RGD-modified alginate scaffold. *Tissue Eng Part A, 20*(3-4), 611-621. doi:10.1089/ten.TEA.2013.0229

Ono, T., & Takayanagi, H. (2017). Osteoimmunology in Bone Fracture Healing. *Curr Osteoporos Rep, 15*(4), 367-375. doi:10.1007/s11914-017-0381-0

Peppicelli, S., Bianchini, F., Toti, A., Laurenzana, A., Fibbi, G., & Calorini, L. (2015). Extracellular acidity strengthens mesenchymal stem cells to promote melanoma progression. *Cell Cycle, 14*(19), 3088-3100. doi:10.1080/15384101.2015.1078032

Ritting, A. W., Weber, E. W., & Lee, M. C. (2012). Exaggerated inflammatory response and bony resorption from BMP-2 use in a pediatric forearm nonunion. *J Hand Surg Am, 37*(2), 316-321. doi:10.1016/j.jhsa.2011.10.007

Rouas, R., Fayyad-Kazan, H., El Zein, N., Lewalle, P., Rothe, F., Simion, A., . . . Badran, B. (2009). Human natural Treg microRNA signature: role of microRNA-31 and microRNA-21 in FOXP3 expression. *European Journal of Immunology, 39*(6), 1608-1618. doi:10.1002/eji.200838509

Shekaran, A., Garcia, J. R., Clark, A. Y., Kavanaugh, T. E., Lin, A. S., Guldberg, R. E., & Garcia, A. J. (2014). Bone regeneration using an alpha 2 beta 1 integrin-specific

hydrogel as a BMP-2 delivery vehicle. *Biomaterials, 35*(21), 5453-5461. doi:10.1016/j.biomaterials.2014.03.055

Tannoury, C. A., & An, H. S. (2014). Complications with the use of bone morphogenetic protein 2 (BMP-2) in spine surgery. *Spine J, 14*(3), 552-559. doi:10.1016/j.spinee.2013.08.060

Ti, D., Hao, H., Fu, X., & Han, W. (2016). Mesenchymal stem cells-derived exosomal microRNAs contribute to wound inflammation. *Sci China Life Sci, 59*(12), 1305-1312. doi:10.1007/s11427-016-0240-4

Waning, D. L., Schmitt, A. P., Leser, G. P., & Lamb, R. A. (2002). Roles for the cytoplasmic tails of the fusion and hemagglutinin-neuraminidase proteins in budding of the paramyxovirus simian virus 5. *J Virol, 76*(18), 9284-9297.

Wei, H., Chen, Z., Elson, A., Li, Z., Abraham, M., Phan, S., . . . He, B. (2017). Developing a platform system for gene delivery: amplifying virus-like particles (AVLP) as an influenza vaccine. *NPJ Vaccines, 2*, 32. doi:10.1038/s41541-017-0031-7

Wojtowicz, A. M., Shekaran, A., Oest, M. E., Dupont, K. M., Templeman, K. L., Hutmacher, D. W., . . . Garcia, A. J. (2010). Coating of biomaterial scaffolds with the collagen-mimetic peptide GFOGER for bone defect repair. *Biomaterials, 31*(9), 2574-2582. doi:10.1016/j.biomaterials.2009.12.008

Zhang, Q., Fu, L., Liang, Y., Guo, Z., Wang, L., Ma, C., & Wang, H. (2018). Exosomes originating from MSCs stimulated with TGF-beta and IFN-gamma promote Treg differentiation. *J Cell Physiol, 233*(9), 6832-6840. doi:10.1002/jcp.26436